REPORT DOCUMENTATION PAGE

1a. REPORT SECURITY CLASSIFICATION	1b. RESTRICTIVE MARKINGS
Unclassified	

AD-A212 411

P 13 1989

2a. SECURITY CLASSIFICATION	3. DISTRIBUTION / AVAILABILITY OF REPORT
	Approved for public release; distribution unlimited.

	5. MONITORING ORGANIZATION REPORT NUMBER(S)
	ARO 23356.6-CH

6a. NAME OF PERFORMING ORGANIZATION	6b. OFFICE SYMBOL (If applicable)	7a. NAME OF MONITORING ORGANIZATION
National Institute of Standards & Technology	.	U. S. Army Research Office

6c. ADDRESS (City, State, and ZIP Code)	7b. ADDRESS (City, State, and ZIP Code)
Gaithersburg, MD 20899	P. O. Box 12211 Research Triangle Park, NC 27709-2211

8a. NAME OF FUNDING / SPONSORING ORGANIZATION	8b. OFFICE SYMBOL (If applicable)	9. PROCUREMENT INSTRUMENT IDENTIFICATION NUMBER
U. S. Army Research Office		MIPR 101-88

8c. ADDRESS (City, State, and ZIP Code)	10. SOURCE OF FUNDING NUMBERS			
P. O. Box 12211 Research Triangle Park, NC 27709-2211	PROGRAM ELEMENT NO.	PROJECT NO.	TASK NO.	WORK UNIT ACCESSION NO

11. TITLE (Include Security Classification)
Fundamental molecular data to support CARS diagnostics of temperature, pressure, and species concentration

12. PERSONAL AUTHOR(S)
Gregory J. Rosasco

13a. TYPE OF REPORT	13b. TIME COVERED	14. DATE OF REPORT (Year, Month, Day)	15. PAGE COUNT
Final	FROM 12/17/85 TO 4/30/89	89/08/10	110

16. SUPPLEMENTARY NOTATION
The view, opinions and/or findings contained in this report are those of the author(s) and should not be construed as an official Department of the Army position, policy, or decision, unless so designated by other documentation.

17.	COSATI CODES		18. SUBJECT TERMS (Continue on reverse if necessary and identify by block number)
FIELD	GROUP	SUB-GROUP	Nonlinear Raman spectroscopy, Raman Q-branch spectra, CO, H_2 self-broadening and -shifting, foreign-gas broadening and shifting, energy-gap laws, rotational energy transfer, (over)

19. ABSTRACT (Continue on reverse if necessary and identify by block number)
The J-, and T-dependence of line broadening and line shifting coefficients are reported for the Q-branch spectra of CO and various hydrogen diatomics. Experimental studies verify our ability to predict, using an energy-gap rate law description of the relaxation matrix equation, the collisionally narrowed Q branch of self-broadened CO. Line shifting is determined experimentally and accounted for by semi-classical calculation. This calculation also is shown to be very accurate for self-broadening in CO and is used to predict line broadening in CO:N_2 from 295 to 1500 K. The Q-branch line shape function for the hydrogen diatomics is studied for a range of collision partners and temperatures. In the low pressure, Dicke narrowed regime, the basic line shape function is understood; however, there is no reliable basis for prediction of the (in some cases complex) "optical diffusion coefficient". In the pressure broadened regime, anomalous, asymmetric lineshapes are reported for the $H_2(D_2)$:Ar system. These are ascribed to inhomogeneous broadening associated with the speed dependence of dephasing cross-sections. This lineshape is shown to, (over)

20. DISTRIBUTION / AVAILABILITY OF ABSTRACT	21. ABSTRACT SECURITY CLASSIFICATION
☐ UNCLASSIFIED/UNLIMITED ☐ SAME AS RPT. ☐ DTIC USERS	Unclassified

22a. NAME OF RESPONSIBLE INDIVIDUAL	22b. TELEPHONE (Include Area Code)	22c. OFFICE SYMBOL

DD FORM 1473, 84 MAR 83 APR edition may be used until exhausted.   SECURITY CLASSIFICATION OF THIS PAGE
All other editions are obsolete.   UNCLASSIFIED

89 9 11 006

18. temperature dependence, pressure dependence, concentration dependence.

19. "collisionally narrow" and symmetrize with increasing $H_2(D_2)$ concentration. The
     J-dependence of the line broadening for the hydrogen diatomics is shown to be
     consistently described by a large (J and T independent) vibrational dephasing
     contribution and a (energy-gap based) rate law modeled rotationally inelastic
     component. Line self-shifting in H_2, which shows a resonance coupling effect, is
     not currently understood. A sensitivity analysis is developed for assessing the
     accuracy of T and P measurements based on use of the N_2 0-1 vibrational Q branch
     CARS spectrum.

Accession For

NTIS GRA&I   ☑
DTIC TAB   ☐
Unannounced   ☐
Justification

By
Distribution/
Availability Codes
        Avail and/or
Dist   Special

A-1

FUNDAMENTAL MOLECULAR DATA TO SUPPORT

CARS DIAGNOSTICS OF

TEMPERATURE, PRESSURE, AND SPECIES CONCENTRATION

FINAL REPORT

GREGORY J. ROSASCO

AUGUST 1989

U. S. ARMY RESEARCH OFFICE

PROPOSAL NO: 23356-CH

U. S. NATIONAL INSTITUTE OF STANDARDS AND TECHNOLOGY

THE VIEW, OPINIONS, AND/OR FINDINGS CONTAINED IN THIS REPORT ARE
THOSE OF THE AUTHOR(S) AND SHOULD NOT BE CONSTRUED AS AN OFFICIAL
DEPARTMENT OF THE ARMY POSITION, POLICY, OR DECISION, UNLESS SO
DESIGNATED BY OTHER DOCUMENTATION.

ii

TABLE OF CONTENTS

LIST OF APPENDIXES

APPENDIX A

Comparison of rotational relaxation rate laws to characterize the Raman Q-branch spectrum of CO at 295 K (manuscript accepted for publication in Chemical Physics Letters)

APPENDIX B

Observation of a speed-dependent collisional inhomogeneity in the H_2 vibrational line profile (manuscript accepted for publication in Physical Review Letters)

LIST OF FIGURES

vi

APPENDIX A

Fig.1 Isotropic Raman Q-branch pressure broadening coefficients as function of rotational quantum number.

Fig.2 The ECS scaling law prediction of the CO Q-branch spectrum at 3.0 and 295 K compared to experimental spectrum.

Fig.3 The MEG law prediction of the CO Q-branch spectrum compared with experimental spectra at a) 3.0 and b) 6.0 atm.

Fig.4 The SPEG law prediction of the CO Q-branch spectrum compared with the experimental spectra at a) 3.o and b) 6.0 atm.

Fig.5 Rotationally inelastic state-to-state rates as a function of initial and final quantum number as given by a) the best MEG law model and b) the best SPEG law model.

APPENDIX B

Fig.1 Experimental IRS spectra of the Q(1) transition of H_2 broadened by Ar at 295 K and 1000 K.

Fig.2 (a) Best fit collision-broadening and narrowing coefficients obtained from IRS spectra of the Q(1) transition of H_2:Ar mixtures at 295 K and 7.3 amagat. (b) Spectral linewidths determined from fitting Lorentzian profiles to the data and to the theoretical profiles calculated using the corresponding parameters in (a).

LIST OF TABLES

Appendix A

Table 1: Experimental values of CO self-broadening coefficients at
295 K.

Table 2: Intermolecular parameters for line broadening calculations.

Appendix B

Table I: Collisional line-shift coefficients $\delta(T)$ for the Q(1)
transition of H_2 at different temperatures, measured with IRS, and
compared to fitted model results.

I INTRODUCTION

A. STATEMENT OF THE PROBLEM STUDIED

As stated in the original proposal, the focus of this research is to "...provide the data and predictive equations necessary..." for "...accurate diagonostic measurements of temperature, pressure, and species concentration by CARS spectroscopy...". These data and predictive equations are to be used to describe the Raman vibrational Q branch for the molecules CO and H_2 as functions of temperature, pressure, and composition.

Within the context of this proposal, the terms "predictive equations" refer both to validated forms for the spectral distribution functions and to a reliable predictive basis for the molecular parameters which specify the distribution function. Foremost among the relevant molecular parameters are the broadening and shifting coefficients for the individual transitions which comprise the branch. Although there is some first principle basis for the predictive equations, the methodology is this area typically (but not exclusively as we demonstrate) is empirical.

The spectral distribution functions need to encompass the effects of both velocity and phase changing collisions. The relative importance of these two types of collisions is very different for the two molecules of interest in this work. In particular, the study of the hydrogen diatomic molecules yields important tests of our fundamental understanding of the role of velocity changing collisions. The correlation of the latter to phase changing collisions also can be revealed by such studies. Prior to our work, there was relatively little known about the temperature and collision partner dependence of line formation for the hydrogens.

For the CO molecule, the dominant line formation process involves the effects of rotationally inelastic collisions which lead to a pressure dependent narrowing (collapse) of the Q branch. In contrast to the situation for the hydrogen diatomics, there is an established framework for description of these spectra. In this case, the predictive basis involves the use of rate laws for rotational energy transfer to specify a relaxation matrix formulation of the Q-branch spectral distribution. However, the efficacy of this basis must be tested against accurate measurements as functions of temperature and pressure. Additionally, first principle calculations can be used to provide a physically realistic assessment of the rate law models. These two areas were the core of our research on the CO system.

B. BRIEF OUTLINE OF THE RESULTS OF THIS STUDY

In the following section (II), we present summaries of the experimental results for both the CO and H_2 systems. These data involve extensive measurements of the the rotational quantum number and temperature dependence of line broadening and shifting coefficients and detailed comparisons of the predictions of various spectral models to spectral distribution functions determined over large ranges of temperature, pressure, and collision partner. In the case of the hydrogens, previously unobserved lineshape anomalies, which are pressure, temperature, and concentration dependent, are reported.

1

Because of the different level of our understanding of the physics of line formation for the two systems, the comparison of these data to the predictions of theory is discussed from somewhat different points of view in Section III.

For the CO system, the discussion in Section III focuses on the use of energy-gap rate law models and the simultaneous prediction of line broadening coefficients and spectral collapse. In this study we are interested in the accuracy of our prediction of the details of the CO Q-branch spectrum as a function of P and T. It is shown that the familiar, energy-corrected sudden (ECS) scaling approach is not consistent with the data on CO. However, the Raman spectral data are adequately fit by two different exponential gap law models which have radically different assumptions about the role of dipolar symmetry forces in the line broadening process. We are able to resolve this ambiguity through a first principle, semi-classical line broadening calculation which we describe in Section IV.

For the hydrogens, Section III focuses on situations where spectral models appear reliable and therefore we need to predict certain molecular line shape parameters. The majority of the discussion involves attempts to account for the J and T dependence of the line broadening coefficients in terms of both vibrational dephasing and rate-law-modelled inelastic collisions.

In Section IV, we turn from predictive equations to first principle theory. The CO line broadening calculation, mentioned above, is described. This newly developed computational tool is shown to give remarkably accurate agreement with infrared and Raman line broadening data over a large range of J and T. The state-of-the-art in the calculation of line broadening and shifting in the hydrogens also is reviewed in the context of our experimental results. With some minor exceptions, we find that first principle calculations are reliable only for the case of D_2:He.

Foreign gas broadening of CO is addressed in Section V. Here the line broadening calculation, discussed in Section IV, is applied to the Q branch of CO in a N_2 host from 300 to 1500 K.

To assess the accuracy of measurements of temperature and pressure derived from CARS diagnostic Q-branch spectra, an extensive sensitivity analysis which utilizes the N_2 Q branch as a model system is presented in Section VI. From this analysis we estimate the errors in T and P which arise from uncertainties ("noise") inherent in the measurement of multichannel, single-shot CARS spectra of N_2. The approach developed in this section establishes a useful framework for response to questions concerning the accuracy of the information derived from spectroscopic measurements. Further, this methodology allows an assessment of the sensitivity of such measurements to inaccuracies in the spectroscopic data-base and can assist the experimentalist in the selection of measurement schemes which are optimally insensitive to "noise" and/or systematic data uncertainties.

In the final (Conclusions) section, we discuss the limits of our ability to predict the Q-branch spectrum of the simple diatomic molecule systems studied in this work. We also suggest areas for future research in support of CARS diagnostics.

2

II SUMMARY OF EXPERIMENTAL STUDIES

The experimental results reported here were obtained using two different high-resolution Raman gain/loss spectrometers: a cw-laser based inverse Raman system with nominally 10 MHz resolution and a quasi-cw inverse Raman apparatus, which uses a pulsed Raman-pump laser, with an effective resolution of 45 MHz. These systems are adequately described in the experimental sections of the publications previously reported for this project, cf. for example, Refs. [P2], [M10], [P3], and [P5]. We note for completeness that these experimental systems provide very high accuracy measurements of the imaginary part of the third order nonlinear susceptibility. The resonant part of the CARS susceptibility is fully determined from these measurements. Highlights of the experimental results are summarized for each molecular system in the following.

A. CO:CO

1) LINE BROADENING COEFFICIENTS

In Fig. II.1 we display the J and T dependence of the line broadening coefficients of self-broadened CO. The solid lines (denoted theory) through the data points are predictions of a modified exponential gap rate law (MEG). This MEG law expresses the rate for upward rotational transitions from state J to state J' as

$$W_{J'J} = P \alpha \bullet \left[\frac{1 + A\ E(J)/kT\delta}{1 + A\ E(J)/KT} \right]^2 \bullet \exp\left[\frac{-\beta\{E(J') - E(J)\}}{kT} \right] \quad (II.1)$$

with α, β, and δ being adjustable parameters, A a constant (a measure of the duration of a collision), $E(J)$ the energy of the rotational level J, P pressure, T temperature, and k Boltzmann's constant. The downward $J' \to J$ transitions are found from the condition of detailed balance. The value A=2 is assigned in Ref. [P5]. The parameters β (=1.346) and δ (=1.322) have been refined relative to those presented in Ref. [P5] in the course of the work discussed in Ref. [P3]. The coefficient α is a function of T of the form

$$\alpha(T) = \alpha(T_0) \frac{1 - \exp(-m)}{1 - \exp(-mT/T_0)} (T_0/T)^{0.5} \quad (II.2)$$

with $\alpha(T_0)$ = 0.01265 cm^{-1}/atm for T_0= 295 K and m= 0.212.

2) LINE SHIFTING COEFFICIENTS

Our measurements of line shifting were described in Ref. [P3]. The procedures described therein were repeated in the vicinity of 600 and 1000 K. For the determination of accurate values of line shifting coefficients it is important to utilize relatively isolated transitions and to include first order corrections for line interference. This requirement results in the

3

Figure II.1
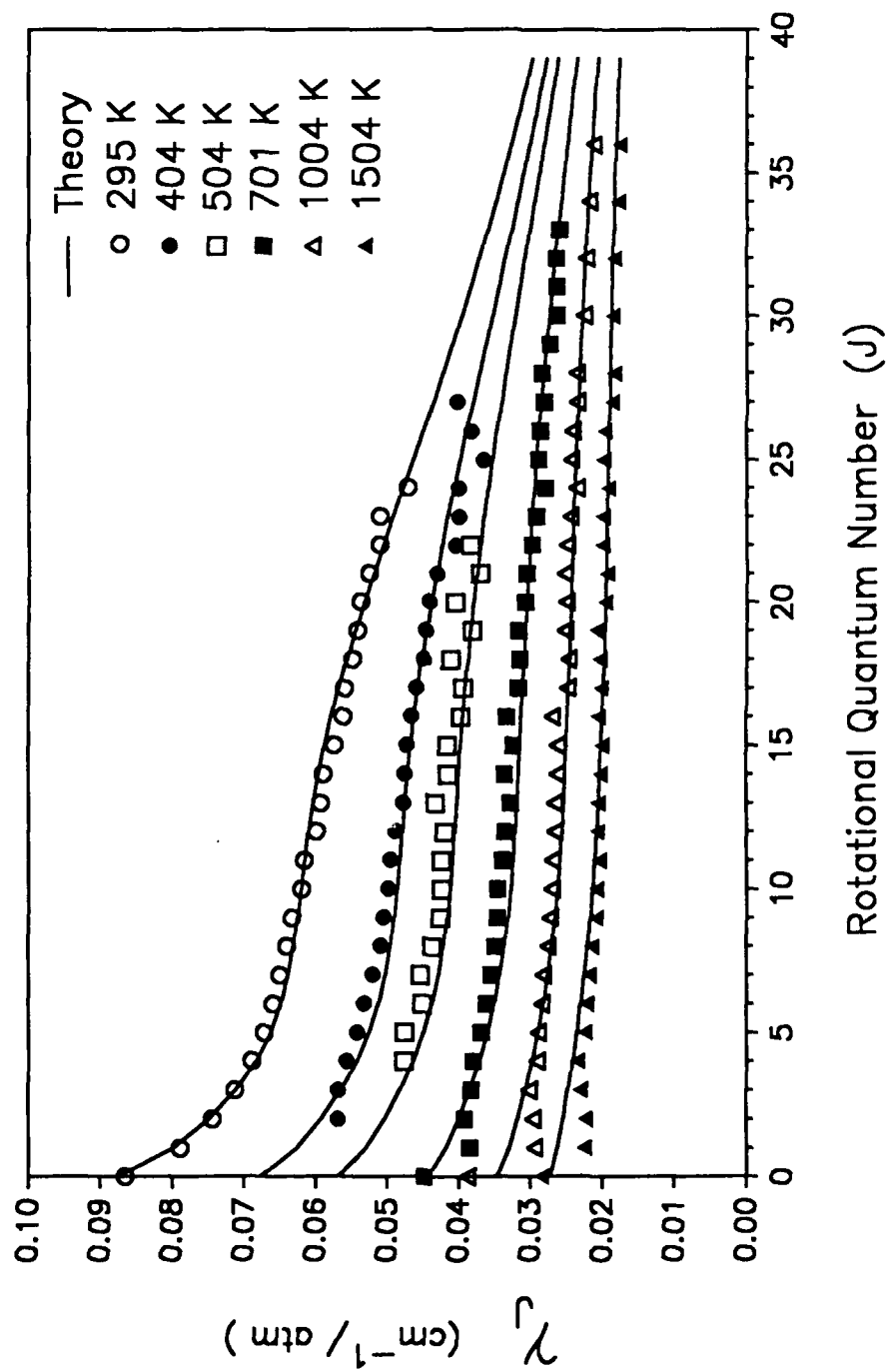
study of the relatively weak, high J transitions; however, we were able to establish reasonably accurate values and set limits to the J-dependence of the shifts. Since the latter dependence is very small, we can establish a single, temperature dependent shift coefficient for the entire Q branch. All the results are displayed in Fig. II.2.

These experimental findings are corroborated by semi-classical calculations of the shift coefficients, see Section IV. The calculated Q-branch shifts, based only on a parameter determined from the room T shift, are shown as the solid line in the figure. The variation with T is described by

$$\Delta\nu/\Delta P = -0.0032 \ (T_0/T) \ cm^{-1}/atm \qquad\qquad (II.3)$$

with T_0= 295 K with estimated uncertainty of ±0.001 cm^{-1}/atm. We note that the results for CO, discussed above, are completely analogous to those obtained for N_2 [R1].

3) SPECTRAL DISTRIBUTIONS

One of the most difficult aspects of the experimental research is the accurate determination of the shape of the collapsing Q branch as a function of P and T. These measurements require high accuracy in both the frequency and intensity axes over large ranges of dye laser wavelength. In addition, we found that the pump and probe beams must be precisely co-focussed at their crossing point in order to minimize spurious signals (i.e. apparent power modulations of the probe laser caused by the pump laser). We ascribe these spurious signals to beam steering effects, essentially "schlieren effects", which therefore depend on the real part of the third order susceptibility. Having reduced these systematic errors to a minimum, we estimate the uncertainies in our measurements of the spectral distributions to be approximately at the level of 2-3% of the peak signal, cf. for example the results in Appendix A.

We have studied the collapse of the Q branch at room temperature very extensively, incorporating the results of three independent series of measurements. This work is discussed in detail in the manuscript included as Appendix A. Representative results from the lineshape studies above room temperature are shown in Fig. II.3. In this figure, the data (symbols) are compared to the predictions of the MEG law (solid lines), Eqs. II.1 and II.2, with the shifts from Eq. II.3. Residuals are displayed, offset for clarity, below the spectral comparison. We will return to consider the analysis of these data in Section III.A, below.

5

CO:CO Q-Branch Lineshift vs T

Figure II.2

Figure II.3
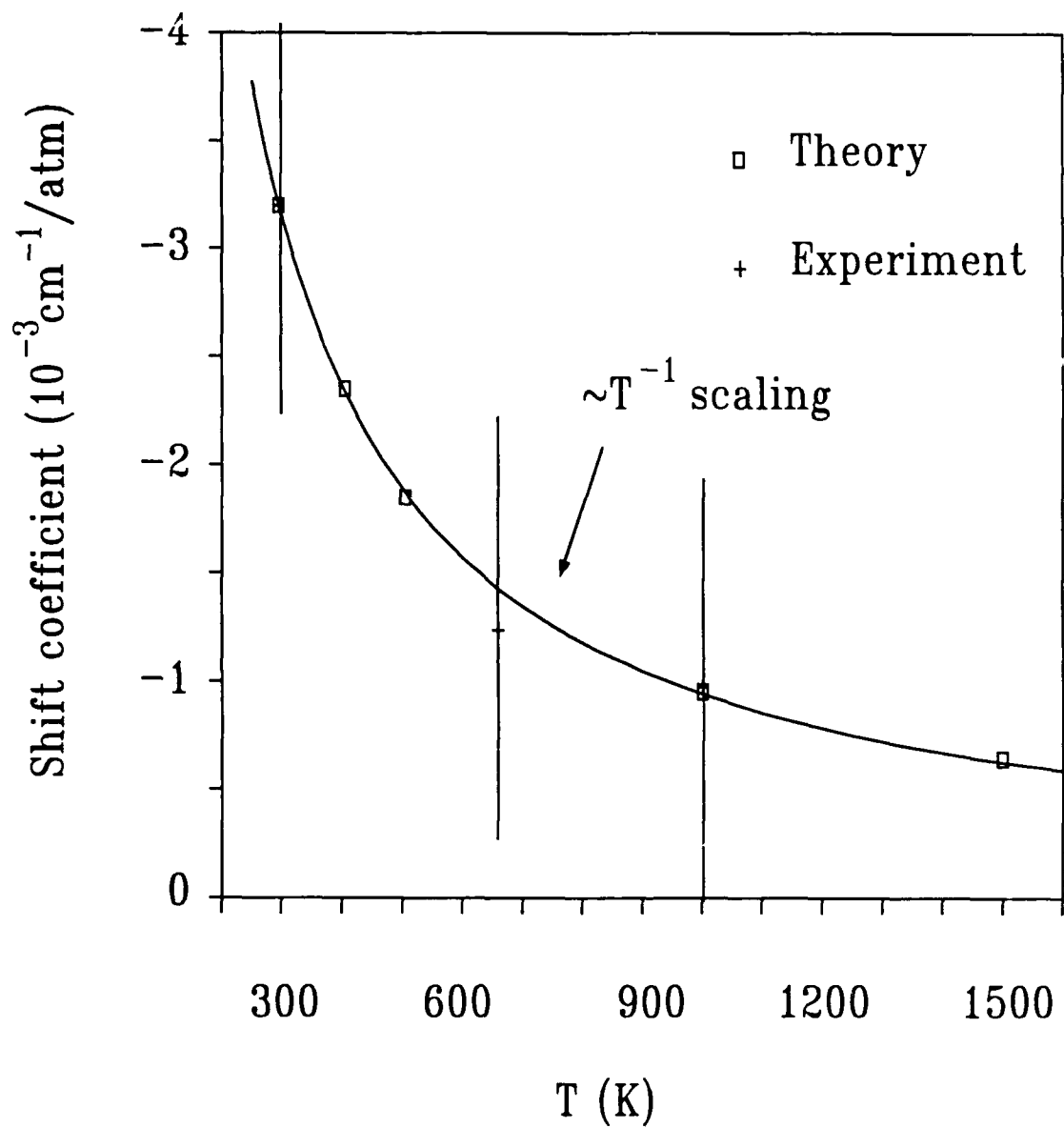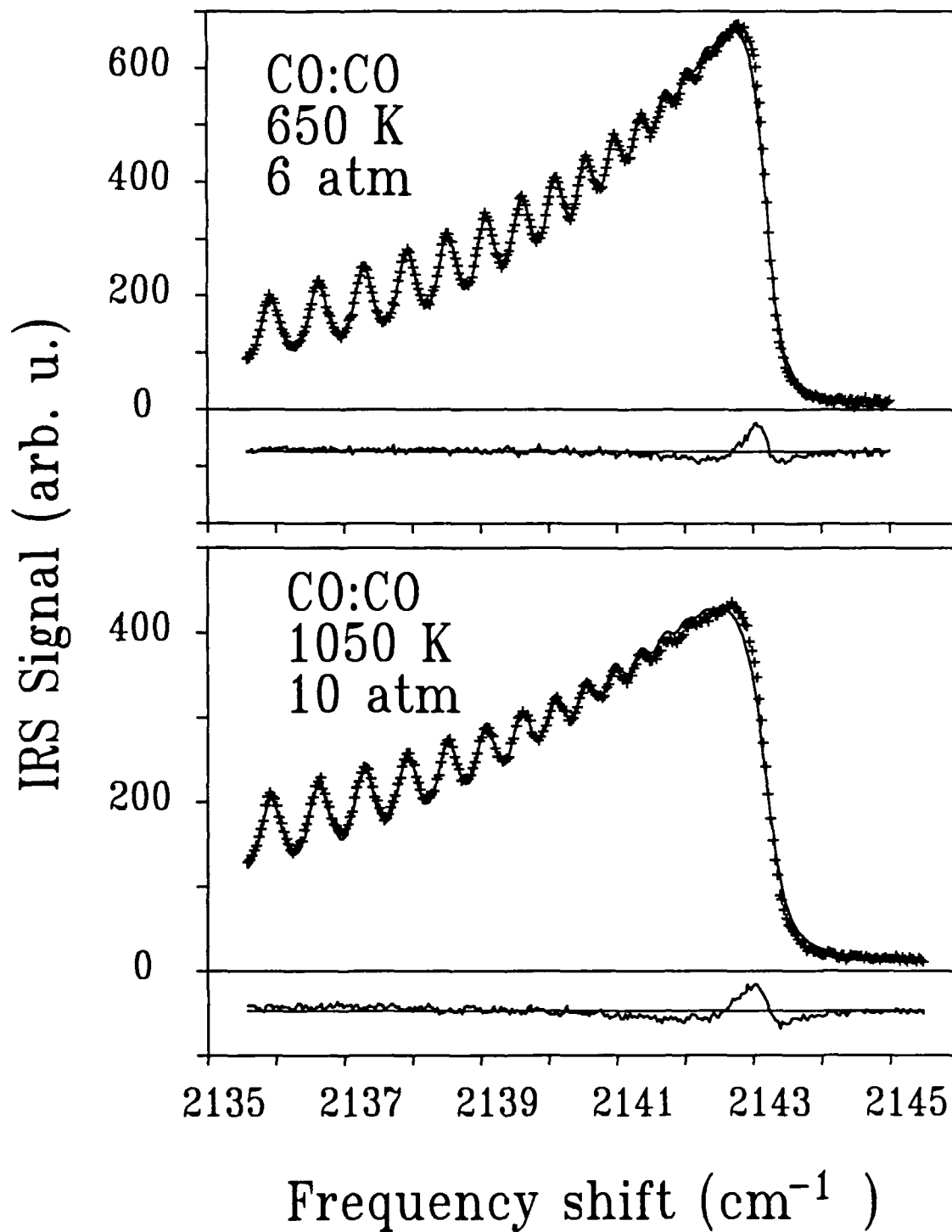
B. DIATOMIC HYDROGEN SYSTEMS

1) LINE BROADENING COEFFICIENTS

The first system studied in this work was $D_2:X$ ($X=D_2$, H_2, He, Ar, CH_4) at room T. Selected results are summarized in Fig. II.4 (for a more complete discussion see Ref. [P2]). The solid line through the points in Fig. II.4 is based on an analysis which includes both vibrational dephasing (indicated by the dash-dot line) and rotationally inelastic components in the total line broadening coefficient. Line broadening coefficients also have been determined for the $H_2:H_2$ system from 295 to 1000 K. These are presented in Fig. II.5 (note that these data are presented as /atm broadening coefficients) along with a parametrizaton [M9], in the spirit of that applied to D_2, in terms of vibrational dephasing and rotationally inelastic contibutions. These analyses will be discussed in Section III.B.

2) LINE SHIFTING COEFFICIENTS

We have measured line shifting for selected transitions and perturbers for a number of hydrogen diatomics during the course of this work. These data are collected in Table II.1.

TABLE II.1

Line shifting coefficients at 298 K (10^{-3} cm^{-1}/amagat)[a]

Molecule:Host	Q(0)	Q(1)	Q(2)	Q(3)	Q(4)	Q(5)
HD:HD[b]	-5.0(1)	-4.3(1)	-3.9(1)	-3.1(1)		
$D_2:D_2$	-1.9(1)	-1.9(1)	-1.8(1)	-1.5(1)	-1.6(1)	
$D_2:He$	+6.1(1)	+6.5(1)	+6.8(1)	+7.6(10)	+6.4(10)	
$D_2:Ar$	-10.3(2)	-9.5(2)	-9.4(2)	-9.5(8)	-9.0(8)	-8.9(8)
$D_2:CH_4$		-18.2(4)	-18.4(4)			

[a] uncertainties in the last digit are indicated by numbers in parentheses
[b] see Ref. [P4].

Only for self-shifting in H_2 have we made an extensive study of both the J and T dependence. The results are presented in Fig. II.6 (this study will be published [M8]). Finally, we note that the T dependence of the Ar-shifting of the H_2 Q(1) line is reported as part of the study, discussed below, on anomalous line shapes, see Appendix B.
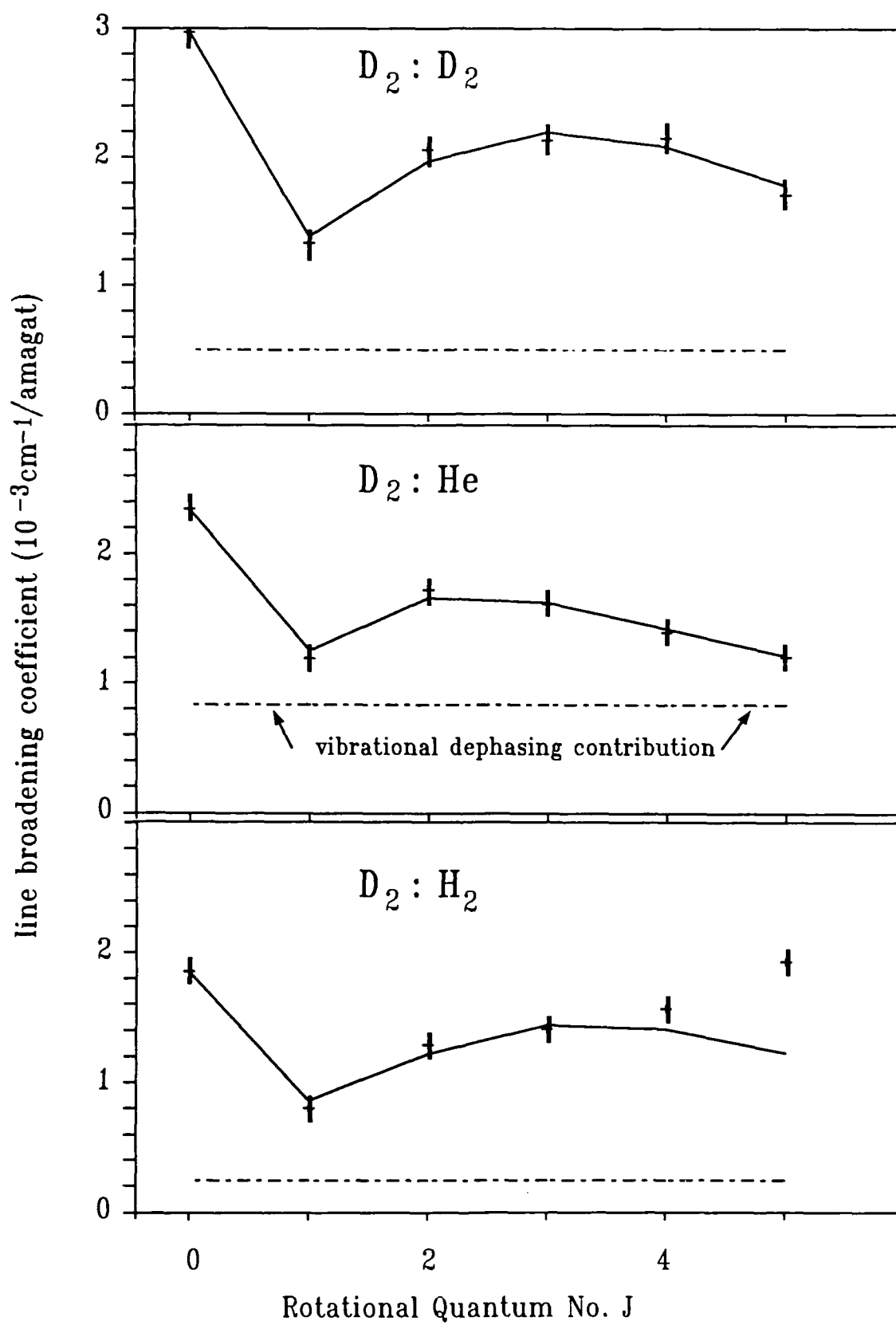
Figure II.4

Exper. vs. ECS H_2-H_2 Linewidths with Constant Dephasing

Figure II.5

10

H$_2$: H$_2$ Q branch shifting

shift (10^{-3} cm^{-1}/amagat) vs Rotational quantum number J

1000 K

725 K

450 K

295 K
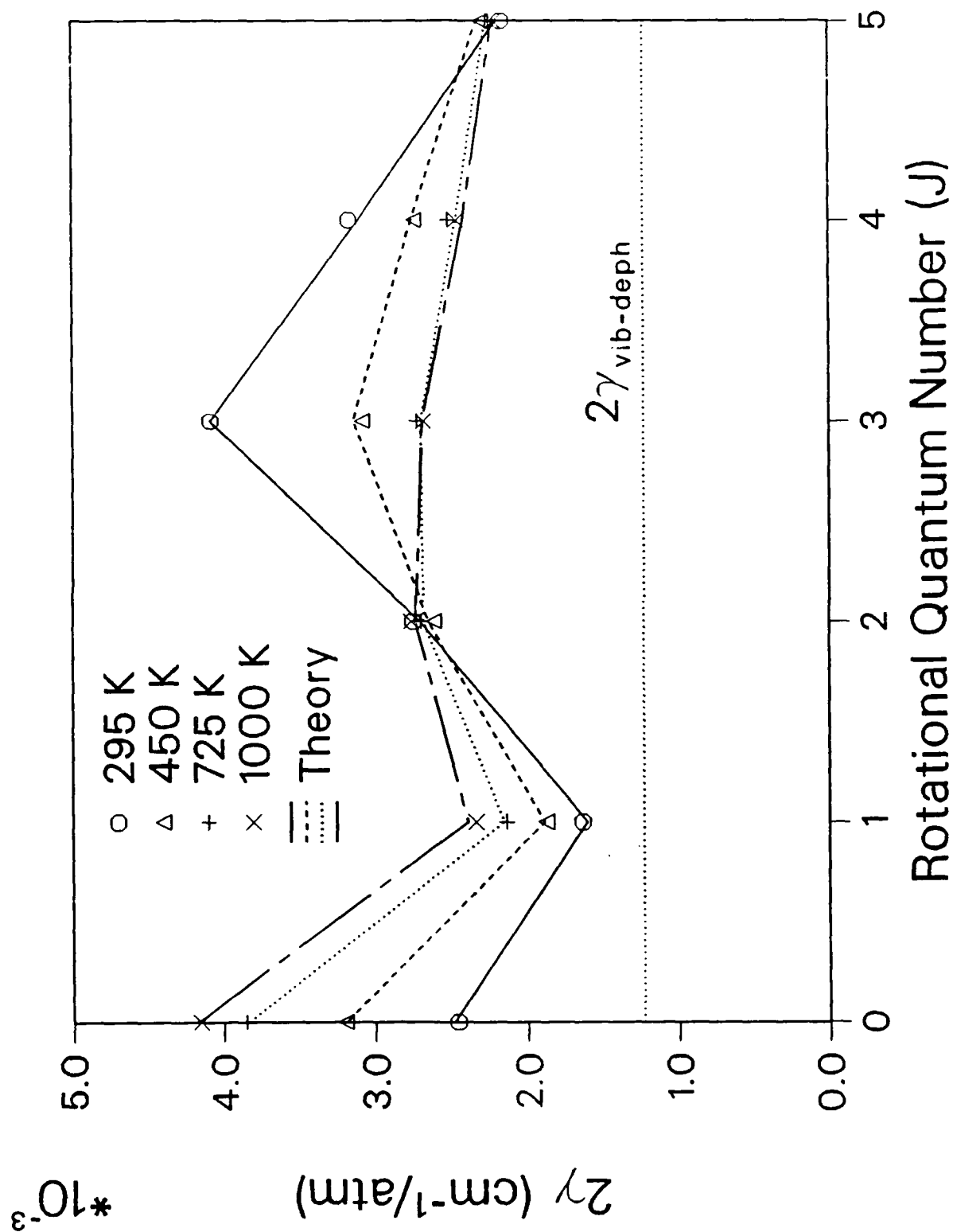
Figure II.6
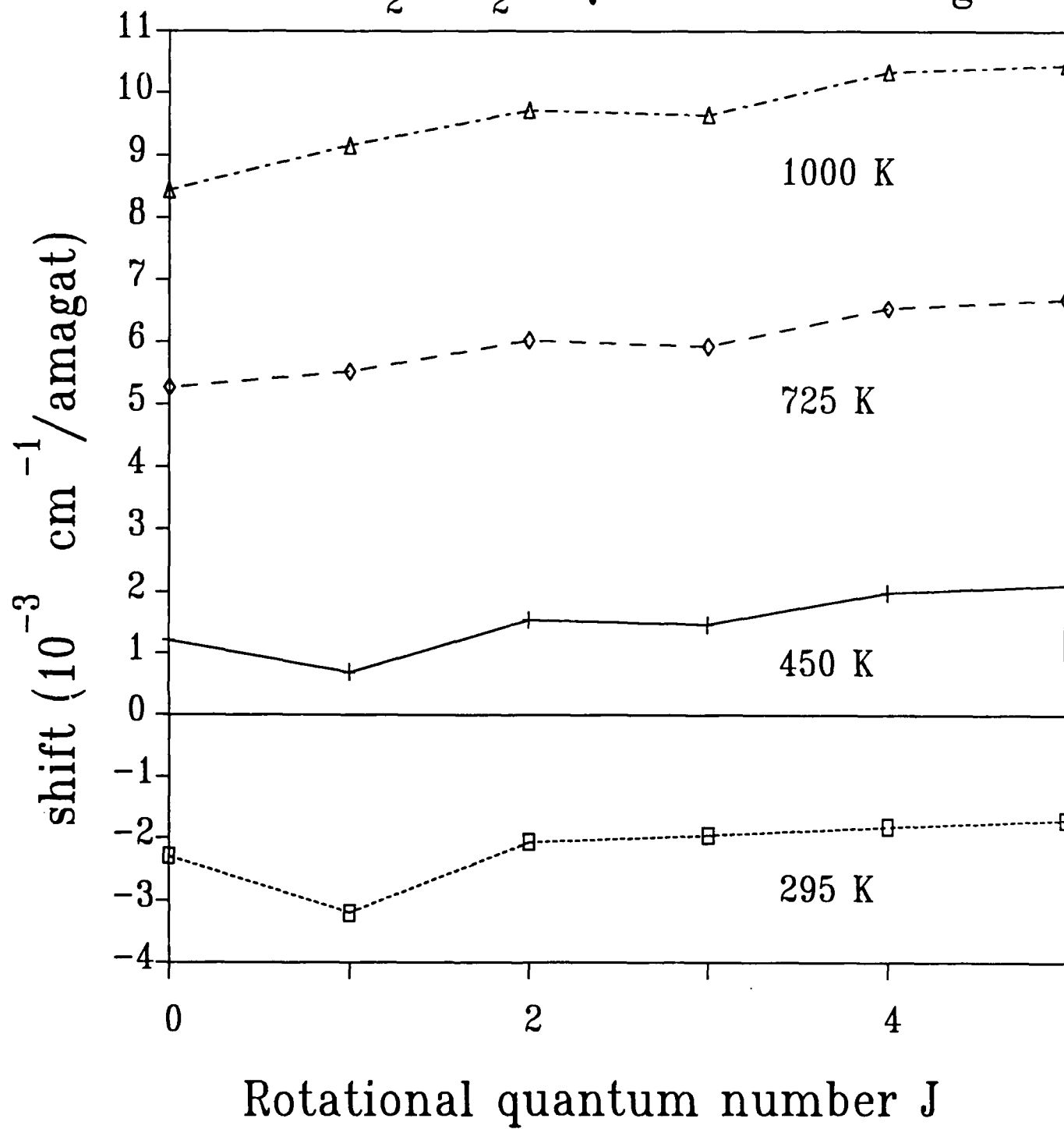
3) SPECTRAL DISTRIBUTIONS

The hydrogen diatomics have long been of interest as systems in which one could accurately test our understanding of the way velocity changing collisions lead to a reduction of Doppler broadening with increasing density, i.e. the well known phenomenon termed Dicke narrowing. The state of this understanding was briefly reviewed in a paper [P1] written as part of the work under this research project. Our subsequent experimental work is summarized in the following.

The D_2:D_2 and D_2:He systems, preliminary results having been reported in Ref. [P2], were extensively studied at room T over a large range of pressures and for both forward and backward scattering. This study (which will be published [M10]) took advantage of the fact that forward and backward scattering geometries simultaneously exist in the multi-pass mirror cell used for the cw-inverse Raman system. (The last mentioned fact explains the shapes of the spectral distributions reported in [P2].) The most important result of this investigation, for the purpose of this project, is that the soft-collision model quantitatively describes all the pressure, scattering wavevector, and J-dependence of these spectra. For completeness we include a short description of this soft-collision model.

This model is a solution to a Fokker-Planck type kinetic equation for the evolution of phase in the presence of both velocity and phase changing collisions. The frequency dependence of the third order susceptibility we use is then

$$\chi \propto \int dt \exp(-i[\omega-\omega_0]t)\exp(-\Gamma t)\exp(\frac{-k^2 v^2}{2T^2}\{Tt-1+\exp(-Tt)\}) \qquad \text{(II.4)}$$

$$\Gamma = \rho\gamma \qquad \text{(II.5)}$$

$$T = \rho\upsilon \qquad \text{(II.6)}$$

$$k = |\mathbf{k_p}-\mathbf{k_s}| \qquad \text{(II.7)}$$

where Γ and T are, respectively, the phase and velocity changing collision rates, ρ is the density, k is the magnitude of the momentum transfer, and v is the most probable speed $=(2k_B T/m)^{1/2}$. In Eq. II.4 ω is the pump-probe frequency difference and the resonance occurs at ω_0. This soft collision lineshape has the proper Gaussian lineshape characteristic of Doppler broadening at very low densities, i.e. T → 0, and at higher densities approaches the Dicke limit. The latter results at densities such that the quantity $\kappa \equiv k^2 v^2/(2T^2) \ll 1$. In this limit the lineshape is Lorentzian with width (HWHM)

$$\Gamma_D = \frac{D_0 k^2}{\rho} + \gamma\rho \qquad \text{(II.8)}$$

with

12

$$D_0 = \frac{v^2}{2\upsilon}$$

(II.9)

the optical diffusion constant. The magnitude of κ determines deviations from the Dicke limit. Increasing κ will give, at lowest order, corrections which cause the lineshape to become slightly sub-Lorentzian, i.e. corrections which will allow the shape to approach the Gaussian, low-density limit. κ depends inversely on the square of the density and directly on the square of the momentum transfer. Variable density, forward and backward scattering allows a careful test of the accuracy of the lineshape function.

An observation, not yet reported in the literature, relevant to the applicability of the soft-collision model to the D_2 lineshape is shown in Fig. II.7. The host gas in this case is Ar, and the principal scattering geometry is backward. The concentration (mole fraction) of D_2 is 50% in this approximately 4 atm room T sample. The experimental spectra and theoretical models displayed in Fig. II.7a show the forward and backward components which make up the observed spectrum and the residual of the fit. The characteristic shape of this residual can be used to infer that the data would be better fit by a complex soft-collision model, cf. [R2]. The complex soft-collision model (in which T, Eq. II.6, is a complex number) results from a solution to the generalized Fokker-Planck equation for the time development of the optical coherence. The result shown in Fig. II.7b indicates the improvement in accuracy provided by this spectral distribution function. The latter form of the lineshape function is expected under conditions where there are correlations between velocity and phase changing collisions. Further evidence for such a correlation is presented below when we discuss anomalous lineshapes in the pressure broadened regime for the D_2:Ar and H_2:Ar systems.

Studies of the T dependence of the lineshapes of the hydrogen diatomics have focussed mainly on the H_2:Ar system; however we have determined the lineshape as a function of P at 1000 K for the self-broadened Q(1) transition of H_2. The results are consistent with the Dicke model, which is the form of the soft-collision model in the density region studied. The lineshape is a symmetric Lorentzian whose half-width is shown in Fig. II.8. The effective diffusion constant in this case is not equal to the mass diffusion value, in sharp contrast to all room T observations on this system, see Ref. [P1]. It is difficult to interpret this result at our current of understanding line formation in the hydrogens, see the following and Appendix B.

Our studies of D_2:Ar and H_2:Ar have revealed previously unknown characteristics of the spectral lineshapes and their dependence on pressure, concentration, and temperature. These are discussed in detail in Appendix B. The essential physics which explains these results has two important aspects. The first involves the fact that for light, optically active molecules in a bath of heavy perturbers the collision energy is strongly correlated with the laboratory speed of the optically active molecule. Since shifting (and broadening) coefficients are functions of the collision energy, we encounter a situation where there potentially is a significant inhomogeneous component in the observed lineshape. This is the source of the asymmetric lineshapes shown in Figs. II.9 and II.10. Under conditions where the collisional dephasing rate is small relative to the speed changing rate, and when the latter rate is of the order of the reciprocal of the

13

D$_2$:Ar [0.5:0.5] Q(1) 3.70 amagat

14

Figure II.7a
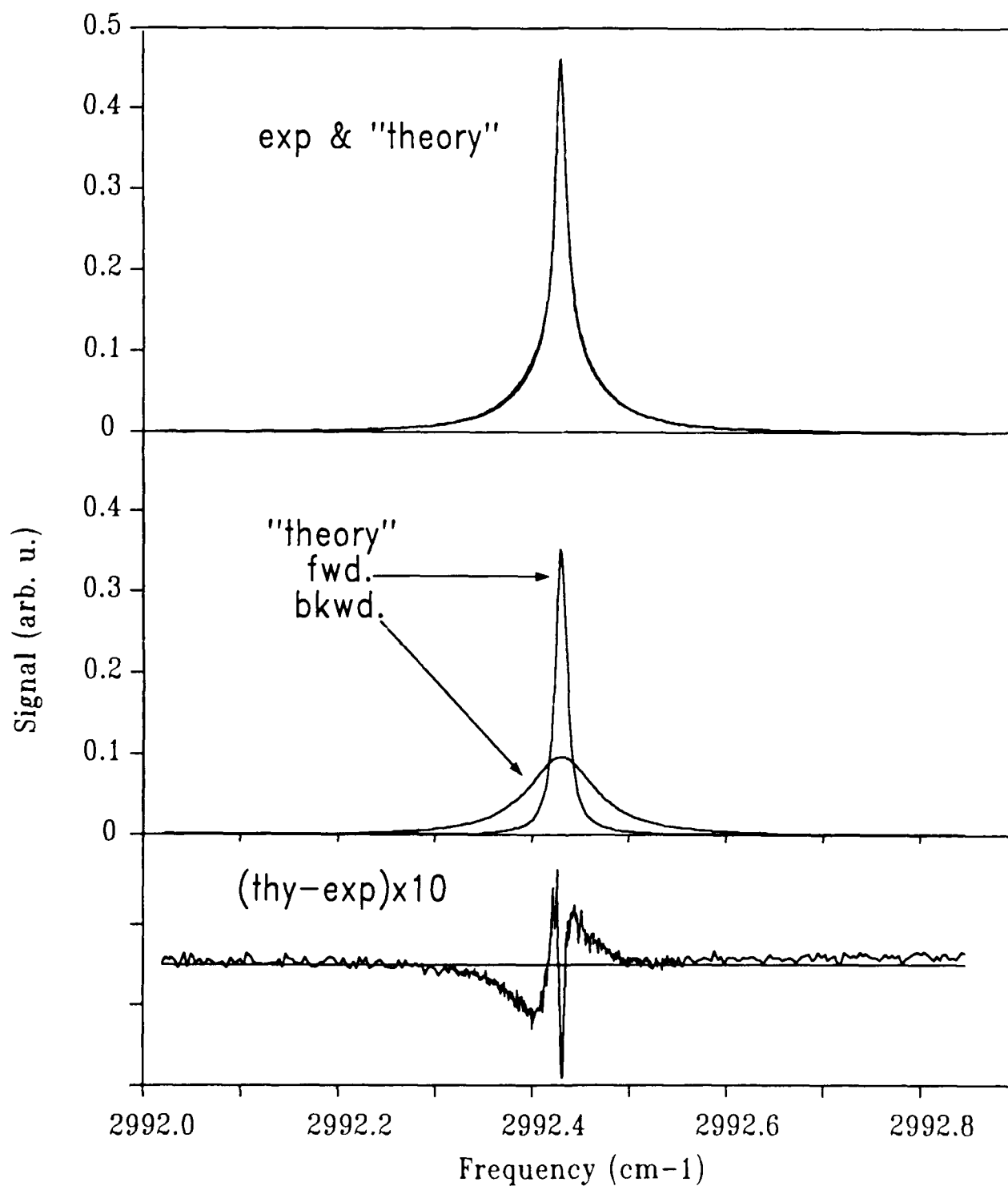
Complex Soft Collision Model
D$_2$:Ar [0.5:0.5]   Q(1)   3.70 amagat

Figure II.7b

H₂ Q₁ at 1000 K

Figure II.8

D$_2$ in Ar; 7.3 Amagat; 297 K

IRS INTENSITY (arbitrary units)

0.1% D$_2$

x2

5% D$_2$

x2

20% D$_2$

x2

2987   2987.2   2987.4

17

Figure II.9

H$_2$ in Ar; 7.3 Amagat; 295 K

2% H$_2$

20% H$_2$

50% H$_2$

IRS Intensity (arbitrary units)

Raman Shift (cm^{-1})

x2

Figure II.10
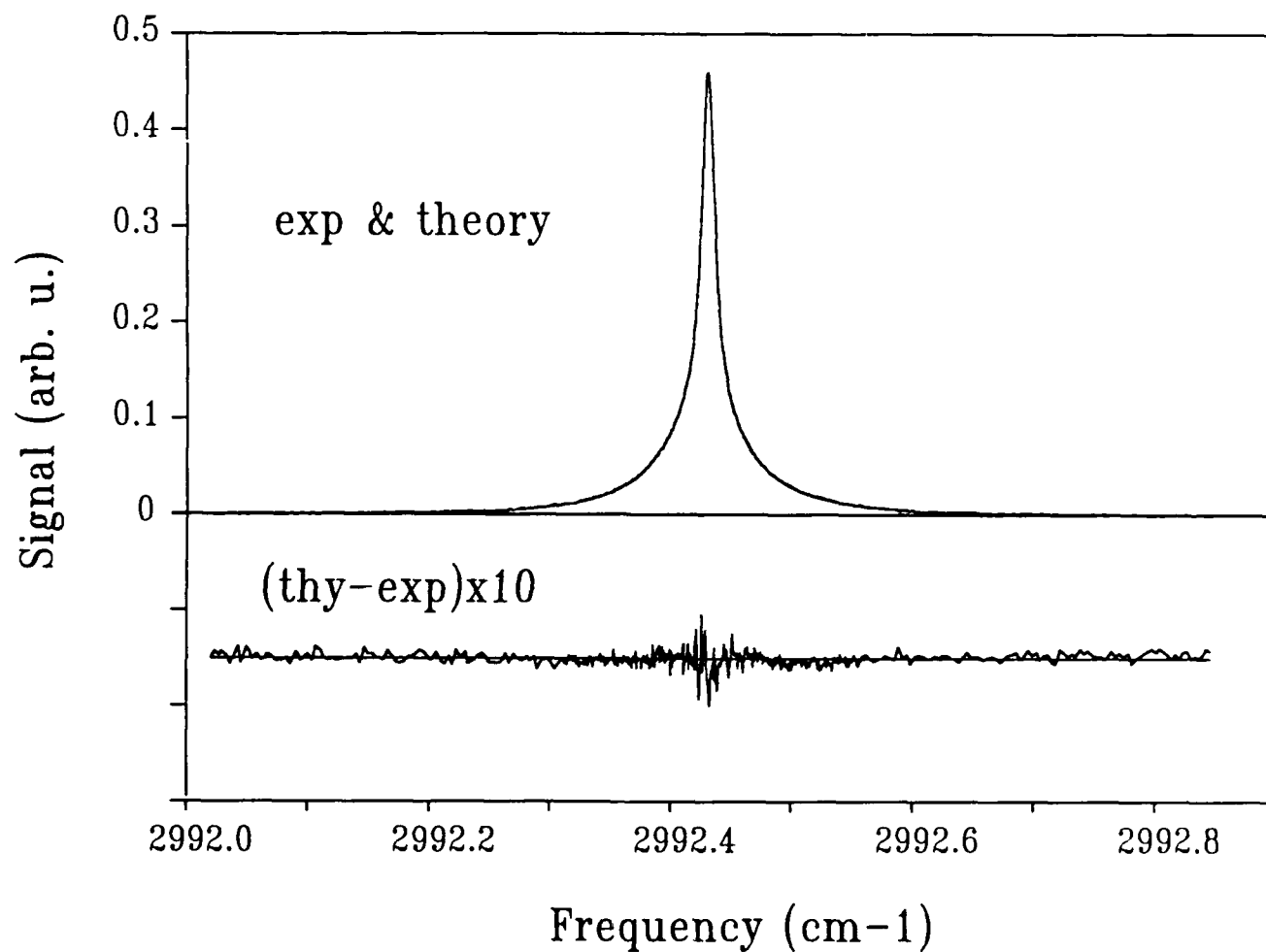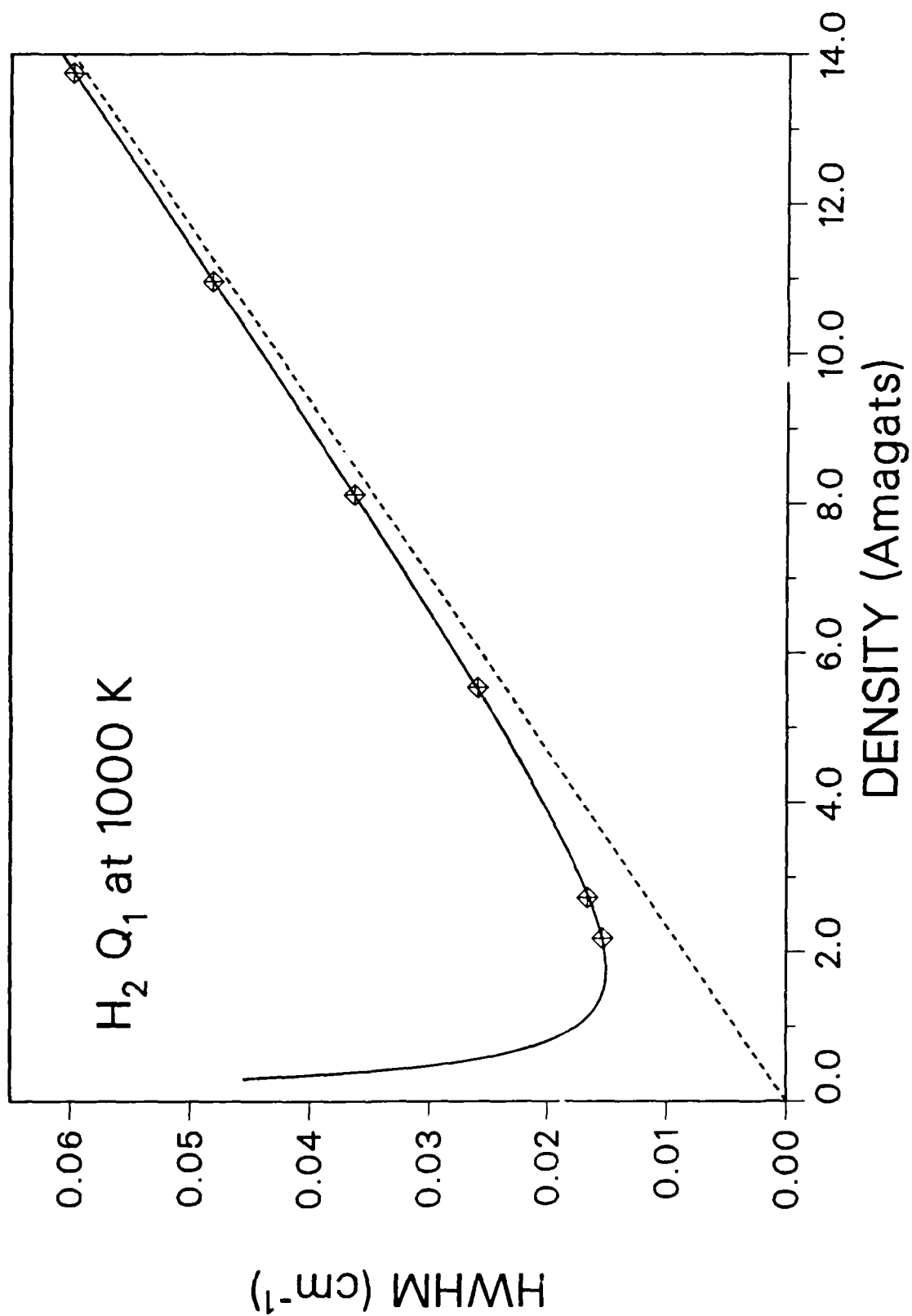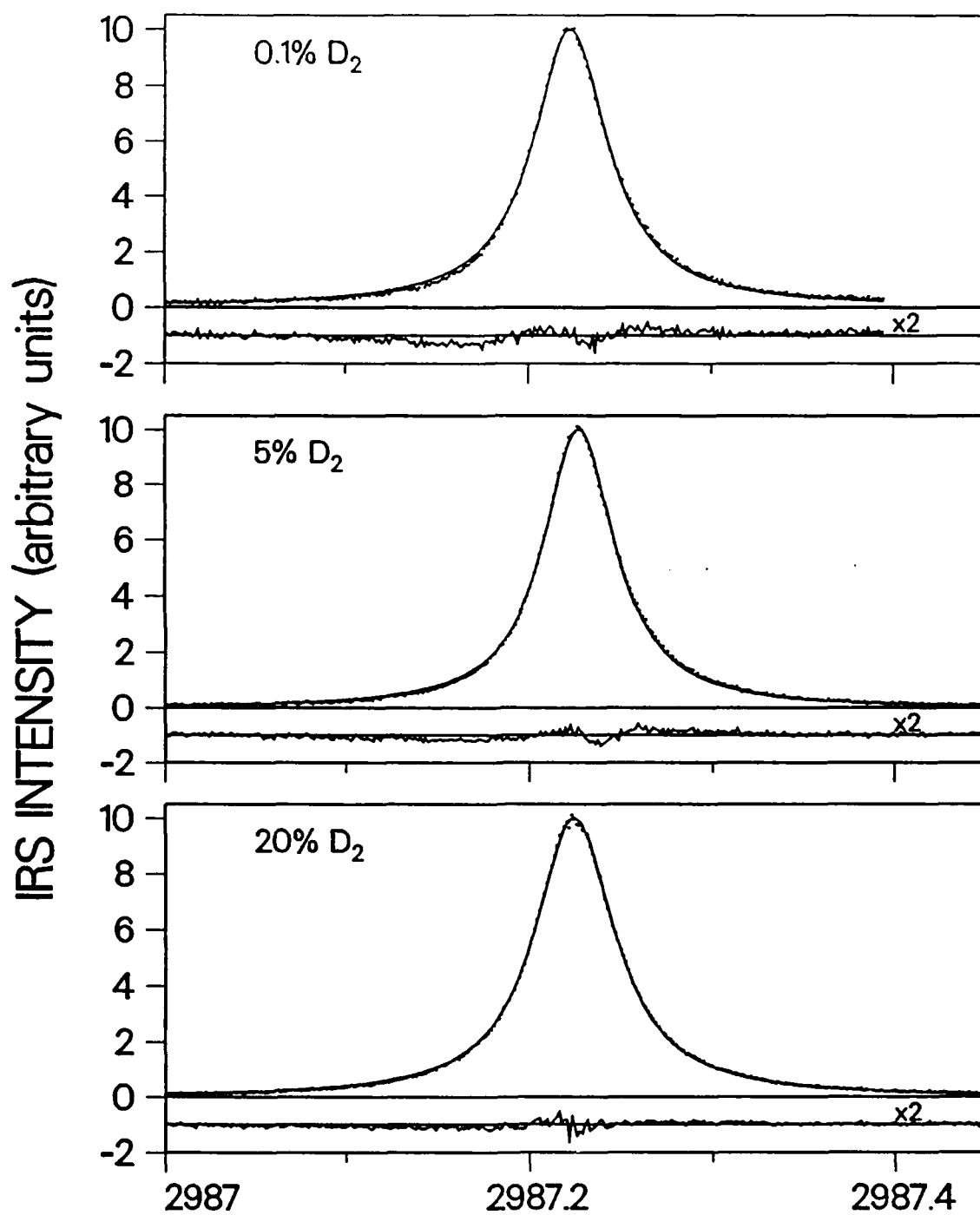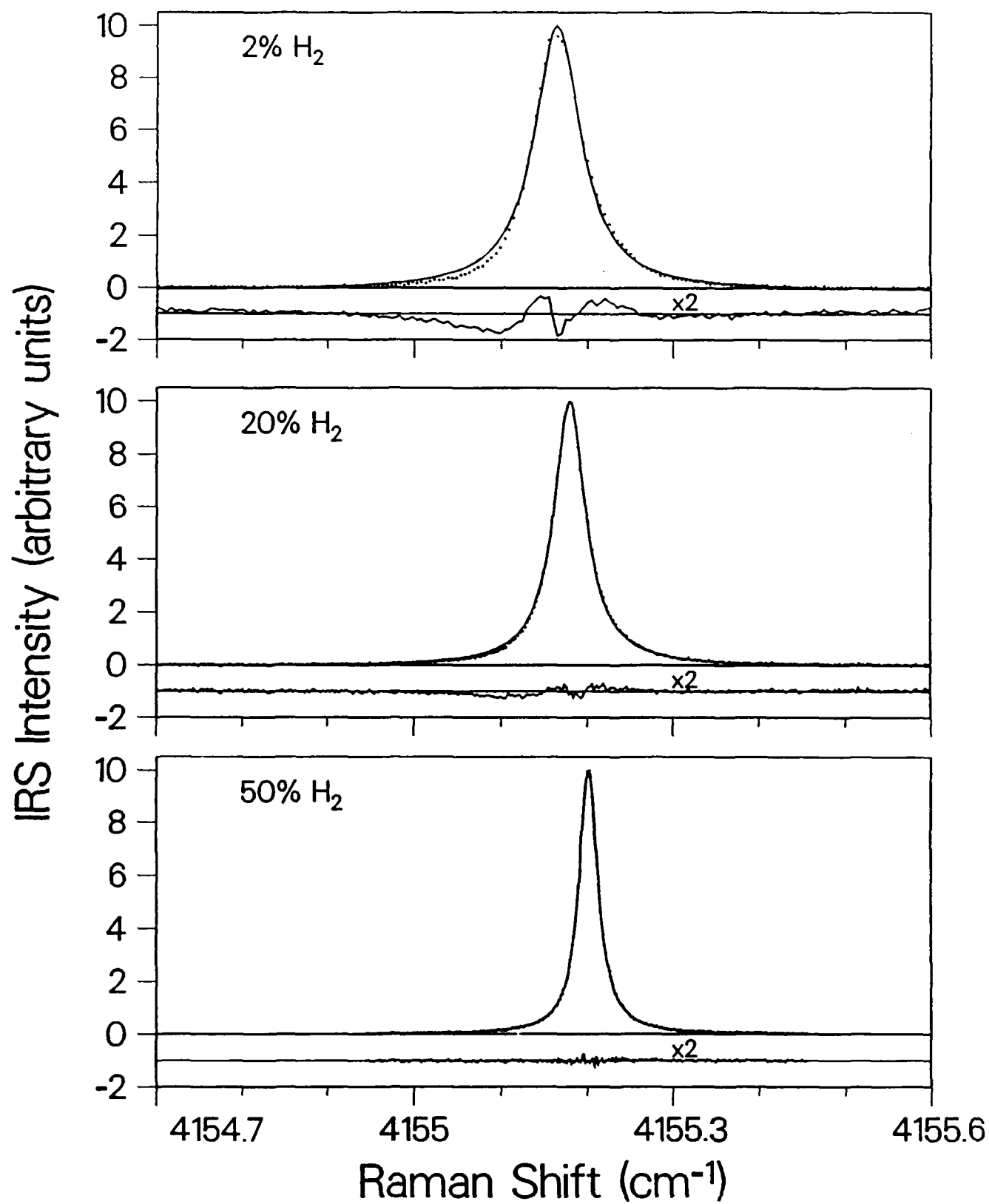
inhomgeneous width, we have the possibility of collisional narrowing of the speed dependent inhomogeneous width, in analogy to Dicke narrowing, discussed above. This second aspect of the process of line formation is evidenced by the concentration dependence of the lineshapes, cf. Figs. II.9 and II.10, and the nonlinear variation of linewidth with concentration shown in Fig. II.11. An analytical model which incorporates the two aspects, discussed above, and which is consistent with a large range of experimental observations on the H_2:Ar system, is described in Appendix B.

H₂ in Ar at 7.3 Amagat, 295 K

Figure II.11
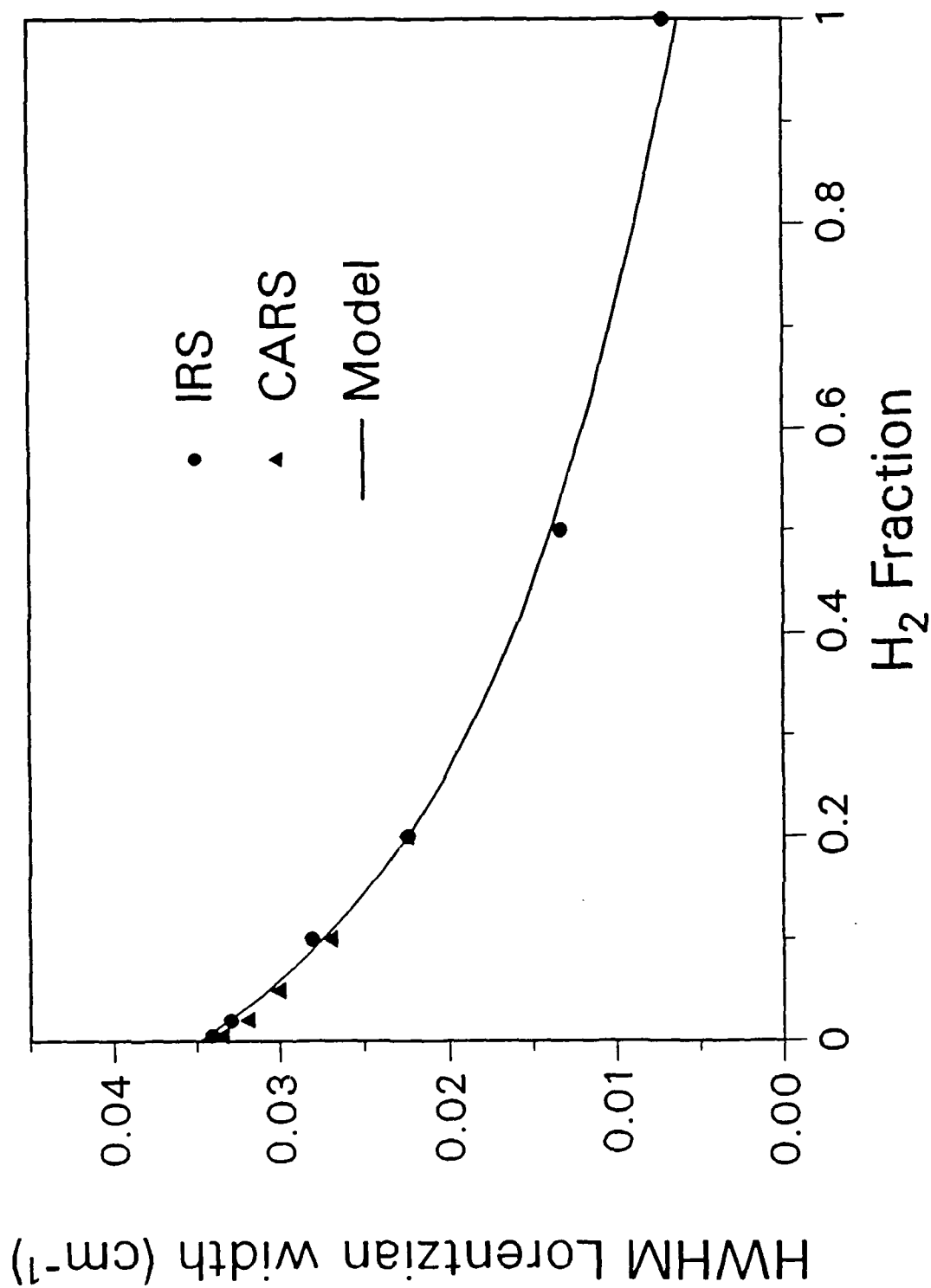
III COMPARISON TO PREDICTIVE EQUATIONS

The state of our knowledge of the Q-branch spectrum is much more highly developed in the case of CO than for the H_2 molecule. In the former case the broadening mechanisms and spectral distribution function are reasonably well understood and the research involves the development of a reliable predictive basis for the fundamental parameters which specify the spectrum. For the diatomic hydrogens there are questions with respect to the fundamental "pressure broadening" mechanisms, e.g. rotational inelasticity versus elastic vibrational dephasing, and with respect to the form of the spectral distribution function, for example, what is the spectral shape in the presence of simultaneous velocity and phase changing collisions? The research reported here (Section II.B.3.b and Appendix B) has revealed another contribution to the H_2 lineshape in the "pressure broadened, impact regime". In this section, we will concentrate on an enumeration of the results of tests of our ability to predict the Q branch spectrum for those cases where the broadening mechanisms and form of the spectral distribution function is reasonably well verified.

A. CO:CO

1) ROOM TEMPERATURE

Although our first studies [P3, P5] of the CO system employed the MEG law, we subsequently expanded consideration to other, well-established rate law models for rotationally inelastic collisions. The details of this work are discussed in Appendix A. A conclusion derived from this work is that the energy corrected sudden scaling law analysis (ECS) of CO [R3], although it gives good account of the J-dependence of the line broadening coefficients, does not properly describe the collapse of the Q branch with increasing pressure at room temperature. In contrast to this result, we also demonstrated that the modified exponential energy gap law (MEG) and the statistical power-exponential energy gap law (SPEG) cannot be distinguished on the basis of agreement with both linewidths and Q-branch collapse. This is surprising in that these two laws fit the data only if radically different assumptions with respect to the propensity for odd delta-J transitions are invoked. In the case of the MEG law, the best fit to the complete data set requires that all delta-J values are allowed with the consequence that more than 50% of the total width must be associated with dipolar (more generally odd multipolar) symmetry forces. The SPEG law on the other hand fits the data set best for the assumption that only even delta-J transitions are allowed. Although the latter selection rule is not required by the symmetry of the CO molecule, the appearance of large rates for odd delta-J transitions does appear to be at variance with the observation that CO is almost homonuclear in its electrical and transport properties. This ambiguity was resolved (in favor of the SPEG law with quadrupolar symmetry forces) by a first principle semi-classical line broadening calculation. This calculation is summarized in Section IV.

The room temperature CO Q branch is now well understood. The subtle differences between the collapsed spectra and the SPEG law based relaxation matrix are at the limit of the uncertainties in our measurement of the Q-branch spectrum. Further experimental verification of the predictions of

theory, summarized above, most likely will result only from direct measurements of state-to-state rates for rotational energy transfer. We now turn to extension of our study of the CO Q branch to elevated temperatures.

2) ABOVE ROOM TEMPERATURE

We presented a reasonably accurate MEG law based parametrization of the J and T dependence of the line broadening coefficients in Section II. In light of the discussion above, it appears that this is a rather "unphysical" description of the Q branch. We persist in the use of the MEG law two reasons. First, the description of the line broadening coefficients is simple and accurate. A similar quality description based on the SPEG law does not appear possible. Second, the description of the Q-branch collapse at elevated temperatures is not significantly improved by use of the SPEG law. Thus, our assessment is that the MEG law, albeit microscopically inaccurate, does provide a remarkably simple, accurate, and useful method of predicting the CO Q-branch spectrum over a large range of T and P.

Judging solely on the basis of the room temperature results we might expect that the SPEG law would be more accurate in the description of the high T Q branch. We have tested this idea by adjusting the SPEG law to agree with the 1050 K line broadening coefficients (calculated from the MEG law of Section II) and then comparing to the experimental data on the Q-branch collapse at $\approx$1050 K. This result is shown in Fig. III.1a. The systematic differences between the SPEG model and the experimental data are quite comparable to those found for the MEG law, cf. Fig. II.3b. We observe that the differences seen in these two figures are characteristic of an underestimate of the degree of collapse. Again, as with the room temperature analysis, the two laws make very different assumptions about the propensity for odd delta-J transitions. In an attempt to better understand these observations, we again turn to the theoretical calculations.

From the calculations, discussed in Section IV, we know that the dipolar symmetry forces make a finite contribution to the total line width at all temperatures. Further, we know from the temperature dependence of either the MEG or SPEG laws that the total inelastic rate spreads over a larger range of delta-J as T increases. Thus, the relative contribution to the collapse of the Q branch from the delta-J=±2 and delta-J=±4 (and higher) transitions decreases with increasing T. This suggests that the small dipolar symmetry component in the inelastic rate may play a more significant role in the collapse of the Q branch at elevated temperatures. To test this idea, we examine the predictions of collapse for the case where we allow approximately 5% of the total linewidth to be associated with delta-J=±1 transitions and readjust the SPEG law (even delta-J) to the experimental linewidths (from the MEG law, less 5%) at 1050 K. Thus, we have a relaxation matrix which has the even delta-J SPEG law symmetry with the addition of nearest-neighbor (delta-J=±1) line interference (from dipolar symmetry forces) and the same total inelastic rate (linewidth) as the MEG and the SPEG discussed previously. The comparison of this "modified SPEG model" to the experimental data is shown in Fig. III.1b. We suggest that the improved agreement displayed in this figure reflects a more physically realistic treatment of the microscopic details of the collapse. It should be noted however that this simple modification of the relaxation matrix is not a highly accurate approximation for the J-dependence of the inelastic contributions of the dipolar symmetry forces.

22

CO:CO 1050 K; 10 atm

SPEG (delta J even)

SPEG (delta J—even) +
|delta J| = 1

Frequency shift (cm^{-1})

Figure III.1
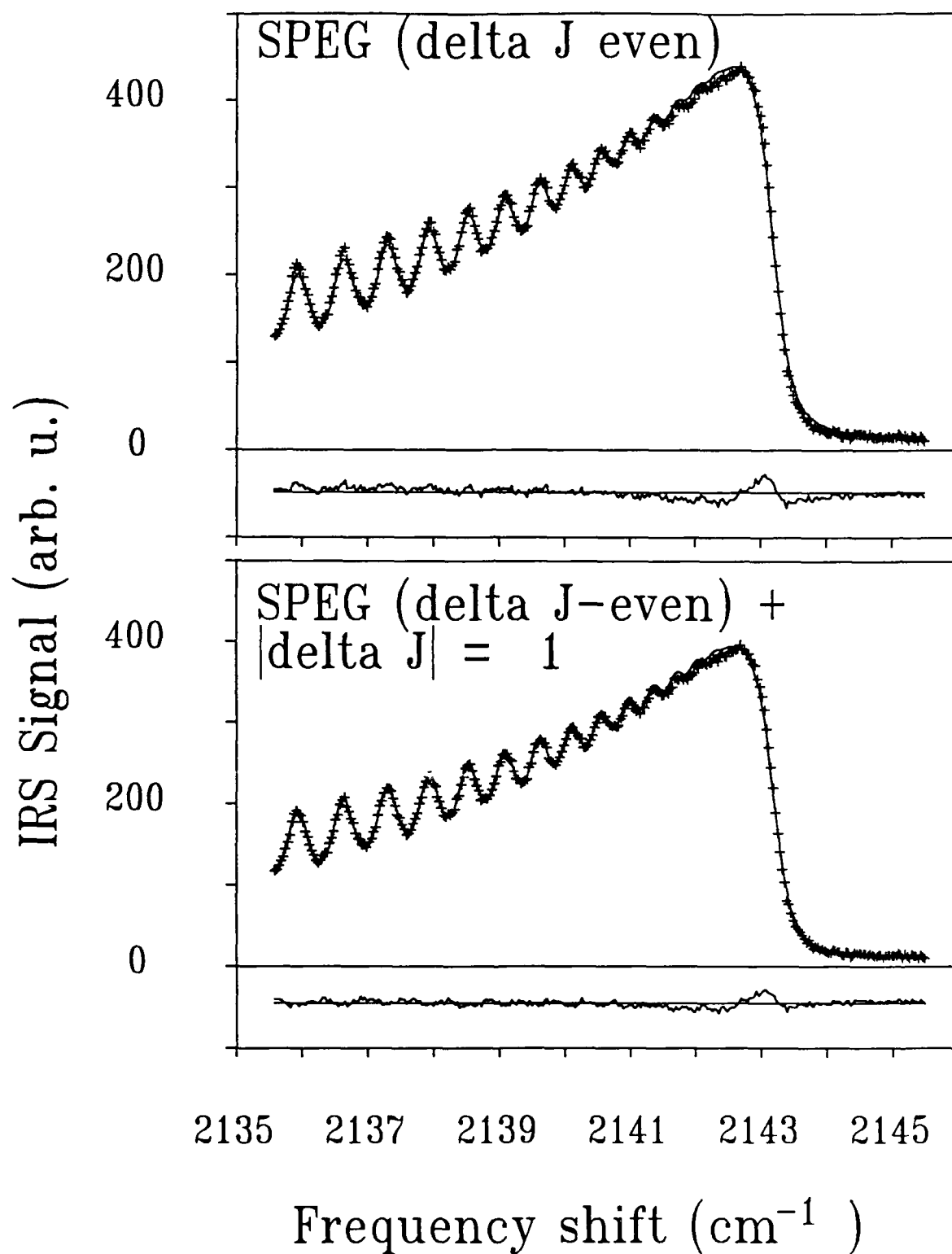
The extension of this analysis to a <u>simple</u>, accurate predictive basis for all temperatures does not appear to be straightforward or particularly valuable in light of the current needs for accurate data. The current status of our understanding of the high temperature Q-branch spectrum of simple diatomics will be the subject of a future publication [M13].

B. DIATOMIC HYDROGEN SYSTEMS

1) ROOM TEMPERATURE

a) LINE BROADENING COEFFICIENTS

We have shown that the MEG law can provide a physically reasonable basis for the description of the J-dependence of line broadening coefficients for the D_2:X system, see Section II and Ref. [P2], and for the HD:HD system [P4]. In both systems, all available linewidth (both infrared and Raman for multiple branches) and inelastic rate data were included in the analysis. Most significant among the results of these analyses was the assignment of a reasonable value for the contribution of (elastic) vibrational dephasing and the identification of a significant vibrational state dependence in the inelastic rates for HD. A similar parametrization, utilizing the MEG law, was made for our measurements of H_2:H_2; however, the form of the law had to be significantly modified (with no clear physical motivation) in order to account for the T-dependence. This has led to a re-examination of the use of rate laws for this system which we will discuss in Section III.B.2.a, below.

b) SPECTRAL DISTRIBUTION

For all the hydrogen diatomics Doppler broadening and Dicke narrowing are important components of the Q-branch spectral distribution function. For the systems H_2:H_2 [P1,R4] and D_2:X (X=D_2, He, H_2) [P2, M10] at room temperature, the soft-collision (Galatry) model [R5, R2] has been shown to quantitatively describe the spectrum with the collisional narrowing parameter determined from the mass diffusion constant. In the case of HD:HD, the large amount of pressure broadening to some extent masks the details of the Dicke narrowing process; however, we were able to quantitatively predict the spectrum with an optical diffusion constant only slightly smaller than the mass diffusion coefficient [P4]. To interpre this observation, it is important to remember that it is the collision controlled diffusion of the optical coherence (created by the applied fields) which we measure spectroscopically, not strictly the diffusion in space of the molecule.

Our studies of D_2 in collision with Ar (see Section II), N_2, and CH_4 and the results for H_2:Ar, discussed in Section II and Appendix B, reveal that we currently have no general predictive basis (for the lineshape or for some of the relevant spectral parameters) for these systems.

2) ABOVE ROOM TEMPERATURE

a) LINE BROADENING COEFFICIENTS

24

As suggested above, it was the J and T-dependence of the line broadening coefficients which motivated a re-examination of rate law models for the $H_2 : H_2$ system. Additional interactions which should be considered in a model for self-broadening of H_2 are the strong role of resonant R-R transfer [R6] and the possibility of resonant (J-dependent) vibrational dephasing [R7] (which plays a strong role in the shifting coefficients, see Section IV).

To explicitly allow for both R-T and R-R rotationally inelastic processes, we have invoked the use of the ECS scaling law (discussed and referenced in Appendix A). Additionally, a J-dependent vibrational dephasing component was considered. The outcome of the analysis [M9] is shown in Figs. II.5 and III.2. The results displayed in these figures are for the case of J-independent vibrational dephasing. The last mentioned model is more consistent with other (pure rotational Raman) linewidth data. This J-independent vibrational dephasing for the room temperature and above data can be reconciled with the observation of resonant vibrational dephasing at low temperature [R7] and is in accord with the previously mentioned analyses of the other hydrogen diatomics.

Although, this ECS based scaling law model is predictive, it is far from simple. It involves the assumption of an exponential gap base-rate for the R-T process and a single base-rate for R-R processes. Each process has a characteristic scaling length and magnitude, and for the R-T process there is an energy gap parameter. It is quite satisfying, to our physical intuition, that the scaling lengths and the energy gap parameters are found to be temperature independent and that the two magnitudes have reasonably simple T-dependent scaling. These results appear to give a physically realistic and reliable description of the J and T-dependence of the line broadening in $H_2 : H_2$.

We observe that modelling the various systems described above required a great deal of information on the specific system (state-to-state rates, multiple spectroscopic branches). When temperature and collision partner dependence are added to the problem, we are forced to conclude that our level of understanding and ability to predict are rather limited at present.

b) SPECTRAL DISTRIBUTION

The study of Dicke narrowing in self-broadened H_2 at 1000 K, discussed in Section II, illustrates our inability to quantitatively predict even this component of the spectrum of the self-broadened hydrogen diatomics. In this case, the optical diffusion constant is found to be larger than the mass diffusion constant. This observation is exactly the inverse of the conclusions of studies of all other systems for which a reasonably complete analysis has been completed. The latter systems give results consistent with our expectation that the optical coherence moves through the gas as fast as an individual molecule. The H_2 result suggests that resonant v-v (vibration to vibration) transfer may play a significant role in enhancing the optical diffusion constant.

The lineshape functions associated with the speed dependence of broadening and shifting extend the need to predict additional "kinetic" coefficients, e.g. speed changing rates, even when we are interested in the normal pressure broadened regime. Currently, there is no predictive basis

H$_2$-H$_2$ ECS Linewidths with Constant Dephasing

(a)
R-T

295 K
450 K
725 K
1000 K

(b)
R-R

2γ (cm^{-1}/atm)

(c)
Pure Dephasing

ROTATIONAL QUANTUM NUMBER (J)

26

Figure III.2
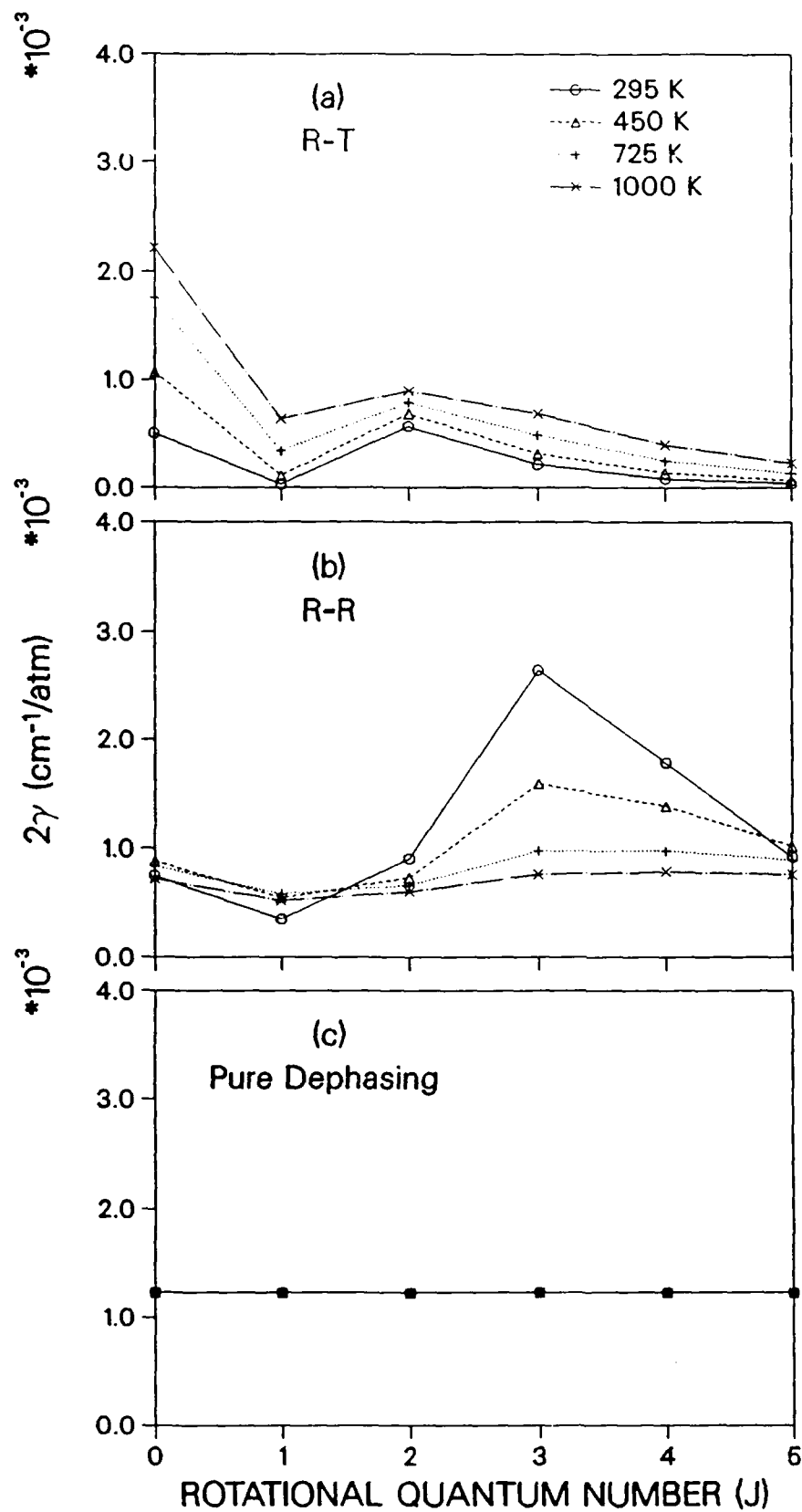
for the complete range of kinetic and line broadening parameters necessary to specify the spectra of the hydrogen diatomics in an arbitrary host gas over an extended range of temperature and pressure.

IV COMPARISONS TO FIRST PRINCIPLE THEORY

The predictive equations discussed in the preceeding section are essentially empirical expressions having physically realistic bases but no simple expression derived from or value determined from first principle theory. In this section we turn to a consideration of the level of our ability to understand and predict the lineshape and its relevant parameters from fundamental theory. Our discussion is limited to a few topics specifically related to the molecular systems of interest in this work.

A. CO:CO

1) LINE BROADENING

It became clear early in our research that we would be well served to initiate a first principle computational study of the CO system to support the measurement program. The motivation involved two primary elements. First, there were insufficient experimental data, for example on state-to-state rates, to allow a critical analysis of rate law models. This situation would become more difficult as we extended measurements above room temperature. Second, the experimental difficulties associated with making accurate spectral measurements under conditions of foreign gas broadening would probably preclude our making substantial new contributions in this area. Reliable theory could then significantly improve our understanding and supply needed data.

Our approach to the calculation of molecular line broadening and shifting was guided by a few simple criteria. First, the theorertical formulation of the problem must result in a manageable computational requirement when applied to moderately heavy diatom-diatom systems. Second, this formulation must be based on intermolecular potentials which have been independently verified as accurate and which can be readily incorporated into the calculational scheme. Finally, the approach must provide line broadening values such that we can test against the wide variety of experimental data available for CO over a temperature range from 100 K to 1500 K. We choose as our theoretical basis the well established Robert and Bonamy [R8] semi-classical formulation of molecular line broadening. The salient features of this formulation are:

(1) through the use of cumulant or linked-cluster expansion techniques, all terms which are bilinear in the anisotropic part of the intermolecular potential are accounted for to infinite order of perturbation theory. This yields a form for the broadening cross section which remains analytic for all impact parameters and therefore avoids the need for any cut-off procedures.

(2) a parabolic trajectory model, based upon the isotropic part of the intermolecular potential, is used to represent collision trajectories near the distance of closest approach.

(3) long range electrostatic forces are accounted for through the use of point multipoles; in the case of CO this involves the dipole (essentially negligible) and quadrupole moments.

(4) the use of a pairwise, site-site Lennard-Jones 6-12 potential to realistically model interactions at short range.

We note that all terms given in Refs. [R8-R11] are explicitly included in these calculations and that the forms for the resonance functions were adapted from [R11]. Relavent molecular interaction parameters are given in Table II of Appendix A. Full details of these calculations will be presented elsewhere [M11].

The results of our calculations are compared in Fig. IV.1a with the experimental results of Nakazawa and Tanaka [R12, R13] for the infrared R-branch. In Fig. IV.1b, the calculations are compared with our experimental data for the Raman Q branch. From these figures, we see that there is excellent agreement between observed and calculated linewidths over a large range of J and T for both infrared and Raman transitions. The temperature range of these calculations involves over an order of magnitude in mean collision energy, thereby probing a large extent of the CO:CO intermolecular potential. It is important to note that this potential is derived from the literature and not adjusted to predict the experimental linewidths.

The quality of the agreement shown in Fig. IV.1 is indicative of the accuracy of the calculational tool developed for this work. Some of the critical features of this tool are the inclusion of all terms in the fourth-order expansion of the atom-atom potential and the use of a very fine grid to evaluate the integrals over impact parameter. We note that the short-range portions of the potential make significant contributions to the total line width in CO:CO and thus this computational approach must provide a reasonably accurate representation of the short-range, anisotropic potential and of the path for close collisions. These observations are analyzed and discussed in more detail in the forthcoming publication [M11].

2) LINE SHIFTING

The isotropic Raman Q branch lines, in contrast to other spectroscopic branches, do not exhibit elastic reorientational phase shifts. Line shifts for these transitions arise from the vibrational state dependence of the isotropic part of the intermolecular potential, and in our analysis we treat this in the lowest order (linear in $V_{interaction}$) of perturbation theory. As described in Appendix A, the isotropic potenial is represented by a Lennard-Jones model. Line shifting is accounted for via a vibrational state dependence of the Lennard-Jones well-depth ϵ. A fractional change, $(\delta\epsilon/\epsilon)=0.55\%$, is found to give agreement with the experimentally determined shifts at 295 K. From the calculation we verify the experimental observation that the shift is very weakly J-dependent (the calculated values vary less than 0.001 cm^{-1}/atm variation from J=0 to J=24). Further, this vibrational dephasing makes less than 0.0005 cm^{-1}/atm contributions to the linewidths. Finally, the calculation predicts a T^{-1} scaling of the shift with temperature. These observations are in agreement with all the experimental results presented in Section II.A.2.

B. DIATOMIC HYDROGEN SYSTEMS

1) LINE BROADENING

(a) Infrared R-branch

(b) Raman Q-branch

Figure IV.1

30
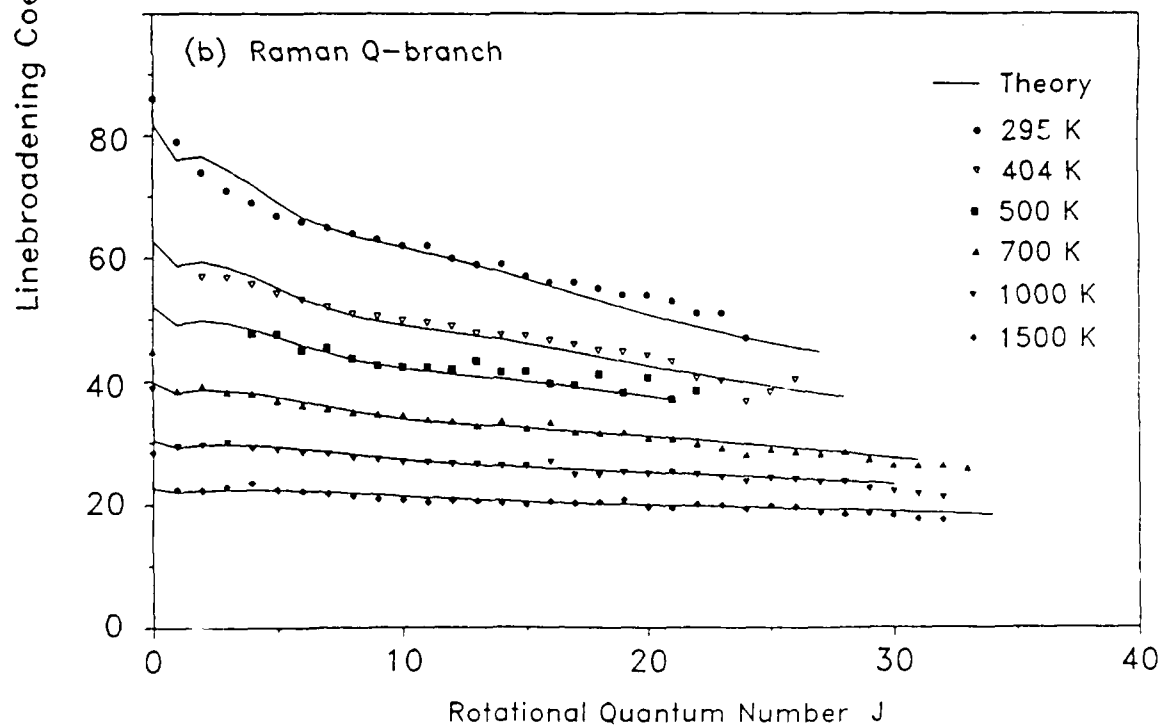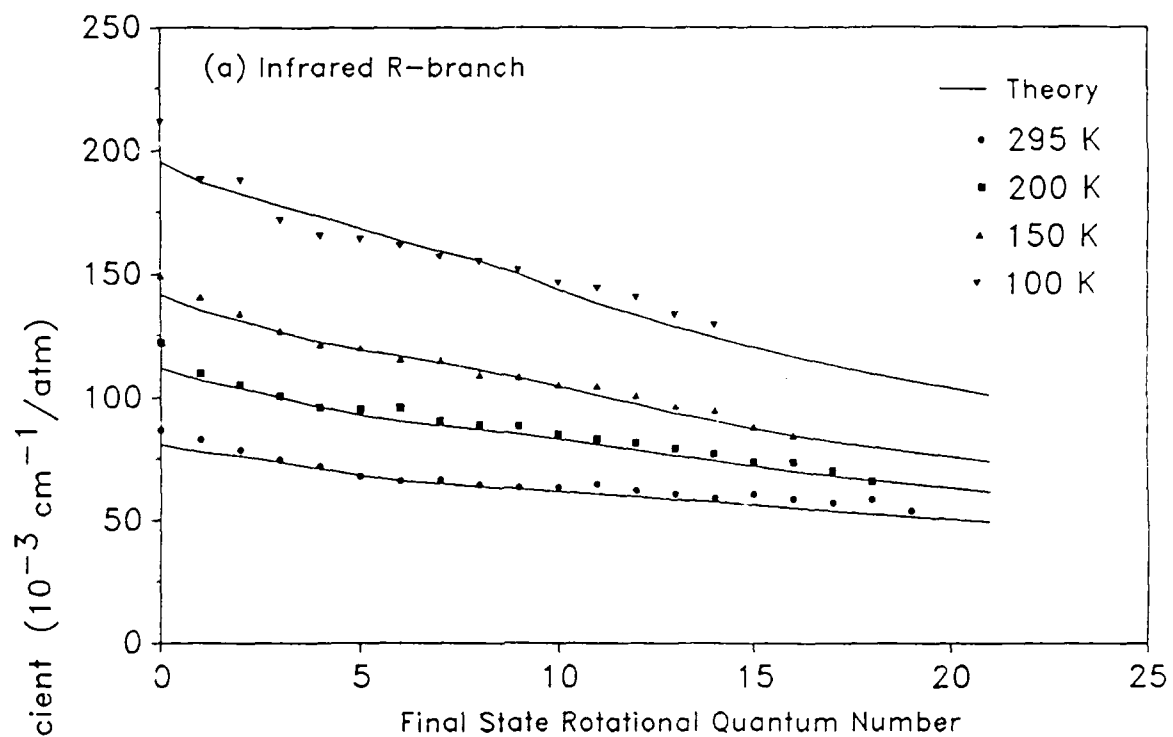
Although the H_2 molecule was the subject of the very first calculation of a Raman Q-branch linewidth [R6], there remain many gaps in our ability to predict line broadening in the hydrogen diatomic systems. We have reviewed much of the theoretical work on these systems and made comparisons to our experimental studies in Refs. [P2] and [P4]. The most complete and successful first principle calculation has recently been made to account for our measurements on D_2:He. The theoretical work grew out of discussions with Dr. Louis Monchick of the Applied Physics Laboratory of The Johns Hopkins University. This work has resulted in three separate publications which include line broadening [R14, R15], line shifting [R15], and the shape of the Dicke-narrowed spectrum [R16].

The calculations of Monchick and co-workers are based on a completely ab initio potential surface, use "standard" (S-matrix based) expressions for the cross-sections, and determine the latter from converged, quantum mechanical, close-coupling scattering calculations. The computational dimensions of this problem are tractable because we are interested in D_2, with only a few populated rotational levels at room temperature, in collision with a monatomic equal mass host.

In their second publication [R15] they provide the following table (we add our vibrational dephasing estimate and slightly change the experimental shifts for J=3 and 4, cf. Table II.1):

Table IV.1
Line broadening and shifting coefficients for D_2:He at 295 K
(units 10^{-3} cm^{-1}/amagat)

| | γ exp't | | γ theory | | | | shift | |
| | | | | inelastic | | | | |
J	total	deph.	total	v=0	v=1	deph.	exp't.	thy.
0	2.35	0.84	2.33	0.73	1.00	0.60	6.1	7.2
1	1.20	0.84	1.11	0.18	0.24	0.69	6.5	7.7
2	1.73	0.84	1.66	0.40	0.54	0.72	6.8	7.7
3	1.62	0.84	1.54	0.34	0.45	0.75	7.6	7.9
4	1.40	0.84	1.29	0.22	0.29	0.78	6.4	8.0
5	1.20	0.84	1.14	0.16	0.23	0.82	---	8.2

The calculated line broadening is in excellent agreement with our experimental results. They identify an elastic vibrational dephasing component which is relatively J-independent and quite commensurate with our estimate. In addition they find a vibrational state dependence to the inelastic rates which we also have identified in our study of HD [P4]. Agreement at this level of detail is very encouraging support for the empirical analyses we have applied to the hydrogen systems, cf. Section III. Although there have been calculations for other H_2:rare-gas systems, the

31

current state of our experimental characterization for these systems does not warrant detailed comparisons.

Turning now to self-broadened H_2, we have added significant new data at elevated temperatures. Unfortunately, there are no calculations which cover this range. At room temperature, the ECS analysis (discussed in Section III.B.2.a) identifies an R-R dominated, inelastic contribution in agreement with the calculation of Van Kranendonk [R6] and a vibrational dephasing contribution to the linewidth in agreement with the calculation of Kelley and Bragg [R17]. The model of the latter study would not predict a J dependence for the vibrational dephasing contribution to the linewidth; however, these authors do predict an almost linear increase in this component as temperature is raised from 295 to 500 K. We note in this regard that the shifting coefficient (which arises from the same interaction as the vibrational dephasing portion of the line broadening) predicted by these authors shows a too rapid increase with T above room temperature, see the discussion below.

2) LINE SHIFTING

The situation with respect to theoretical treatments of line shifting is similar to, but even more limited than, that described above. There is excellent agreement between theory and experiment in the case of D_2:He, cf. Table IV.1. The only other system for which comparison can be made is self-broadened H_2.

The work of Kelley and Bragg [R17] attempted to account for the overall temperature and J dependence of the shifting coefficients displayed in Fig. II.6. To understand the context of their analysis, which stems from the earliest measurements of Q-branch shifting [R18], we replot these data versus the fractional population of the J state in Fig. IV.2. We have added to this plot the previously determined shifts at low temperatures [R19]. The linear-with-population trend observed in these data has been attributed to resonance coupling [R18]. More recently this notion has been incorporated into the impact theory of line broadening by Ben Reuven, cf. Ref. [R20.]. Our data show this effect up to 1000 K. The significant outliers (seen above room T) to the linear-with-population trends in these data are the Q(0) line shift values. What is remarkable in these data is that the coupling shift (determined from the slopes of the straight lines in Fig. IV.2) is essentially temperature independent from 80 to 1000 K, whereas the overall shift, as measured by the zero-population intercepts of the straight lines, changes from strongly negative to strongly positive over this same temperature range. Our current understanding of the H_2:H_2 intermolecular potential, in particular its vibrational state dependence, will not provide a reasonable explanation for either of these observations. This topic will be discussed in some detail in Ref. [M8]. For the present we limit the discussion to the observation that present theory [R17] differs significantly with the overall shift coefficient at elevated temperatures, cf. Fig. IV.3; and thus, we have no reliable predictive basis for either the J or the T dependence of the line shifting coefficients.

3) SPECTRAL DISTRIBUTIONS

Let us begin with the observation that there is no formal, theoretical derivation or justification for the form of the spectral distribution

H$_2$: H$_2$ Q branch shifting

Figure IV.2

33
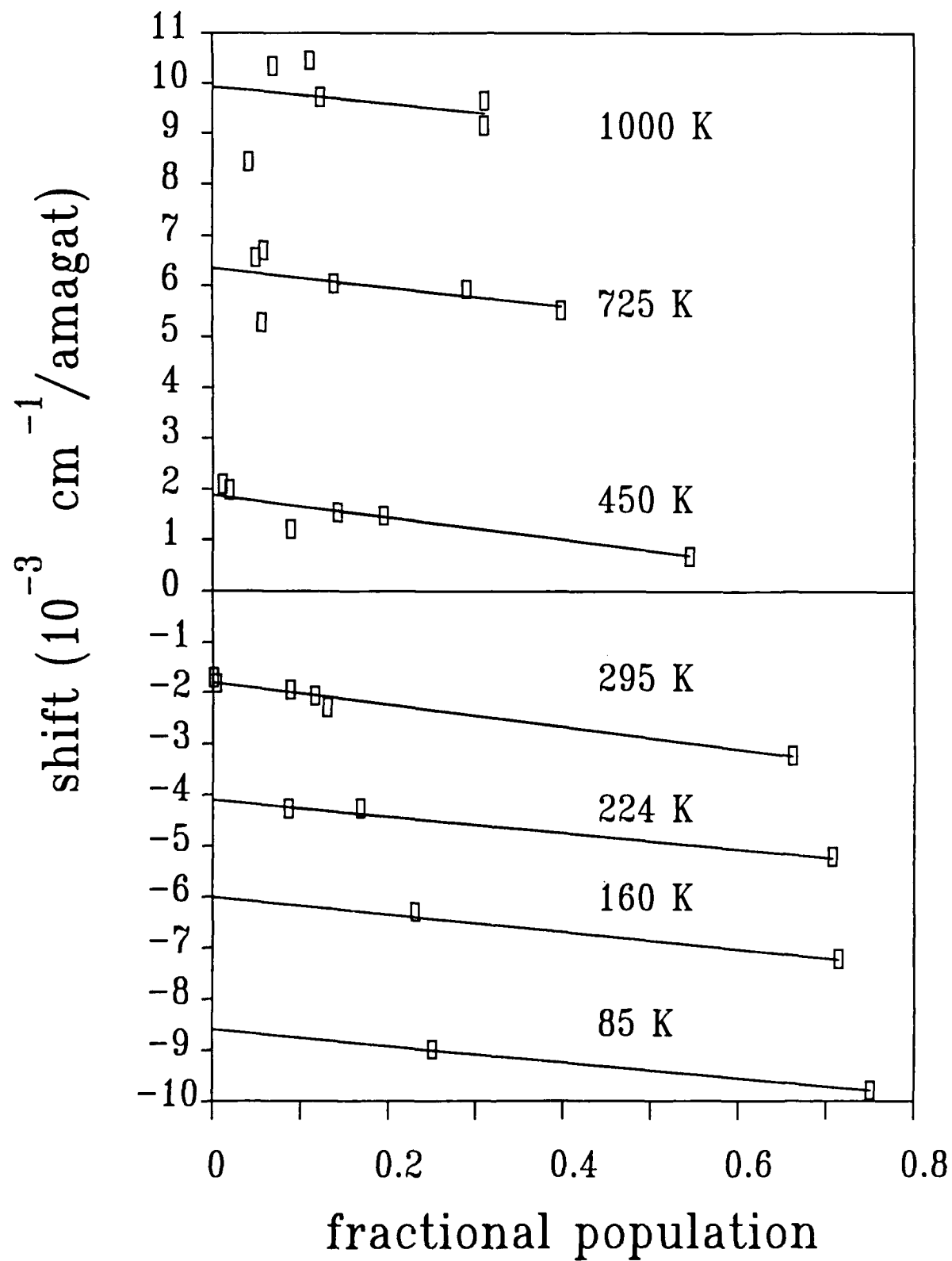
Zero population intercept vs theory (Kelley and Bragg)

Figure IV.3
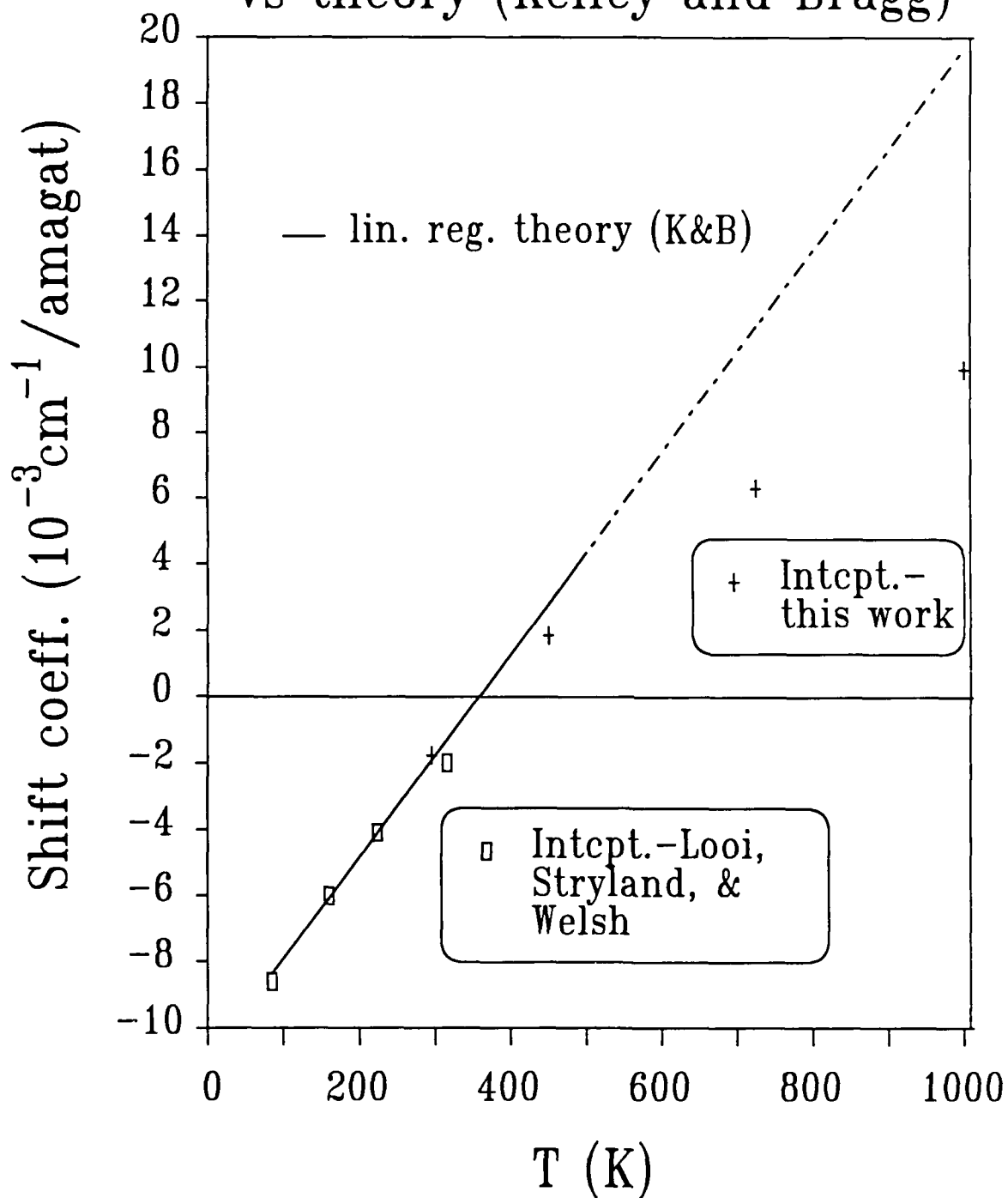
function which we applied to the pressure broadened line shape of the H_2:Ar system. Our approach was phenomenological and derived from argument-by-analogy from the theory of Doppler broadening and Dicke narrowing. This appears as an area which would benefit from a careful theoretical analysis. It is generally true that we still lack a good understanding of spectral line formation when there are correlations among the velocity, speed, or phase changes associated with collisions. Fortunately, the simple kinetic models, applied to this point, do appear to give reasonable account of the observations. We lack a means of predicting the "kinetic" parameters at present, and this is due in part to the lack of a good formal theory.

The quality of our formal theory and a demonstration of its utility for first principle predictions are both evidenced by the theoretical work, discussed in-part above, on D_2:He. The final subject of this work [R16] was the shape of the Q branch in the density regime intermediate to the Doppler and fully pressure-broadened limits. In this work, the authors use recently derived extensions (which explicitly treat spectral line formation) of the Waldmann-Snider kinetic equation. They examine several approximation schemes for solution of the generalized kinetic equations and determine line shape functions in good agreement with our experimental results. As an illustration of this we show in Fig. IV.4 a comparison between the the soft-collision model which we verified (see Section II.B.3) as appropriate for our measurements and the numerically calculated result supplied by Dr. Monchick [R21]. Again, we emphasize that the calculation is based on an ab initio potential, involves generalized kinetic cross-sections which appear in the approximate solutions to the extensions of the Waldmann-Snider equation, and employs S-matrices calculated from close-coupled quantum scattering calculations. We are encouraged by such calculations to suggest that a generally useful basis for understanding and prediction spectra not only is possible but soon will be realized in fact.

Q(1) D$_2$:He

Figure IV.4
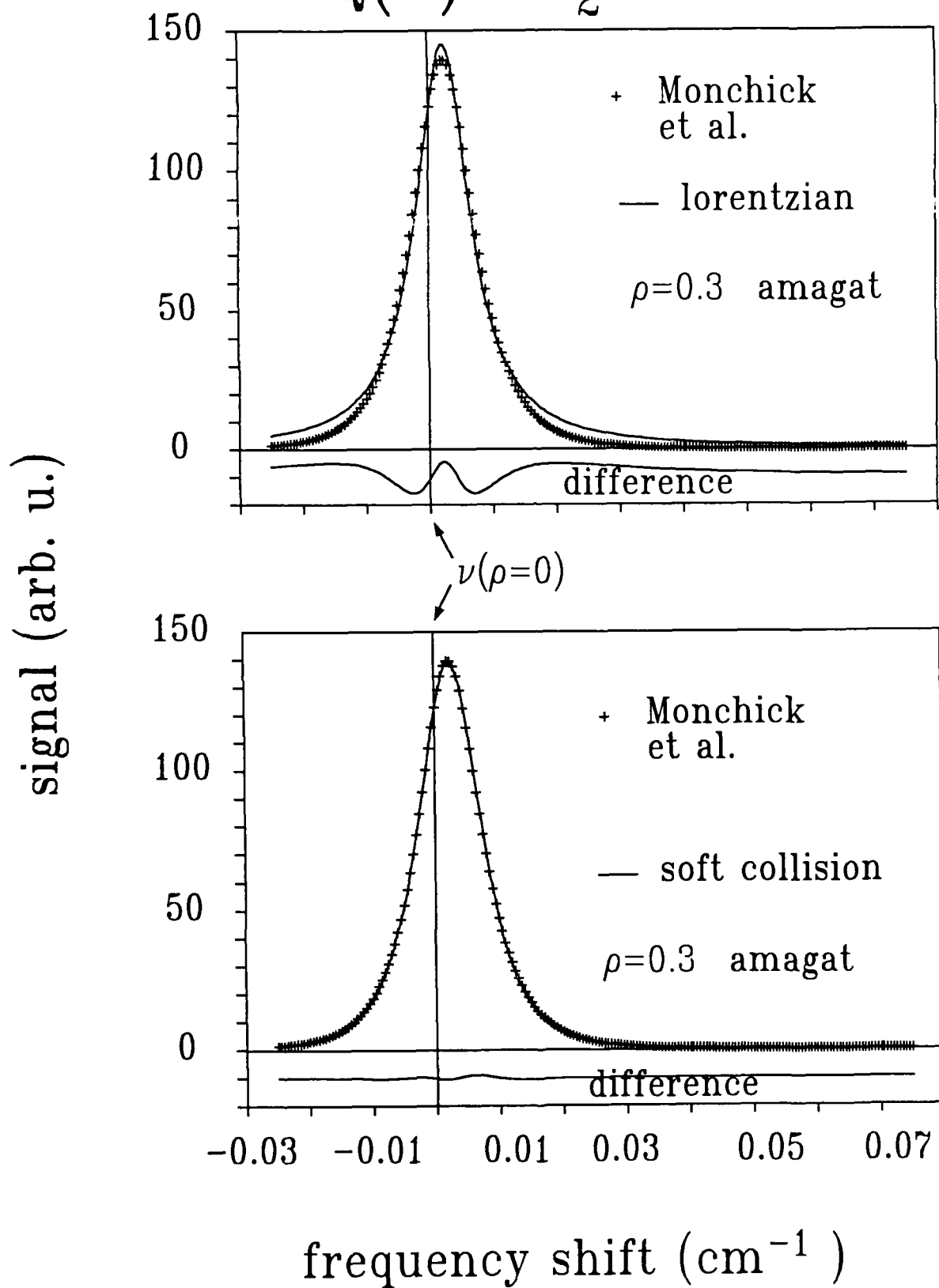
V THEORETICAL PREDICTION OF LINE BROADENING FOR CO:N$_2$

The theoretical/computational development, described in the preceeding section, provides a powerful tool for the prediction of line broadening for simple diatomic systems. In particular, there is a great deal of interest, for example on the part of the combustion research community, in the prediction of Q-branch spectra for the CO molecule in a N$_2$ host.

To address this problem, the collision partner in the previous calculation is replaced by N$_2$ using the parameters contained in Table V.1. These values supplement the CO values given in Appendix A, Table 2.

Table V.1

N$_2$ and N$_2$:CO Potential Parameters for Line Broadening Calculations[a].

Quantity	Value	Ref.
μ $(10^{-30}$ C m)	0.00	
Q $(10^{-40}$ C m^2)	-4.67	[R22]
ϵ_{n-n} $(10^{-22}$ J)	5.03	[R23]
σ_{n-n} $(10^{-11}$ m)	3.32	[R23]
ϵ_{c-n} $(10^{-22}$ J)	5.96	[R24]
σ_{c-n} $(10^{-11}$ m)	3.335	[R24]
ϵ_{o-n} $(10^{-22}$ J)	4.72	[R24]
σ_{o-n} $(10^{-11}$ m)	3.235	[R24]
l_{n-n} $(10^{-11}$ m)	1.098	[R25]
ϵ_{iso} $(10^{-22}$ J)	13.0	[R26]
σ_{iso} $(10^{-11}$ m)	3.75	[R26]

---

[a]Intermolecular potential parameters given here
are related to the potential parameters of Refs [R8-R10] through
$4\epsilon_{\alpha\beta}$ $(\sigma_{\alpha\beta})^6 = e_{\alpha\beta}$; $4\epsilon_{\alpha\beta}$ $(\sigma_{\alpha\beta})^{12} = d_{\alpha\beta}$ and $|r_{1n}| + |r_{1n}| = l_{n-n}$.

On the basis of our experience with self-broadened CO and N$_2$ [M11], we estimate the inaccuracy of the calculated line broadening to be of the order of 5%. The comparison, displayed in Fig. V.1a, with the experimental infrared data of Refs. [R12, R13] shows an excellent level of agreement. The

CO:N$_2$ R-BRANCH LINEWIDTHS
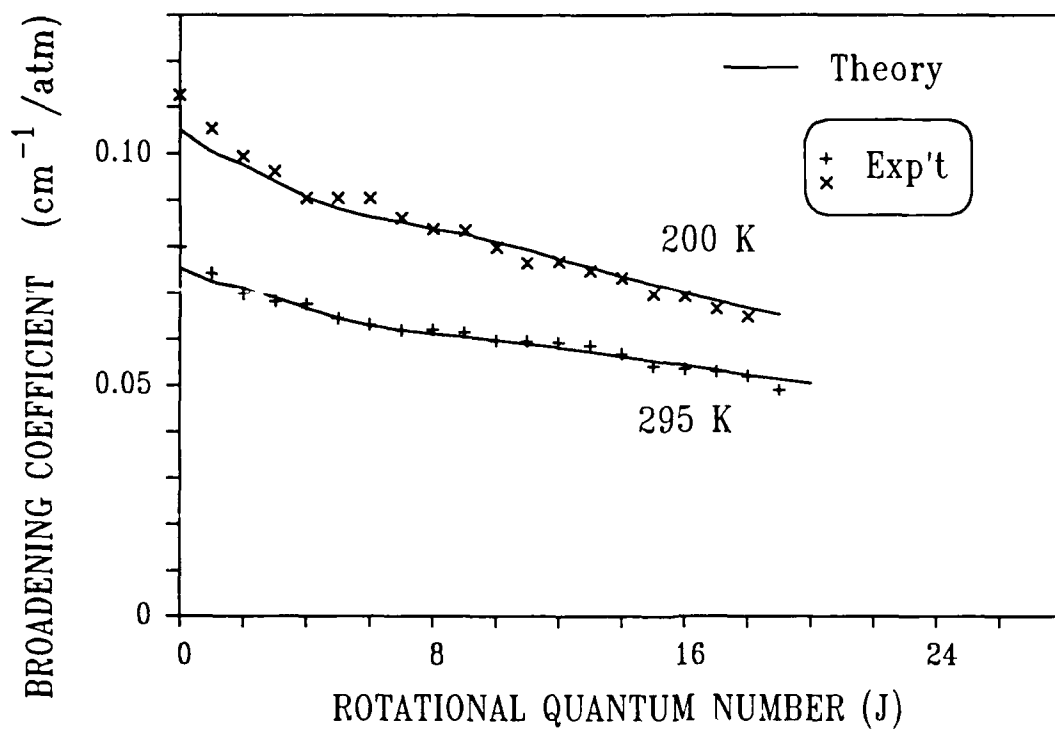
CO:N$_2$ Q-BRANCH LINEWIDTHS

Figure V.1
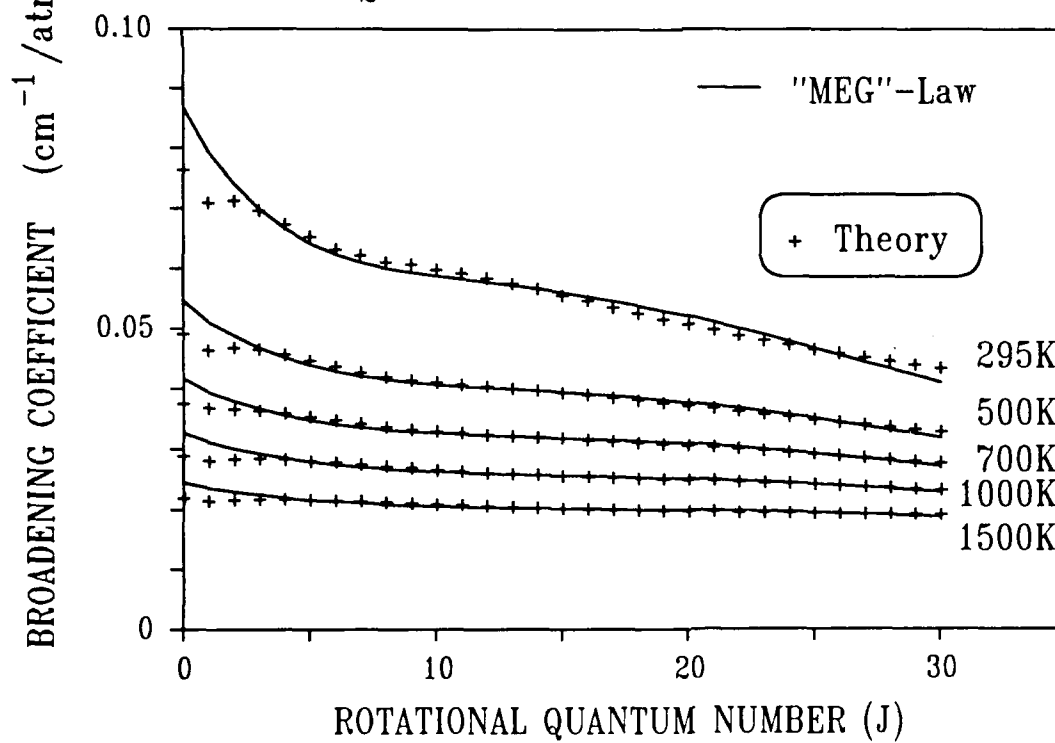
calculated values of the Q-branch line broadening as functions of J and T are listed in Table V.2.

Table V.2

$CO:N_2$ Q-branch line broadening coefficients (cm^{-1}/atm)[a]

J	295 K	500 K	700 K	1000 K	1500 K
0	0.07631	0.04902	0.03747	0.02883	0.02179
1	0.07086	0.04638	0.03673	0.02796	0.02129
2	0.07124	0.04686	0.03659	0.02825	0.02152
3	0.06962	0.04652	0.03634	0.02830	0.02158
4	0.06729	0.04570	0.03590	0.02820	0.02157
5	0.06531	0.04474	0.03536	0.02799	0.02151
6	0.06318	0.04368	0.03477	0.02773	0.02140
7	0.06219	0.04278	0.03419	0.02742	0.02128
8	0.06108	0.04202	0.03368	0.02709	0.02113
9	0.06059	0.04148	0.03326	0.02677	0.02097
10	0.05981	0.04104	0.03292	0.02648	0.02081
11	0.05918	0.04070	0.03264	0.02623	0.02065
12	0.05839	0.04039	0.03241	0.02602	0.02049
13	0.05749	0.04007	0.03220	0.02584	0.02036
14	0.05664	0.03975	0.03199	0.02568	0.02023
15	0.05557	0.03938	0.03178	0.02554	0.02012
16	0.05467	0.03902	0.03157	0.02540	0.02001
17	0.05357	0.03859	0.03137	0.02527	0.01992
18	0.05266	0.03818	0.03114	0.02514	0.01983
19	0.05161	0.03772	0.03089	0.02501	0.01975
20	0.05073	0.03728	0.03063	0.02487	0.01967
21	0.04977	0.03680	0.03036	0.02472	0.01959
22	0.04895	0.03634	0.03009	0.02457	0.01950
23	0.04810	0.03587	0.02980	0.02441	0.01942
24	0.04735	0.03541	0.02951	0.02425	0.01938
25	0.04660	0.03496	0.02922	0.02408	0.01933
26	0.04591	0.03452	0.02892	0.02391	0.01928
27	0.04524	0.03409	0.02863	0.02373	0.01923
28	0.04461	0.03368	0.02834	0.02355	0.01918
29	0.04401	0.03329	0.02806	0.02337	0.01913
30	0.04342	0.03291	0.02778	0.02319	0.01908

[a] the five significant figures represent only the numerical precision of the calculation; the values are considered accurate at the 5% level

These values are presented in Fig. V.1b along with a "MEG" law (no restriction on delta-J) description based on Eqs. II.1 and II.2 with the following parameters:

$$A = 1.75 \tag{V.1}$$

$$\alpha(T_0) = 0.01204; \quad (T_0 = 300 \text{ K}) \tag{V.2}$$

$$m = 0.204; \quad (T_0 = 300 \text{ K}) \tag{V.3}$$

$$\beta(T) = \{ 2 - 0.5131(1000/T)^{0.3} \} \tag{V.4}$$

$$\delta(T) = \{ 1 + 0.18(1000/T)^{0.75} \} \tag{V.5}$$

The value of A is assigned on the basis of the average of the N_2 and CO values. We use the temperature dependent forms for β and δ in order to give a reasonably accurate representation of the calculated Q-branch linewidths over the complete range of J and T. This calculation will be the subject of a forthcoming publication [M12].

VI   SENSITIVITY ANALYSIS

In this section we will summarize selected results from a study [M14] of the accuracy which can be achieved in the determination of T and P from a single-shot, multi-channel CARS spectrum.   The widely used, well studied N_2 vibrational (v=0 → v=1) Q-branch spectrum is selected as the basis for this analysis.   The approach is to generate (via computer calculations) a set of "data" for self-broadened N_2 for values of T and P over the range 295-1500 K and 1-100 atm.   We select the 9 combinations of 295, 1000, and 1500 K and 1, 10, 100 atm as our "known" set of T_0 and P_0 .   The spectral data are determined from the best, currently available description of the N_2 Q branch [R27, R28], i.e. a modified exponential gap (MEG) rate law [R29] for the state-to-state rates for rotationally inelastic collisions combined with the relaxation matrix formalism for describing the CARS Q-branch spectral distribution function.   To more closely model diagnostic spectra, the CARS spectral distribution also is calculated for finite spectrometer resolutions (0.5 cm^{-1} and 2.0 cm^{-1} Gaussian convolutions).   The three "data" sets (infinite resolution, 0.5 cm^{-1} and 2.0 cm^{-1} convolutions) are shown (as the symbols, which may appear as heavy solid lines) in Figs. VI.1-3.

An estimate of the uncertainty limits, "noise-band", found in the measurement of a single-shot, multi-channel spectrum is derived from a number of literature sources [R30-R36].   Since a wide-variety of noise sources have been considered in the referenced studies, we make an operational definition (consistent with the literature) that the frequency dependent noise-band, $\Delta I(\omega)$, is given by

$$\Delta I(\omega) = \pm \sqrt{(\sigma^2 + (\kappa I(\omega))^2)} \qquad\qquad (VI.1)$$

with $I(\omega)$ the CARS spectral intensity in "counts".   In this expression, we ignore the shot-noise (proportional to the $\sqrt{I(\omega)}$) because it is usually of the order of the noise-proportional-signal component only at the 1%-of-I_{max} level in the spectrum.   We eliminate consideration of these low intensity regions of the experimental spectra by setting an effective reading-noise limit σ of

$$\sigma = 2\% \ I_{max} \qquad\qquad (VI.2)$$

The noise proportional-to-signal component is set at the $\kappa=7.5\%$ level; a reasonably typical value for diagnostic spectroscopic systems.   This representation of the uncertainty limits is appropriate to broadband-Stokes laser and single-mode Raman-pump laser configurations.

In order to estimate uncertainty limits we choose as our error criterion the condition that no point in the "fit" spectrum differ from the "data" by an amount greater than the error band defined in Eq. (VI.1).   This condition is illustrated in Fig. VI.4.   We find the uncertainty limits by searching P,T-space around the "known" P_0 and T_0 to locate the points at which the error condition is violated.   At each search point the overall amplitude of the spectrum is adjusted to minimize the weighted (Eq. (VI.1))

N₂ MEG law; no convolution

42
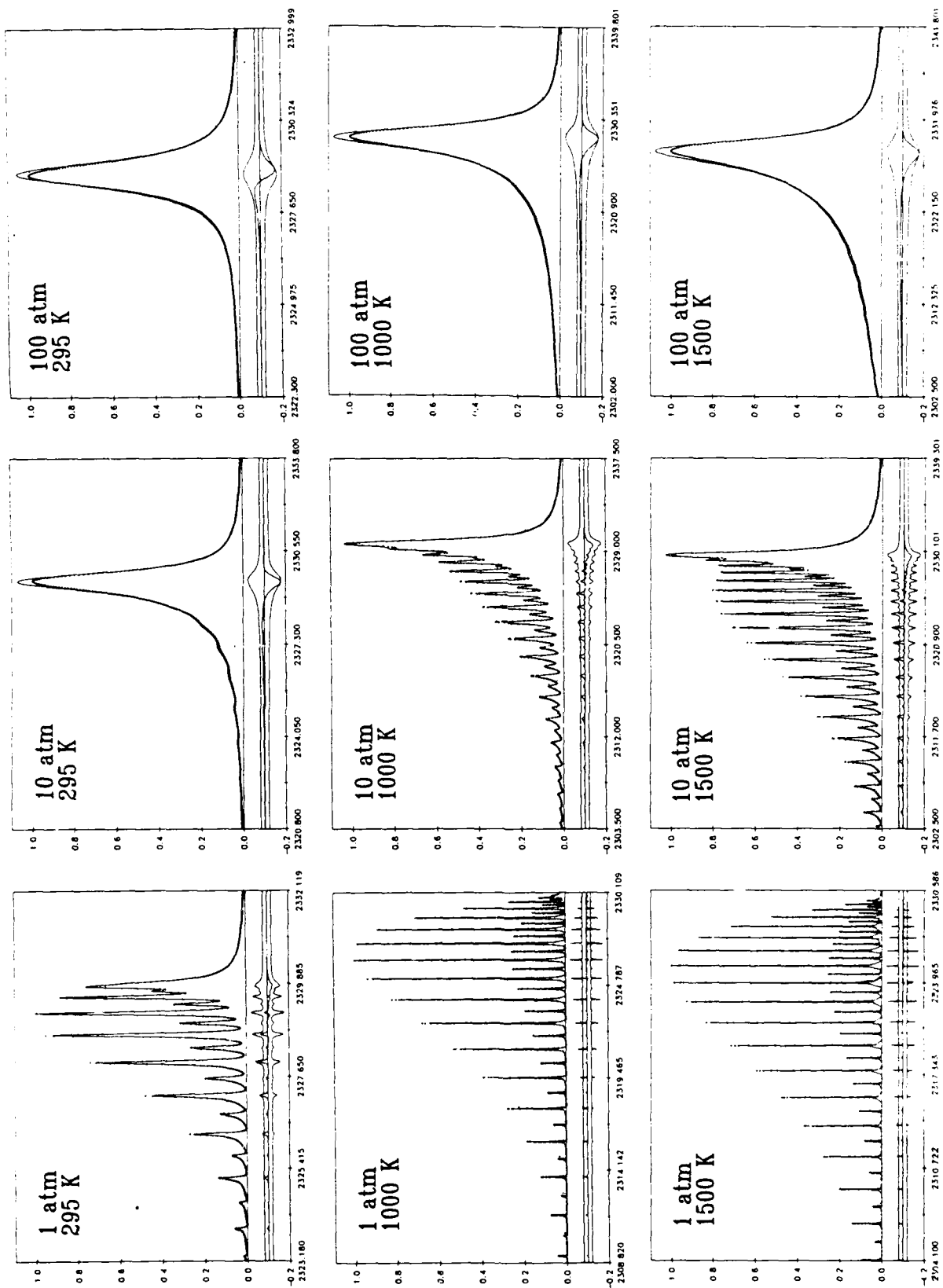
Figure VI.1

N₂ MEG law; 0.5 cm⁻¹ convolution

43
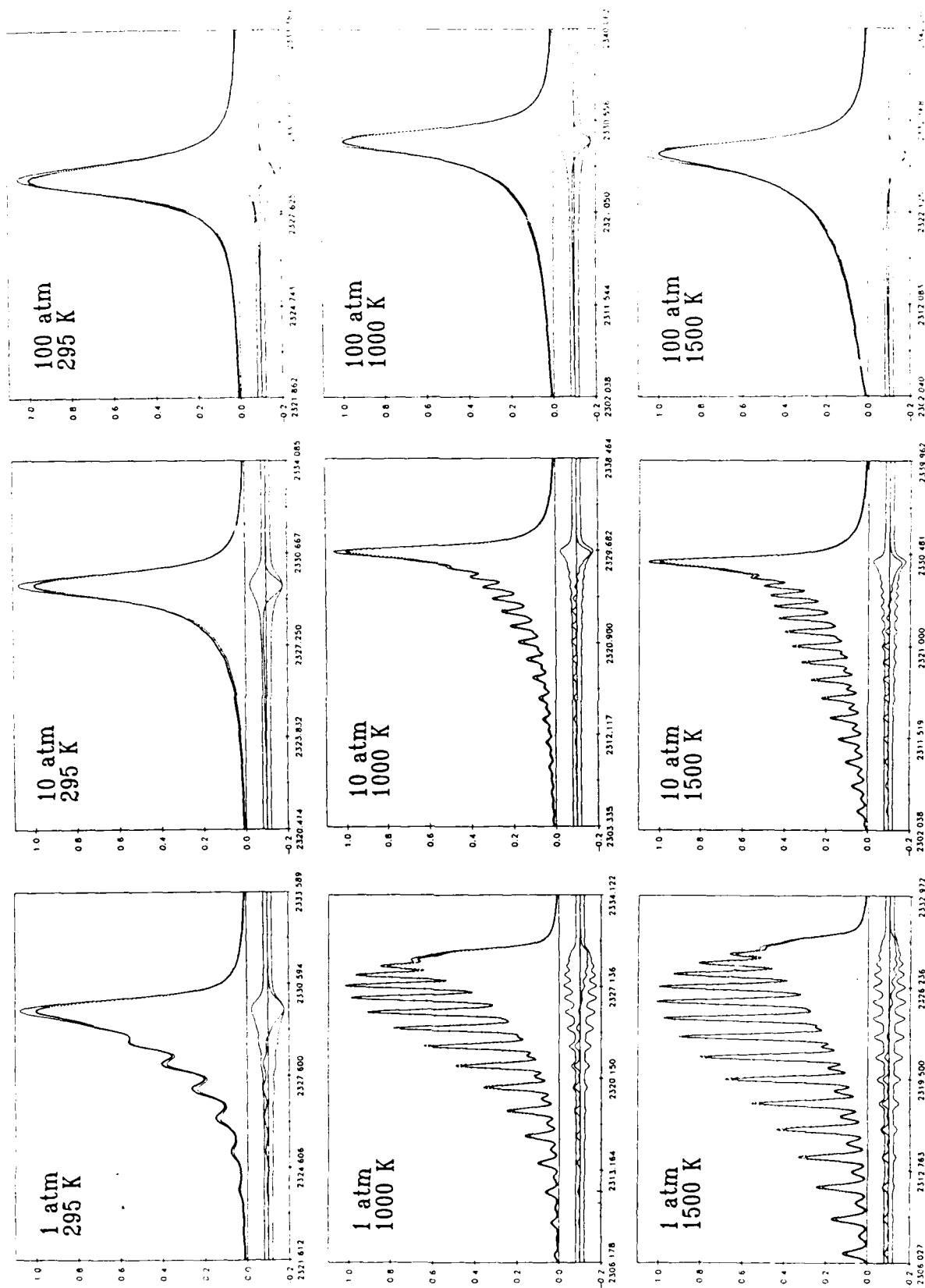
Figure VI.2

N₂ MEG law; 2.0 cm⁻¹ convolution
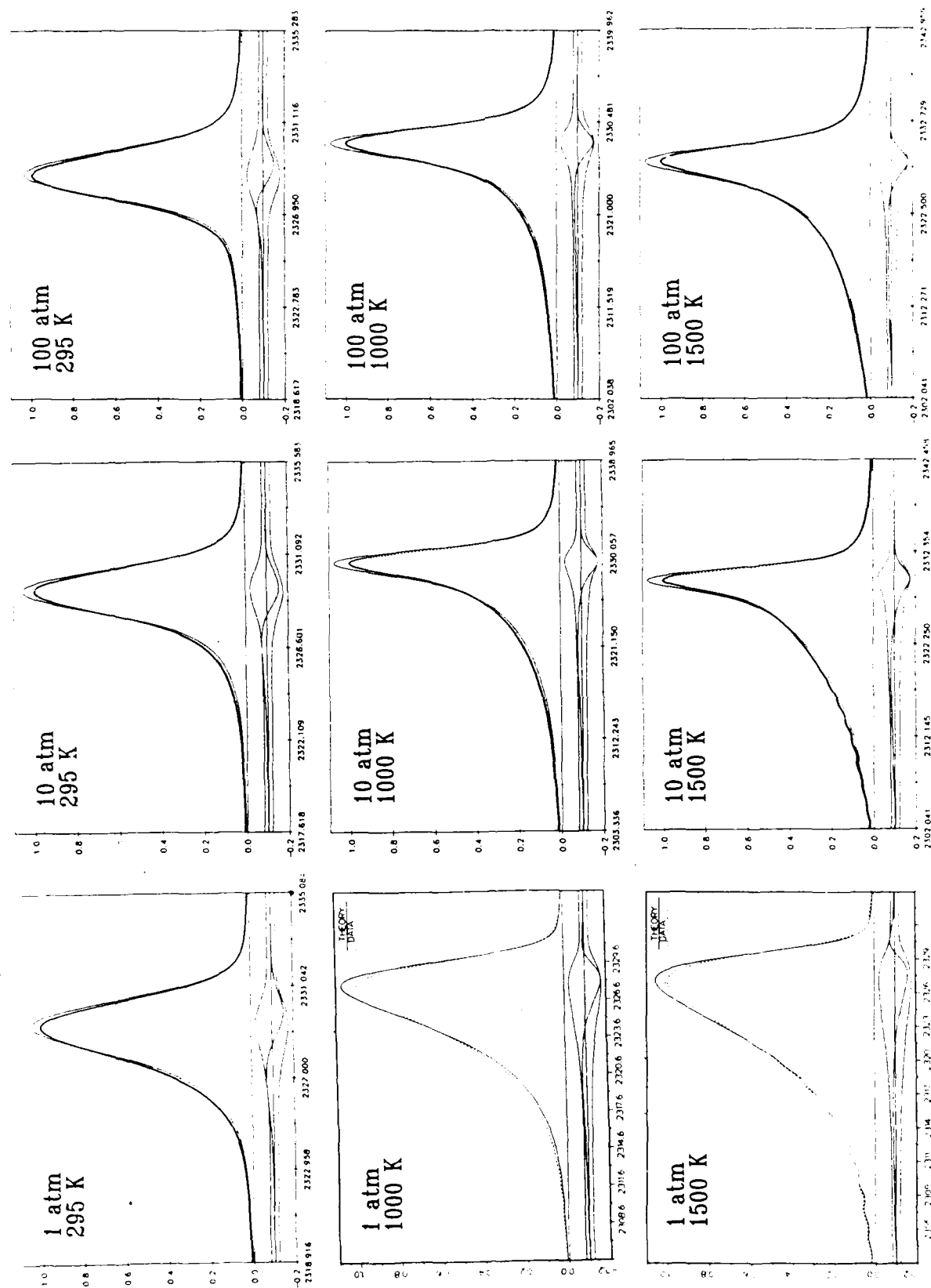
Figure VI.3

N₂ MEG law; no convolution

10 atm
1000 K

Figure VI.4

45
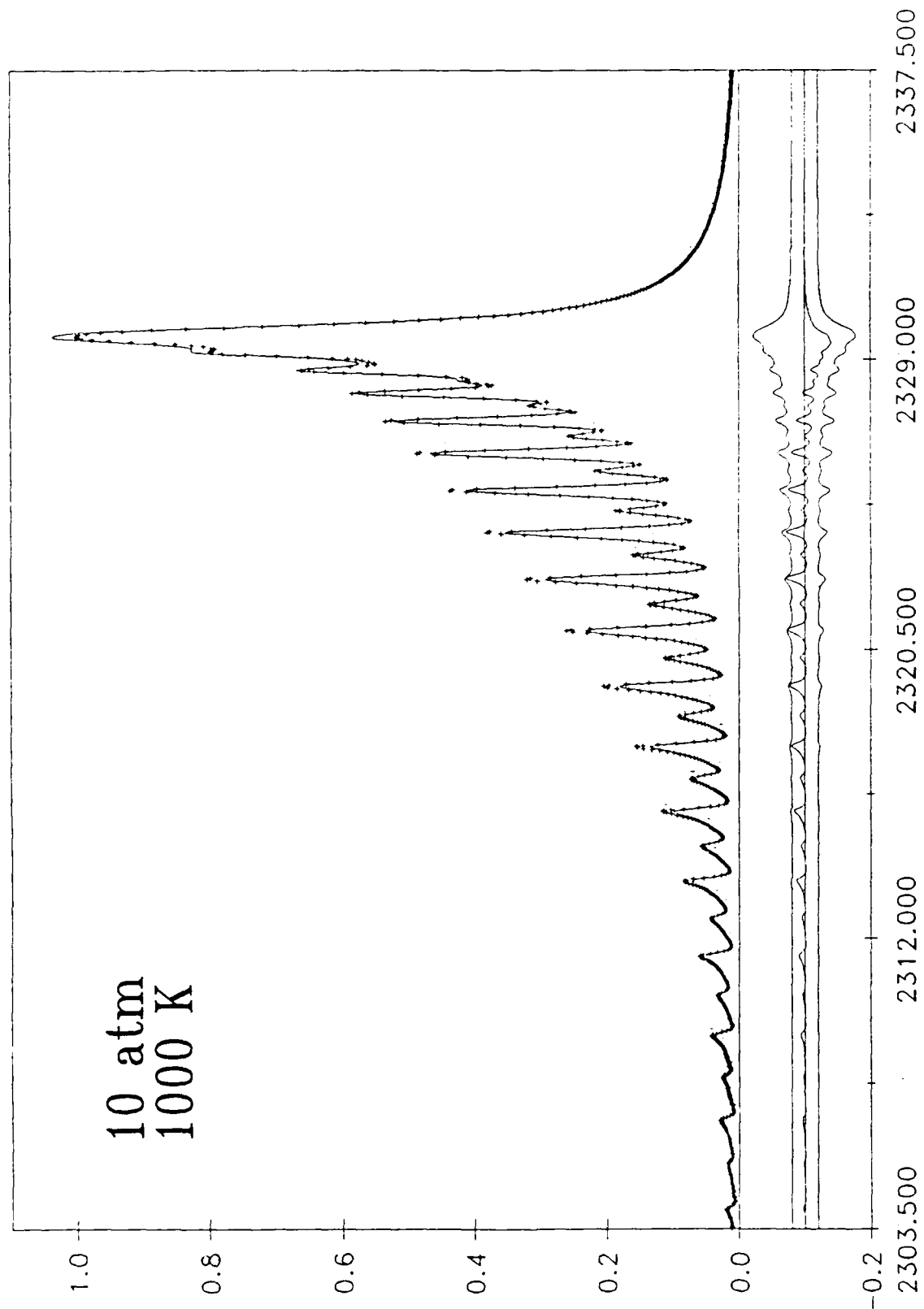
mean-square deviation of the "fit" relative to the "data". The locus of such points, the "error-limit surface", for the three data sets is plotted in Figs. VI.5-7. In these figures, the T,P limits are expressed as fractional deviations from the reference T_0, P_0.

Since this representation of the error-limit surface has not previously been presented in the literature, we suggest the following interpretation of these plots. Consider an ensemble of single-shot spectra, each with its own unique noise component. If we applied a least-mean-squares fitting procedure to each of these spectra, we would expect to find a distribution of "best fit" P's and T's in the vicinity of P_0 and T_0. This distribution is a mapping of the spectral noise through the instrument response function and the CARS spectral distribution function onto the T,P plane. Such a mapping is shown schematically in Fig. VI.8. Since the most probable T and P for the set of measurements should be T_0 and P_0, we would expect that the distribution function can be approximated by a figure of revolution of a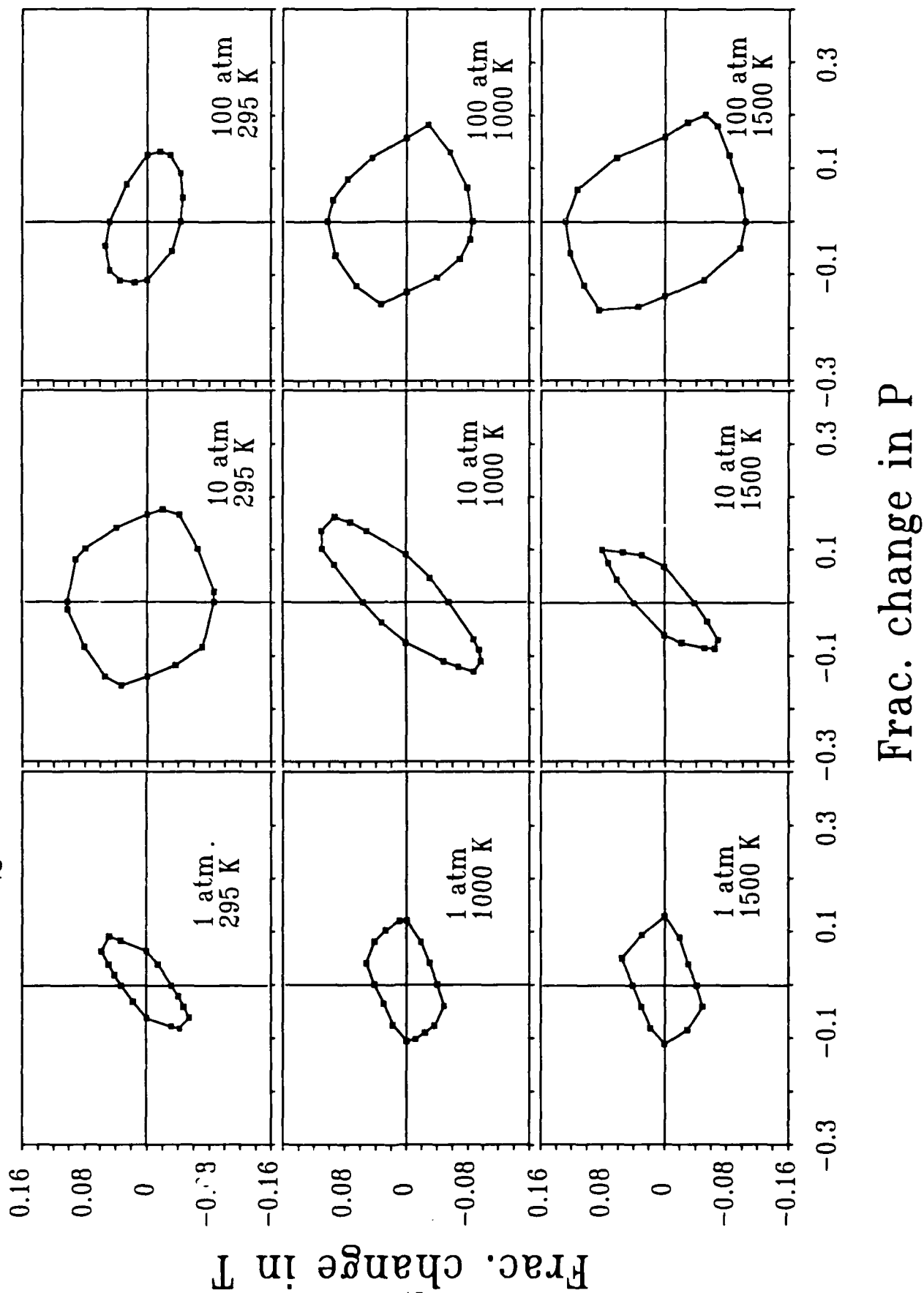 statistical distribution which maximizes at T_0 and P_0. A Gaussian distribution is used to generate Fig. VI.8, although the actual distribution need not be Gaussian or symmetric. For the mapping displayed in Fig. VI.8 it is easy to show that the most probable values for constant P or constant T cuts through the surface are approximately as shown by the solid and dash-dot lines on the figure. The error-limit surface then represents a measure of the limits of the probability distribution, e.g. the 2-sigma points are suggested by the illustration.

With the interpretation of the preceeding paragraph in mind, we have performed least-mean-squares fits for P at constant T (and vice versa) for the entire, instrumentally convolved "data" set. In each case the amplitude is adjusted to minimize the weighted mean-square deviation as discussed above. The solid and dot-dashed lines in Figs. VI.6 and VI.7 are the locus of these weighted least-squares fits with P and T held constant, respectively. We show in Fig. VI.9 an expanded view of the 100 atm, 295 K panel from Fig. VI.6. It can be seen from this figure that the constant P and constant T curves approximate those we expected from the statistical argument of the preceeding paragraph. That is, if we consider, as an example, that subset of fits enclosed within the limit-surface in Fig. VI.9 for which the pressure is between 9 and 10% greater than P_0=100 atm, we will find from this subset a most probable temperature which is 2% lower than T_0=295 K. If we consider the limit-surface at 1 atm, 1500 K, shown expanded in Fig. VI.10, we see that errors in P imply essentially no correlated error in T. We also note from this last figure that temperature uncertainties in the range of ±5% would be expected from single-shot CARS data on high temperature atmospheric pressure N_2. This estimate is in good agreement with the observations of Ref. [R34] on flames and Ref. [R31] on a high temperature furnace.

We also observe, from a comparison of Figs. VI.5-7, that the effect of the finite resolution of diagnostic multi-channel instruments is, by-and-large, simply to expand the error-limit surface, particularly along the pressure axis, but otherwise to preserve the basic shapes and orientations of the limit-surface. We note in this regard that the magnitude of the P,T axis in Fig. VI.7 is approximately twice that in Figs. VI.5 and VI.6.

An important observation derived from the shapes of the limit-surfaces and locus of constant P and constant T least-squares minima is that there are

46

N₂ infinite resolution

Frac. change in P

Frac. change in T

Figure VI.5

N₂ 0.5 cm⁻¹ convolution

N₂ 0.5 cm⁻¹ convolution

Constant T ------   Frac. change in P   Constant P ———

48   Figure VI.6

N₂ 2 cm⁻¹ convolution

Figure VI.7

Constant T ------   Frac. change in P   Constant P ——

$\bar{P}$

1

0.5

0

constant T

T

P

0

0.5

1

$\bar{T}$

constant P

50

Figure VI.8

N₂ 0.5 cm⁻¹ convolution

100 atm
295 K

Frac. change in P

Constant T - - - - -   Frac. change in P   Constant P ———

Frac. change in T

Figure VI.9

N$_2$ 0.5 cm^{-1} convolution

Frac. change in T

0.16

0.08

0

−0.08

−0.16

−0.3

−0.1

0.1

0.3

Frac. change in P

1 atm
1500 K

Constant T -----   Frac. change in P   Constant P ——

Figure VI.10

cases where errors in P and T are correlated. These cases are: 1 atm, 295 K; 10 atm, 1000 and 1500 K; and 100 atm, 295 K. It is important to note that the exact form and degree of correlation is a func ion of the CARS spectral distributioi. (i.e. a strong function of P_0 and T_0), the spectral resolution, and the spectral distribution of the error (e.g. the weighting function). We illustrate sensitivity to the latter by the results presented in Fig. VI.11. For the upper three panels the weighting function includes a shot-noise component, $\sqrt{(.5I(\omega))}$, a noise floor, $\sigma_0 \approx 2$ (cts.), with $I_{max}=10^4$ (cts.), and the noise-proportional to signal at the 7.5% level as previously. These values are typical of diagnostic applications to laboratory flames, cf. Ref. [R34]. The lower three panels (in which we indicate only the locations of constant P and constant T least squares minima) utilize a constant, unit weight, i.e. commonly referred to as "unweighted" fitting. Upon comparing this figure to Fig. VI.6, we see distinct changes in the magnitude and orientations of the error-limit surfaces and associated constant P and constant T least squares minima. In some cases the degree of correlation in the P and T errors is increased, while in others it is decreased.

We conclude this section with a brief discussion of the errors in T and P which arise if there are systematic errors in our knowledge of the parameters of the rate law which is the basis for describing the CARS spectrum. These (and other sources of systematic error) are studied in Ref. [M14]. We find, from an analysis similar to the above, that systematic errors in linewidths of the order of 5-10% in general lead to similar errors in derived T and P. We illustrate this type of sensitivity in Fig. VI.12. In this figure we see that the entire error-limit surface, and the location of the most probable T and P, are shifted of the order of 4-5% as a result of a (-10%) variation in the MEG law parameter β. This variation in the β parameter produces the linewidth variations shown in Fig. VI.13; these variations have average magnitudes of 4.6% at 295 K and 3.1% at 1500 K. We see from this analysis the need for an accurate data base to assure the accuracy of spectroscopically derived T and P.

The analysis above centered on use of the fundamental (0 → 1) Q branch for temperature and pressure measurement. We believe that the methodology developed in the course of this study provides a useful approach to sensitivity analyses. Among the many conclusions which we can draw from this this preliminary study, we consider the following to be most significant:

-the nature of the noise spectrum and the CARS spectral distribution determines the shape of the error distribution in P,T space and thus meaningful answers to sensitivity questions require a specification of both the nature of the noise and the spectral region from which T and P will be determined

-it is very difficult to accurately determine pressure from the shape of the Q branch

-accurate temperature measurements for cases where there is significant uncertainty in our knowledge of the MEG law can not be based solely on the spectrum of the fundamental branch.

We do not regard any of these observations s revolutionary, rather we view them as more quantitatively substantiated statements of our expectations as

53

N₂ 0.5 cm⁻¹ convolution

$$\Delta I = \pm\sqrt{(\sigma^2 + 0.5 I + (\kappa I)^2)}$$

Figure VI.11

β (−10%) (0.5 cm⁻¹)

Frac. change in P

Figure VI.12

55

N₂ 295,1500 K Linewidths vs MEG par.

N_2 295,1500 K Linewidths vs MEG par.

90% β_0

HWHM, cm-1

std MEG ^{J} +   b=1.5

□
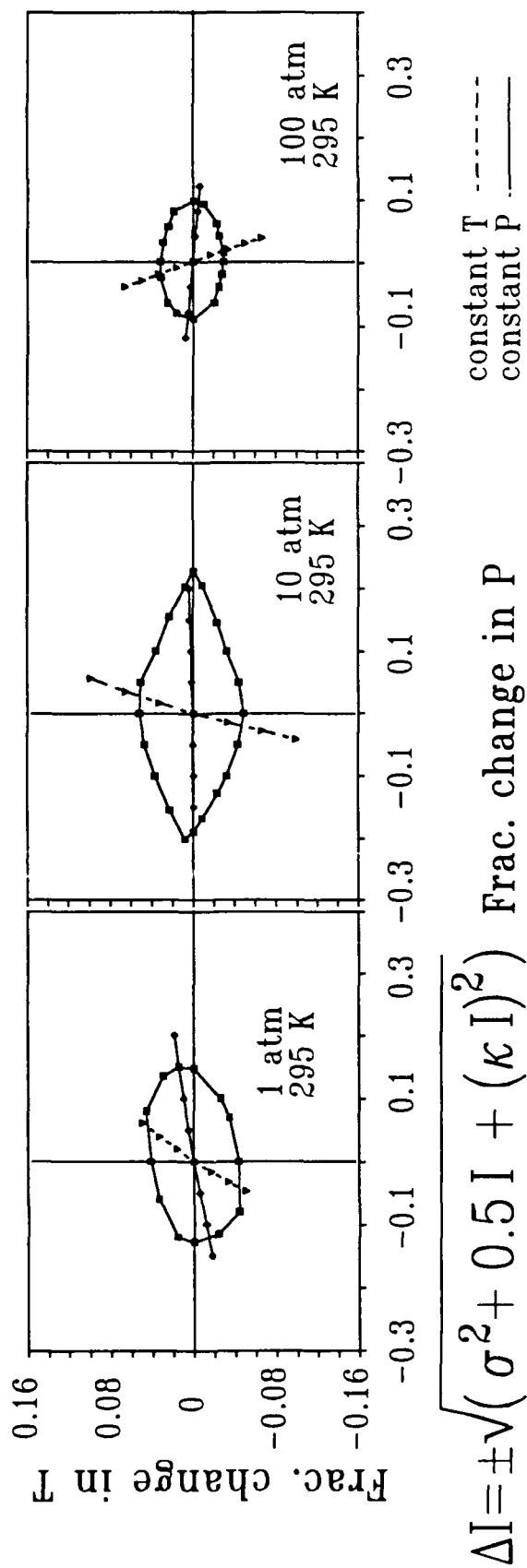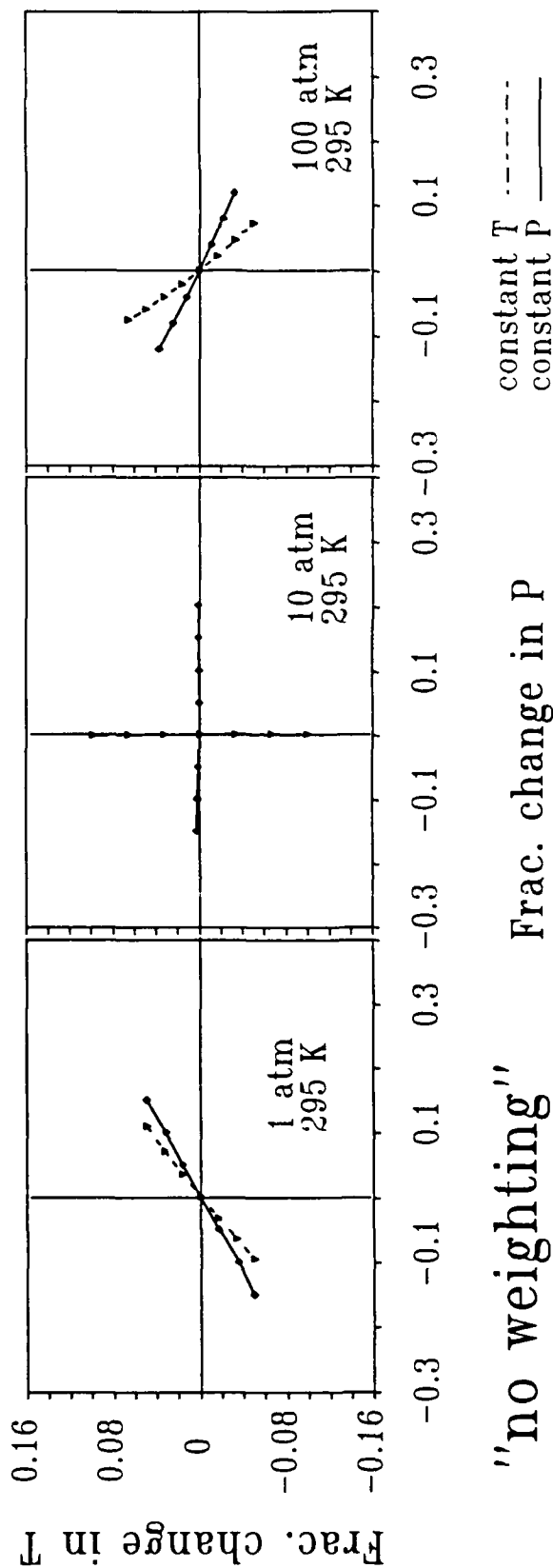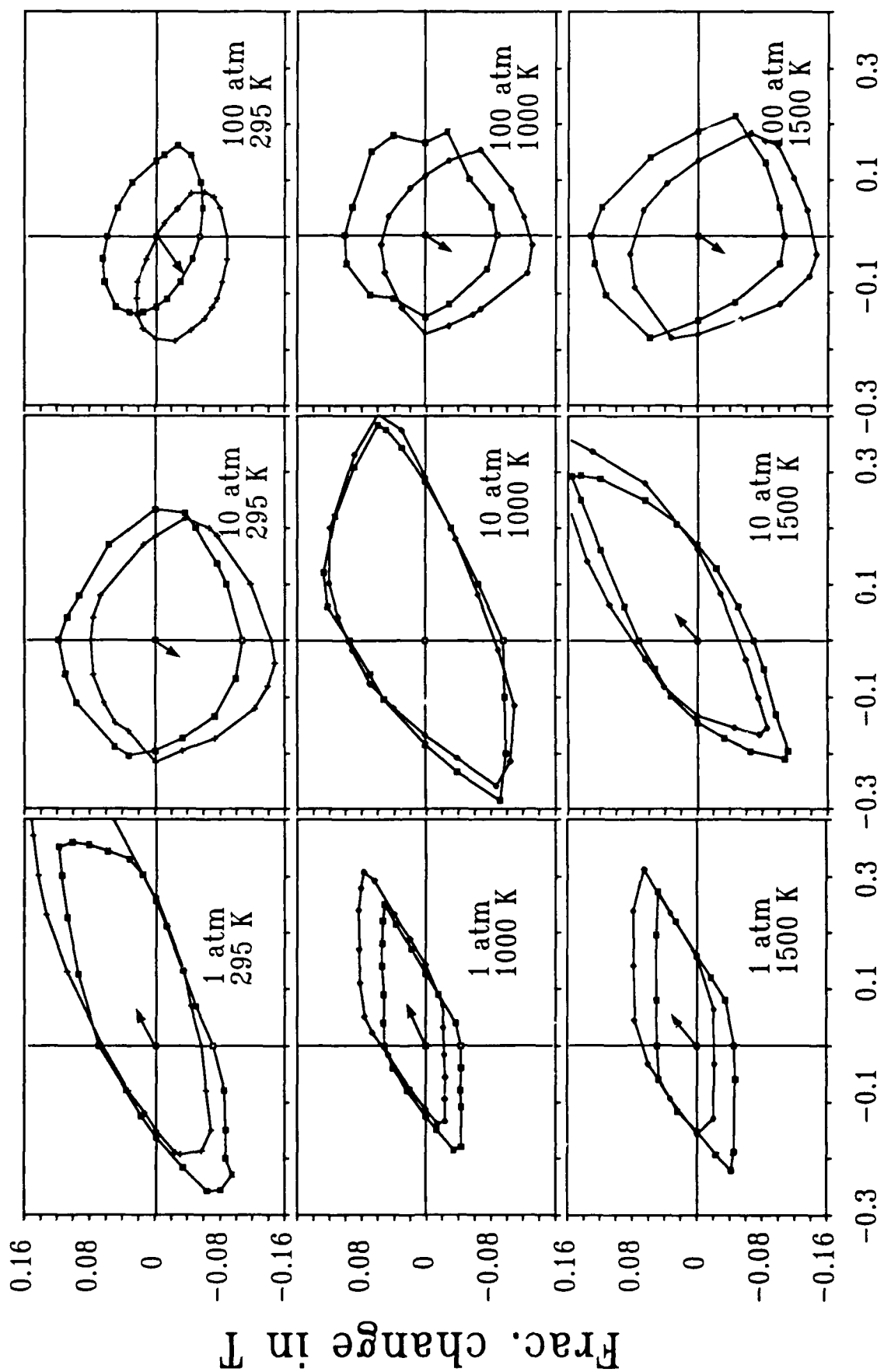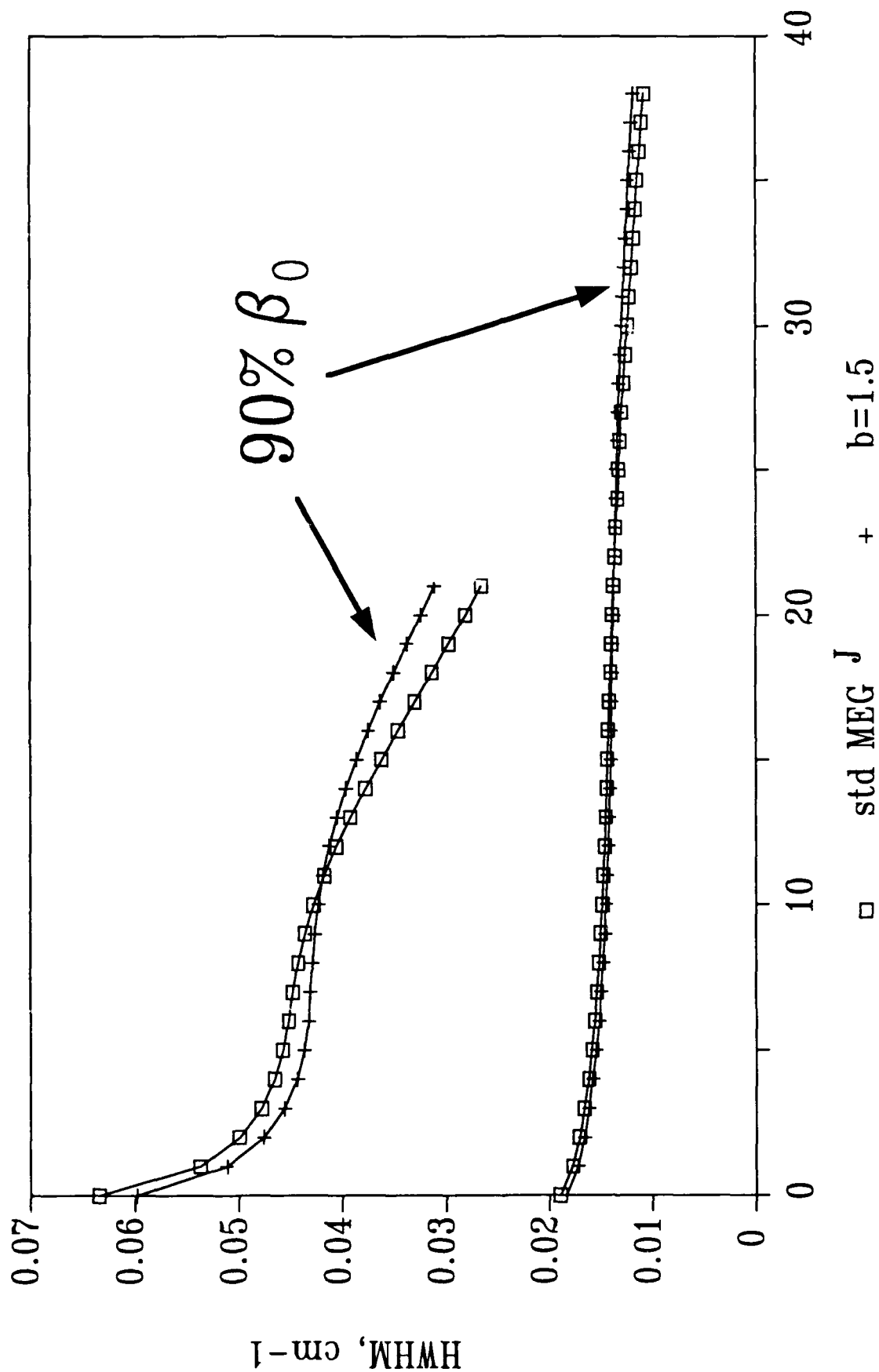
to the limits of error. Further, we note that the methodolgy developed here can be used to suggest possible approaches to the minimization of systematic errors in spectral measurements of T and P.

VII CONCLUSIONS

A reliable predictive basis has been established for simple molecular systems such as self-broadened CO and N_2. The very detailed studies made on the CO system, in particular, support the use of a relaxation matrix, based on rates for state-to-state rotational energy transfer, for describing the Q-branch spectrum. These studies also illustrate the limits of our ability to specify the relaxation matrix. We observe that as we attempt to account more accurately for the elements of the matrix, we encounter a more complex and (currently) less predictable J and T dependence in these elements. Fortunately, the MEG law, in spite of inaccuracies with respect to a number of significant details, does give a simple and remarkably useful representation of the collapse of the Q branch as a function of P and T.

Ultimately, the validity of the predictive model must be judged in the context of our application, i.e. considering the diagnostic approach, the accuracy required, and the ranges of extrapolation in pressure, temperature, and species concentration over which we will try to apply the predictive basis. It is the fact that we almost always must extrapolate our predictive equations into untested ranges which requires that we know the line-formation mechanisms and their basic dependence on the "system" variables.

It is clear from our studies that the reliability of the predictive basis would be greatly enhanced by first principle calculations of the off-diagonal elements of the relaxation matrix. Since these are not strictly state-to-state rates this will require that line-broadening-type calculations be extended to reveal the "distribution of relaxation" as a function of the intermolecular interactions and the magnitudes of angular momentum and energy transfer.

The need for a first principle understanding increases significantly when we include the composition variable in our systems. This situation arises because it is very difficult to empirically study the spectrum of the diagnostically interesting, minority, molecular species in the presence of the foreign gas host. The difficulty involves not only making accurate spectroscopic measurements on a minority species, but also problems associated with producing stable, accurately known reference samples having the required ranges of concentration, pressure, and temperature. In addition, no matter what limitations are set by the experimental difficulty of an empirical validation-study, diagnostic applications will (by definition) almost always involve significant extrapolations of some or all of the system variables. Improved first principle understanding would be extremely valuable.

For molecules such as N_2 and CO, the development of a predictive basis for the mixed-gas systems also will require significant improvements in the sensitivity and accuracy of the spectroscopic measurement techniques applied in model-validation studies. High resolution CARS spectroscopy appears to be a reasonable approach to provide some of this capability. Additionally, the fact that we now have accurately known susceptibilities for certain systems can provide a means of discerning systematic errors in multi-channel (diagnostic) instruments. The last-mentioned instruments, so calibrated, then can be used on reference samples to provide an important level of validation.

The spectrum of the hydrogens is very appealing from the diagnostic point of view, in that the resolved, intense Q branch affords excellent measures of temperature and pressure. We note also that the large pressure-shift to pressure-width ratio characteristic of the hydrogens, especially in foreign gas hosts, suggests a unique approach to pressure measurements which overcomes the large, correlated ambiguities in pressure and temperature measurements which can be encountered when using the Q branch of molecules such as CO and N_2.

On the basis of our studies of the hydrogens, we see that a reasonable conceptual basis for description of these systems is emerging and that empirical, predictive formulae can be used for some important parameters. However, there remain fundamental questions with regard to the physics of line formation as well as problems with respect to reliable prediction of spectroscopic parameters. The hydrogen diatomics, although quite tractable in terms of the spectroscopy, require significant levels of theoretical development, e.g. new kinetic equations, improved intermolecular potentials at short range including vibrational state dependence, and computationally manageable quantal scattering methods. Producing requisite reference samples also can pose significant problems. The study of the hydrogens affords many opportunities for fundamental advances in science and has significant promise for utility in diagnostic application.

We note that an element common to all fundamental and model-validation studies is the necessity of producing the required "reference samples". These must have accurately known conditions of temperature, pressure, and species concentration, selected either to be reasonably representative of the diagnostic environments of interest or to critically test an element of the predictive theory. In this regard, we suggest that shock tubes may serve as sources of these reference samples. Use of these sources will demand accurately calibrated multi-channel spectroscopy; which, as we indicated above, now appears within reach for both low and high resolution applications. The combination of a shock tube source with a "reference quality" spectroscopic instrument could provide important checks on possible systematic errors in pressure, temperature, and species concentration for a wide-range of diagnostic problems.

Finally, we observe that the accuracy required in the data base in order to avoid significant systematic errors should be assessed in terms of some form sensitivity analysis. Such analyses will guide the selection of the range of conditions under which validation experiments are required.

REFERENCES

LIST OF RESEARCH REPORTS RESULTING FROM THIS WORK

accepted for publication

P1. G.J. Rosasco and W.S. Hurst, The effects of velocity and phase changing collisions on Raman Q-branch spectra, in Spectral Line Shapes, Vol. 4, ed. by R. J. Exton, (A. Deepak Publishing, Hampton, VA, 1987), pp. 533-567.

P2. K.C. Smyth, G.J. Rosasco, and W.S. Hurst, Measurement and rate law analysis of D_2 Q-branch line broadening coefficients for collisions with D_2, He, Ar, H_2, and CH_4, J. Chem. Phys. 87, 1001(1987).

P3. G.J. Rosasco, L.A. Rahn, W.S. Hurst, R.E. Palmer, J.P. Looney, and J.W. Hahn, High resolution inverse Raman spectroscopy of the CO Q branch, SPIE Vol. 912, Pulsed Single-Frequency Lasers: Technology and Applications, (Society of Photo-Optical Instrumentation Engineers, Bellingham, WA, 1988), pp. 171-183.

P4. G.J. Rosasco, A.D. May, W.S. Hurst, L.B. Petway, and K.C. Smyth, Broadening and shifting of the Raman Q branch of HD, J. Chem. Phys. 90, 2115(1989).

P5. G.J. Rosasco, L.A. Rahn, W.S. Hurst, R.E. Palmer, and S.M. Dohne, Measurement and prediction of Raman Q-branch line self-broadening coefficients for CO from 400 to 1500K, J. Chem. Phys. 90, 4059(1989).

P6. J.P. Looney, G.J. Rosasco, L.A. Rahn, W.S. Hurst, and J.W. Hahn, Comparison of rotational relaxation rate laws to characterize the Q-branch spectrum of CO at 295 K, accepted for publication Chemical Physics Letters.

P7. R.L. Farrow, L.A. Rahn, G.O. Sitz, and G.J. Rosasco, Observation of a speed-dependent collisional inhomgeneity in H_2 vibrational line profiles, accepted for publication in Physical Review Letters.

manuscripts to be published

M8. L.A. Rahn and G.J. Rosasco, Measurement of the density shift of the H_2 Q(0-5) transitions from 295 K to 1000 K.

M9. R.L. Farrow, L.A. Rahn, and G.J. Rosasco, ECS-rate law analysis of the self-broadening coefficients of the H_2 Q-branch from 295 K to 1000 K.

M10. G.J. Rosasco, W.S. Hurst, and W.B. Bowers, Simultaneous forward-backward nonlinear Raman spectroscopy.

M11. J.P. Looney and G.J. Rosasco, Semi-classical calculations of line broadening in the Raman Q branch of CO, N_2, and O_2.

M12. J.P. Looney, Semi-classical line broadening calculations for the Raman Q branch of $CO:N_2$ from 295 K to 1500 K.

M13. J.P. Looney, G.J. Rosasco, L.A. Rahn, W.S. Hurst, and J.W. Hahn, CO Raman Q-branch collapse at high temperatures.

M14. W.S. Hurst, G.J. Rosasco, and J.P. Looney, Sensitivity analyses of T and P errors resulting from CARS spectroscopic measurements.

OTHER LITERATURE CITED IN THIS REPORT

R1. L. Bonamy, J. Bonamy, D. Robert, B. Lavorel, R. Saint-Loup, R. Chaux, J. ʃ ːos, and H. Berger, J. Chem. Phys. **89**, 5568(1988).

R2. S.G. Rautian and I.I. Sobelman, Sov. Phys. Uspekhi **9**, 701(1967).

R3. J.J. BelBruno, J. Gelfand, and H. Rabitz, J. Chem. Phys. **78**, 3990(1983).

R4. R.L. Farrow and R.E. Palmer, Opt. Lett. **12**, 984(1987).

R5. L. Galatry, Phys. Rev. **122**, 1218(1961).

R6. J. VanKranendonk, Can. J. Phys. **41**, 433(1963).

R7. W.K. Bischel and M.J. Dyer, Phys. Rev. A. **33**, 3113(1986).

R8. D. Robert and J. Bonamy, J. Phys. (Paris), **40**, 923(1979).

R9. J. Bonamy, D. Robert, and C. Boulet, J. Quant. Spectrosc. Radiat. Transfer, **31**, 23(1984).

R10. J. Bonamy and D. Robert, J. Quant. Spectrosc. Radiat. Transfer, **16**, 185(1976).

R11. B. Labani, J. Bonamy, and D. Robert, Internal Report 1985-1, Molecular Physics Group, Faculty of Science, University of Besancon, 25030 Besancon Cedex, France.

R12. T. Nakazawa and M. Tanaka, J. Quant. Spectrosc. Radiat. Transfer, **28**, 409(1982).

R13. T. Nakazawa and M. Tanaka, J. Quant. Spectrosc. Radiat. Transfer, **28**, 471(1982).

R14. R. Blackmore, S. Green, and L. Monchick, J. Chem. Phys., **88**, 4113(1988).

R15. S. Green, R. Blackmore, and L. Monchick, Comment on line widths and shifts in the Stokes-Raman Q-branch of D_2 in He, submitted to J. Chem. Phys.

R16. R. Blackmore, S. Green, and L. Monchick, Dicke narrowing of the polarized Stokes-Raman Q branch of the $v=0 \rightarrow 1$ transition of D_2 in He, submitted to J. Chem. Phys.

R17. J.D. Kelley and S.L. Bragg, Phys. Rev. A, **34**, 3003(1986).

R18. A.D. May, V. Degen, J.C. Stryland, and H.L. Welsh, Can. J. Phys. 39, 1769(1961).

R19. E.C. Looi, J.C. Stryland, and H.L. Welsh, Can. J. Phys. 56, 1102(1976).

R20. A. Ben-Reuven, Phys. Rev. A 4, 2115(1971).

R21. L. Monchick, private communication.

R22. A.D. Buckingham, C. Graham, and J.H. Williams, Mol. Phys. 49, 703(1983).

R23. C.S. Murthy, et al., Mol. Phys. 41, 1387(1980).

R24. The atom-atom interaction parameters are found through the usual combination rules $\epsilon_{ab} = \sqrt{(\epsilon_a \epsilon_b)}$ and $\sigma_{ab} = (\sigma_a + \sigma_b)/2$, cf. Appendix A.

R25. T.A. Scott, Phys. Rep. 27C, 89(1976).

R26. The isotropic potenial is obtained from the angular average of the site-site potentials.

R27. L.A. Rahn and R.E. Palmer, J. Opt. Soc. Am. B. 3, 1164(1986).

R28. L.A. Rahn, R.E. Palmer, M.L. Koszykowski, and D.A. Greenhalgh, Chem. Phys. Lett. 133, 513(1987).

R29. M.L. Koszykowksi, L.A. Rahn, R.E. Palmer, and M.E. Coltrin, J. Phys. Chem. 91, 41(1987).

R30. D.A. Greenhalgh and S.T. Whittley, Appl. Opt. 24, 907(1985).

R31. M. Pealat, P. Bouchardy, M. Lefebvre, and J.-P. Taran, Appl. Opt. 24, 1012(1985).

R32. D.R. Snelling, R.A. Sawchuk, and R.E. Mueller, Appl. Opt. 24, 2771(1985).

R33. R.J. Hall and D.A. Greenhalgh, J. Opt. Soc. Am. B, 3, 1637(1986).

R34. D.R. Snelling, G.J. Smallwood, R.A. Sawchuk, and T. Parameswaran, Appl. Opt. 26, 99(1987).

R35. S. Kroll, M. Alden, T. Berglind, and R.J. Hall, Appl. Opt. 26, 1068(1987).

R36. D.R. Snelling, T. Parameswaran, and G.J. Smallwood, Appl. Opt. 26, 4298(1987).

LIST OF PARTICIPATING SCIENTIFIC PERSONNEL

COLLABORATORS AT THE U. S. NATIONAL INSTITUTE OF STANDARDS AND TECHNOLOGY

Walter B. Bowers
Sharon M. Dohne
Wilbur S. Hurst
John Patrick Looney
Gregory J. Rosasco
Kermit C. Smyth

COLLABORATORS FROM HOWARD UNIVERSITY

Larry B. Petway

COLLABORATORS FROM THE UNIVERSITY OF TORONTO

A. David May

COLLABORATORS FROM THE KOREA STANDARDS RESEARCH INSTITUTE

Jae Won Hahn

COLLABORATORS FROM THE COMBUSTION RESEARCH FACILITY, SANDIA NATIONAL LABORATORIES

Roger L. Farrow
Richard E. Palmer
Larry A. Rahn
Gregory O. Sitz

APPENDIX A

Comparison of Rotational Relaxation Rate Laws to Characterize the Raman Q-branch Spectrum of CO at 295 K.

(accepted by Chemical Physics Letters)

J.P. Looney[a], G.J. Rosasco[a], L.A. Rahn[b], W.S. Hurst[a], and J.W.Hahn[a,c]

[a]Temperature and Pressure Division, U.S. National Institute of Standards and Technology, Gaithersburg, MD 20899 USA

[b]Combustion Research Facility, Sandia National Laboratories, Livermore, CA 94550 USA

[c]Permanent Address : Korean Standards Research Institute, Taejon, Chungnam, Republic of Korea

Abstract

We test the ability of the Energy Corrected Sudden (ECS), Modified Exponential Gap (MEG) and the Statistical Power-Exponential Gap (SPEG) rate laws to characterize line broadening and line interference in the CO Q-branch at 295 K. All three rate laws fit the experimental linewidth data. The ECS law is found to predict too much spectral collapse. The MEG and SPEG laws both adequately model spectral collapse, but with different implications about the role of dipolar and quadrupolar symmetry forces in CO:CO line broadening. From semiclassical calculations of CO linewidths, we conclude that the SPEG law with a restriction to even ΔJ changes is the more physically correct model.

I. Introduction

Numerous studies of the pressure and temperature dependence of Q-branch spectra of simple molecular systems [1] show that collisional broadening and spectral line interference in the Q-branch can be described using the relaxation matrix formalism. [2-5]. When vibrational dephasing (for IR and Raman studies) and elastic reorientation (for IR studies) can be neglected, the elements of the relaxation matrix are expressible in terms of state-to-state rates for rotational energy transfer. This has focused the attention of many studies on tests of the ability of various rotationally inelastic rate law models [6], which provide a simple representation of the relaxation matrix, to yield an accurate characterization of the observed spectra.

The present study is motivated by the desire to test the ability of three, widely applied, rate law models to predict the self-broadened CO Q-branch spectrum. Aside from the potential implications for diagnostics applications, line interference in the CO Q branch is of particular interest for a number of reasons. First, spectroscopic evidence [7-12] gives a clear indication that CO line broadening shows little vibrational state dependence, thus supporting the use of a rate law model to parameterize the relaxation matrix. Second, neighboring transitions in the CO Q branch when overlapped may interfere, thereby causing the spectrum to collapse. This degree of line interference should provide a good test of rate law models. The situation for CO contrasts with N_2 for which the line interference is obscured as the observed spectrum is the superposition of two independent Q

3

branches from the ortho and para molecular species. Finally, there have been inelastic rate law analyses of CO linewidth data [11-13]; however, no rate law model has been adequately tested against the observed spectral collapse.

In this paper, we present experimental results from a series of studies on the pressure dependence of the CO Raman Q-branch from 0.5 to 6.0 atm at room temperature. From these studies we report a J-independent shift coefficient, improved line broadening coefficients for the lower J transitions (J=0-18), and accurate line broadening coefficients for the higher J transitions, up to J=24.

We found from our analyses that linewidths and collapsed spectra were both adequately modelled by either the Modified Exponential Gap (MEG) [14] or Statistical Polynomial-Exponential Gap (SPEG) [6,15] rate laws, but with different implications as to the relative propensity for dipolar (unrestricted ΔJ) and quadrupolar (even ΔJ only) transitions. The Energy Corrected Sudden (ECS) [6,16] scaling law, previously reported, can be discounted as it predicts too much spectral line interference. From the results of a semiclassical calculation of CO line broadening, we conclude that the SPEG rate law model, with a restriction to quadrupolar selection rules governing rotational state changes, provides the more physical description of the CO Q-branch spectrum at 295 K.

II. Experimental Results

The data reported here are derived from three experimental studies of the self-broadened Q branch of CO at room temperature. The earliest of these [10] employed inverse Raman spectroscopy with cw-lasers and determined line

broadening out to J=18 and a line shifting coefficient for Q(14). A second series of experiments [11], conducted with a pulsed Raman pump laser in a quasi-cw inverse Raman spectroscopic system, extended line broadening out to J=24 and measured shift coefficients for Q(J)=18-22. A final set of measurements, using the latter experimental system, were made to accurately determine the spectrum of the partially collapsed Q branch over a large frequency range (above and below the bandhead) at 2.9 and 6.0 atm. These experimental systems, the associated spectral resolution and frequency accuracy, and the sample cells and optical configurations have been described in previous publications [10-12].

A. Line broadening coefficients

Using the fitting procedure discussed in Refs. [11] and [12], we determined the line broadening coefficients given in Table 1 and displayed in Fig. 1. Error estimates, indicated in parentheses, are typically on the order of 2-5%. The low J transitions (0-3) are strongly blended leading to a larger uncertainty. The high J transitions, due to their relative weakness, also have larger uncertainties. It should be emphasized that the values extracted through our fitting procedure are independent of any rate law model.

B. Line shifts

To accurately predict the collapse of a Q branch it is important to have a reliable value of the pressure shift coefficient [11,17]. Since

collisional collapse has the effect of "pulling" Q-branch lines toward the most probable J, it is important that line mixing be small if one is interested in accurate frequency shift determination [11]. The measured transitions J=18-22 display a sufficiently high signal-to-noise ratio, and have small enough line mixing for the pressure range used (0.5 - 2.9 atm), that accurate values of the line shifting coefficient can be determined. For the range J=18-22, there is no discernible J dependence of the pressure shift. We note, that this observation is consistent with measurements [17] and calculations [18] for self broadened N_2, and with the results of our calculation, reported below. A weighted linear regression of the shifts versus pressure yields a value of the CO Q-branch shift coefficient, -0.0032 $\pm$ 0.0003 cm^{-1}/atm at 298 K.

III. Rate Law Analysis of CO Q-Branch Data

The rate law models we investigated are the Energy Corrected Sudden (ECS) [16], the Modified Exponential Gap (MEG) [14], and the Statistical Power-Exponential Gap (SPEG) laws [15]. All three of these rate law models have been applied in the analysis of partially or fully collapsed Q-branch spectra with varying degrees of success.

The ECS scaling law was used by Bel Bruno et al. [13] to derive inelastic state-to-state rates from CO infrared linewidths. The ECS scaling law also has been applied to line broadening and collapse of the isotropic Raman Q-branch spectrum of N_2 with moderate success [18].

The MEG law, which has been the most successful in characterizing the isotropic Raman Q-branch spectrum of N_2 [19], has been applied to the

6

parameterization of the J and temperature dependence of the CO Q-branch linewidths [12]. Preliminary analyses of CO Q-branch collapse using this law have been reported [11,12].

The SPEG law has been employed successfully in the description of the infrared $\nu_2+\nu_3$ Π-Σ band of pure N_2O [20] and to the ν_2 band of CO_2, both self- [21] and N_2-broadened [22]. It has also been applied in the description of the NO isotropic Raman Q-branch spectrum [23]. No analyses of CO linewidths or spectra using the SPEG law have been reported.

A. The ECS Scaling Law Analysis

We turn now to predictions of the Raman isotropic Q branch based upon an ECS scaling law analysis of the CO infrared linewidths [13]. According to this analysis two mechanisms termed R-T and R-R processes, contribute to inelastic rates in CO. The former is essentially a rotation to translation energy exchange process for molecule-"effective" atom interactions and the latter a rotational-quantum number perserving exchange process. The R-T transfer rates are determined by a set of fundamental base rates for J→0 transitions and an associated scaling length. The fundamental base rates for the R-T transfer process are expressed in terms of an exponential gap law with two parameters. The R-R transfer rates are determined by a single $\Delta J=1$ exchange rate and an associated scaling length. We use the parameters given in Ref. [13] along with the definitions and equations given in Refs. [16,24-26] to calculate the ECS rates.

We plot in Fig. 1, along with the experimental broadening coefficients, the total inelastic rates (from both R-T and R-R processes) as

7

given by the ECS analysis. It can be seen that the ECS law gives, overall, reasonably good agreement with measured linewidths. The ECS law, when used to predict the collapsed Q-branch spectra (a comparison with experimental results at 3.0 atm is shown in Fig. 2), is found to overestimate the degree of collapse. This represents an example of the fact that the ability of a rate law to model linewidths does not necessarily indicate its ability to predict spectral collapse.

Although the ECS analysis of Bel Bruno et al. did not discriminate between dipolar and quadrupolar selection rules, we have subsequently performed an ECS analysis of CO linewidths based on quadrupole selection rules, using either an exponential gap or a polynomial gap law for the base R-T rates (no R-R rates). We again find that the ECS law significantly overestimates the degree of collapse and thus it appears inadequate for describing the CO relaxation matrix. The ECS law predicts inelastic rates near the diagonal which are too large and too little a propensity for multi-quanta collision processes.

B. The MEG Law

The MEG law used in Refs. [11] and [12] is an exponential gap law with an energy correction term applied to the initial level. We have generalized the MEG law by applying a similar energy correction to the final state following the prescription of Koszykowski et al. [14]. This MEG law expresses the rate for upward rotational transitions from state J to state J' as

$$W_{J'J} = P \, \alpha \, \bullet \, \left[\frac{1 + A \, E(J')/kT\delta'}{1 + A \, E(J')/kT}\right]^2 \, \bullet \, \left[\frac{1 + A \, E(J)/kT\delta}{1 + A \, E(J)/KT}\right]^2 \, \bullet$$

$$\exp\left[\frac{-\beta\{E(J') - E(J)\}}{kT}\right] \tag{1}$$

with α, β, δ', and δ being adjustable parameters, A a constant (a measure of the duration of a collision), $E(J)$ the energy of the rotational level J, P pressure, T temperature, and k Boltzmann's constant. We note that in the limit that $\delta' = 1$, we recover the form of the MEG law given in [12,14]. Previously the value A = 2 was assigned based upon estimates of effective interaction length and distance of closest approach for CO:CO collisions at 295 K [12]. We note, however, that the value of A is not critical in the ability of the MEG law to fit the data.

A best fit of the MEG law to all the experimental data (both linewidths and partially collapsed spectra) gives α = 0.01395 (cm^{-1}/atm), β = 1.351, $\delta' = \delta$ = 1.17, without any distinction between even and odd ΔJ transitions. In Fig. 1 the MEG law is seen to reproduce the linewidths at a level that it consistent with experimental error at all J. The results obtained with this form of the MEG law and $\delta = \delta'$ yield only slightly better fits to linewidths and predictions of collapse than the MEG law discussed previously in Refs. [11,12] with $\delta' \equiv 1$.

In Fig. 3 a and b we compare MEG law predictions with experimentally measured spectra at 3.0 and 6.0 atm. The residuals, which we assess to be within experimental reproducibility, demonstrate that the MEG law yields an excellent characterization of the Q-branch collapse. It has been found that the degree of collapse observed for the CO spectrum is poorly predicted by a MEG law with the restriction to even rotational quantum number changes, which might be expected for an "almost homonuclear" diatomic. From the MEG

law analysis, we would be led to the conclusion that there is roughly equal propensity for dipolar and quadrupolar transitions in CO:CO collisions.

C. The SPEG Law

The SPEG law is a statistical rate law model which has its origins in surprisal analysis [6,15]. This law expresses the rate for an upward rotational transition from state J to state J' as

$$W_{J'J} = P \alpha \bullet \left[\frac{E(J') - E(J)}{B_0} \right]^{-\delta} \bullet$$
$$\exp \left[\frac{- \beta \{E(J') - E(J)\}}{kT} \right] \tag{2}$$

with α, β, and δ adjustable parameters and B_0 is the ground state rotational constant, the remaining symbols are as defined in section IIB above.

It was found that the overall best fit to the experimental data, both linewidths and collapsed spectra, is given by $\alpha = 0.06428$ (cm^{-1}/atm), $\delta = 0.2646$ and $\beta = 1.295$ with the collisional selection rule $\Delta J = |J'-J| =$ even. The SPEG law is also found to fit the experimental linewidths totally consistent with experimental error, see Fig. 1.

In Figs. 4 a and b we show the excellent agreement of the SPEG law predictions with our experimental spectra at 3.0 and 6.0 atm. A SPEG law without the restriction to even ΔJ is found to significantly overestimate the degree of collapse of the CO Q branch. From this analysis, we would conclude that rotational state changes in CO:CO collisions are dominated by quadrupolar selection rules. This is in contrast to conclusions based on the MEG law analysis. Without further information it was not possible to choose

10

between the MEG and SPEC laws and their different implications about rotational state changes in CO:CO collisions.

IV. Semiclassical Linebroadening Calculations

To discern, on a physical basis, between the SPEC and MEG rate law models, we have turned to theory with the intention to determine the relative importance of dipolar and quadrupolar forces in CO:CO collisions. We use the Robert and Bonamy [27-33] formulation of molecular line broadening to calculate CO self-broadening coefficients. In our calculations, all terms from a fourth-order expansion of the atom-atom potential are explicitly included [27-29,37]. The CO intermolecular interaction parameters, taken from the literature, are given in Table 2. Full details of these calculations will be presented elsewhere [43].

Our calculations show excellent agreement when compared with experimental infrared R-branch [7,44] and Raman Q-branch [12] data over a large range of J (0-30) and T (100 - 1500 K) for both infrared and Raman Q-branch data. Agreement over this range of J and T indicates that this CO:CO potential is very reliable for line broadening calculations.

To determine the role of the quadrupolar and dipolar symmetry forces in CO:CO collisions, we repeated the calculations omitting terms arising from dipolar symmetry forces. We find that the dipolar forces make a small contribution (4-8%) to Q-branch linewidths for the low and intermediate J (J=0-14) transitions and have a larger contribution for high J transitions (J>15), with ≈ 18% of the Q(24) transition linewidth being attributable to these forces. Because of the large interline spacing, the latter region of

11

the Q branch exhibits relatively little line interference; in contrast, at low J where collapse is most important, we infer from these calculations that the CO state-to-state transitions are dominated by quadrupolar selection rules. Finally, we note that this calculation provides only total inelastic collision cross rates, not individual state-to-state rates; so it cannot be used to directly determine the off-diagonal elements of the relaxation matrix.

V. Conclusion

The comparision of the MEG and SPEG law for modeling of the CO Raman Q-branch represents an important example of the fact that it is difficult to draw reliable conclusions about collision dynamics from rate law fits to linewidths and spectra alone. To illustrate the difference between these two rate law models, we plot in Fig. 5a and 5b, respectively, rotationally inelastic state-to-state rates based upon the best MEG and the SPEG laws. As can be seen from this figure, the distribution of state-to-state rates given by the two rate laws is very different. Only the SPEG law analysis is consistent with the dominant role of quadrupolar symmetry forces, as found from our calculations. This observation is also in accord with experimental [45] and theoretical [46,47] studies of CO:He [47] and other "almost homonuclear" diatomics in collision with rare gas [45]. Our conclusions could be tested by measuring the relative $\Delta J=1$ and $\Delta J=2$ state-to-state rates. Finally, we note that this study points out the need for detailed information about state-to-state rates for physically reliable modeling of high pressure Q-branch spectra.

12

Acknowledgements

References

1. This large body of work is reviewed in : G.J. Rosasco and W.S. Hurst, in: Spectral Lineshapes Vol. 4, ed. R.J. Exton (Marcel Deepak, Hampton, 1987); D.A. Greenhalgh, in: Advances in Non-linear Spectroscopy Vol. 15, ed. R.J.H. Clark and R.E. Hester (John Wiley, New York, 1988); D. Robert, to be published in: Vibrational Spectra and Structure, ed. J.R. Durig (Elsevier, New York, 1988); L.L. Strow, Proc. SPIE 928 (1988), in press.

2. U. Fano, Phys. Rev. 131 (1963) 259.

3. A. Ben-Reuven, Phys. Rev. 141 (1966) 34.

4. A. Ben-Reuven, Phys. Rev. 141 (1966) 7.

5. A. Ben-Reuven, Advan. Chem. Phys. 33 (1975) 235.

6. T.A. Brunner and D. Pritchard, Advan. Chem. Phys. 50 (1982) 589.

7. T. Nakazawa and M. Tanaka, J. Quant. Spectrosc. Radiat. Transfer 28 (1982) 409.

8. J.J. BelBruno, J. Gelfand, W. Radigan and K. Verges, J. Mol. Spectrosc. 94 (1982) 336.

9. J.P. Bouanich, J. Quant. Spectrosc. Radiat. Transfer 31 (1984) 561.

10. G.J. Rosasco, W. Lempert, W.S. Hurst and A. Fein, Chem. Phys. Lett. 97 (1983) 435.

11. G.J. Rosasco, L.A. Rahn, W.S. Hurst, R.E. Palmer, J.P. Looney and J.W. Hahn, Proc. SPIE 912 (1988) 171.

12. G.J. Rosasco, L.A. Rahn, W.S. Hurst, R.E. Palmer and S.M.Dohne, J. Chem. Phys. 90 (1989) 4059.

13. J.J. BelBruno, J. Gelfand and H. Rabitz, J. Chem. Phys. 78 (1983) 3990.

14. M.L. Koszkowski, L.A. Rahn, R.E. Palmer and M.E. Coltrin, J. Phys. Chem. 91 (1987) 41.

15. B.C. Sanctuary, Chem. Phys. Lett. 62 (1979) 378.

16. A.E. DePristo, S.D. Augustin, R. Ramaswamy and H. Rabitz, J. Chem. Phys. 71 (1979) 850.

17. B. Lavorel, R. Chaux, R. Saint-Loup and H. Berger, Opt. Commun. 62 (1987) 25.

18. L. Bonamy, J. Bonamy, D. Robert, B. Lavorel, R. Saint-Loup, R. Chaux, J. Santos and H. Berger, J. Chem. Phys. 89 (1988) 5568.

19. L.A. Rahn, R.E. Palmer, M.L. Koszkowski and D.A. Greenhalgh, Chem. Phys. Lett. 133 (1987) 513.

20. L.L. Strow and A.S. Pine, J. Chem. Phys. 89 (1988) 1427.

21. L.L. Strow and B. Gentry, J. Chem. Phys. 84 (1986) 1149.

22. B. Gentry and L.L. Strow, J. Chem. Phys. 86 (1987) 5722.

23. W. Lempert, G.J. Rosasco, W.S. Hurst, J. Chem. Phys. 81 (1984) 4241.

24. A.E. DePristo and H. Rabitz, Chem. Phys. 44 (1979) 171.

25. A.E. DePristo, J. Chem. Phys. 73 (1980) 2145.

26. A.E. DePristo, J.J. BelBruno, J. Gelfand and H. Rabitz, J. Chem. Phys. 74 (1981) 5031.

27. D. Robert and J. Bonamy, J. Phys. (Paris) 40 (1979) 923.

28. J. Bonamy, D. Robert and C. Boulet, J. Quant. Spectrosc. Radiat. Transfer 31 (1984) 23.

29. J. Bonamy and D. Robert, J. Quant. Spectrosc. Radiat. Transfer 16 (1976) 185.

30. J.M. Hartmann et al., J. Quant. Spectrosc. Radiat. Transfer 35 (1986) 357.

31. J.M. Hartmann, L. Rosenmann, M.Y. Perrin and J. Taine, Appl. Opt. 27 (1988) 3063.

32. B. Lavorel, G. Millot, R. Saint-Loup, C. Wenger, H. Berger, J.P. Sala, J. Bonamy and D. Robert, J. Phys. (Paris) 47 (1986) 417.

33. L. Rosenmann, J.M. Hartmann, M.Y. Perrin and J. Taine, Appl. Opt. 27 (1988) 3902.

34. J.P. Looney and R.M. Herman, J. Quant. Spectrosc. Radiat. Transfer 37 (1987) 547.

35. C.G. Gray and K.E. Gubbins, Theory of Molecular Fluids Vol. 1 (Clarendon, Oxford, 1984).

36. The site-site spacing corresponds to the known bond length of the CO molecule; see G. Herzburg, Spectra of Diatomic Molecules, (Van Nostrand Rienhold, New York, 1950).

37. B. Labani, J. Bonamy and D. Robert, Internal Report 1985-1, Molecular Physics Group, Faculty of Science, University of Besancon, 25030 Besancon Cedex, France.

38. W.L. Meerts, F.H. deLeeuw and A. Dymanus, Chem. Phys. 22 (1977) 319.

39. D. Frenkel and J.P. McTague, J. Chem. Phys. 72 (1980) 2801.

40. D.J. Tildesley and P.A. Madden, Mol. Phys. 42 (1981) 1137.

41. The C-O atom-atom interaction parameters are found through the usual combination rules $\epsilon_{ab} = \sqrt{\epsilon_a \epsilon_b}$ and $\sigma_{ab} = (\sigma_a + \sigma_b)/2$.

42. J.O. Hirschfelder, C.F. Curtis and R.B. Bird, Molecular Theory of Gases and Liquids (John Wiley, New York, 1954).

43. J.P. Looney and G.J. Rosasco, to be published.

44. T. Nakazawa and M. Tanaka, J. Quant. Spectrosc. Radiat. Transfer 28 (1982) 471.

45. A.V. Smith and A.W. Johnson, Chem. Phys. Lett. 93 (1982) 608.

46. C.W. McCurdy and W.H. Miller, J. Chem. Phys. 67 (1977) 463.

47. S. Green and P. Thaddeus, Astrophys. J. 205 (1976) 766.

Figures

1. Isotropic Raman Q-branch pressure broadening coefficients as a
   function of rotational quantum number J. The filled circles,
   with error bars, are the experimental values from Table 1.
   The dotted line is the ECS prediction. The dashed line is the
   SPEG law fit given in section III-C. The solid line is the MEG
   law fit given in section III-B. (see text)

2. The ECS scaling law prediction of the CO Q-branch spectrum at 3.0 atm and
   295 K (solid line) d to experimental spectra (dots). The
   residuals (observed minus calculated) are offset for visibility.

3. The MEG law prediciton of the CO Q-branch spectrum (solid line) compared
   with experimental spectra (dots) at (a) 3.0 and (b) 6.0 atm. The
   residuals (observed minus calculated) are offset for visibility.

4. The SPEG law prediciton of the CO Q-branch spectrum (so id line) compared
   with experimental spectra (dots) at (a) 3.0 and (b) 6.0 atm. The
   residuals (observed minus calculated) are offset for visibility.

5. Rotationally inelastic state-to-state rates as a function of intial and
   final quantum number as given by (a) the best MEG law model ($\delta'=\delta$,
   unrestricted ΔJ), and (b) the best SPEG law model (ΔJ = even only).

17

Table 1

Experimenatal values of CO self-broadening coefficients at 295 K
(HWHM in cm^{-1}/atm, (uncertainty in last digit))

J	γ_J
0	0.086(10)
1	0.0789(50)
2	0.0744(30)
3	0.0712(30)
4	0.0690(20)
5	0.0672(10)
6	0.0659(10)
7	0.0650(10)
8	0.0640(10)
9	0.0634(10)
10	0.0620(10)
11	0.0615(10)
12	0.0599(10)
13	0.0593(10)
14	0.0589(10)
15	0.0574(10)
16	0.0561(10)
17	0.0560(10)
18	0.0549(10)
19	0.0543(10)
20	0.0538(10)
21	0.0526(10)
22	0.0511(10)
23	0.0510(40)
24	0.0472(80)

Table 2

Intermolecular Parameters for Line Broadening
Calculations[a].

Quantity	Value	Ref.
μ $(10^{-30}$ C m$)$	.367	[38]
Q $(10^{-40}$ C m$)$	-6.00	[38]
ϵ_{o-o} $(10^{-22}$ J$)$	8.50	[39]
σ_{o-o} $(10^{-11}$ m$)$	2.95	[39]
ϵ_{c-c} $(10^{-22}$ J$)$	7.07	[40]
σ_{c-c} $(10^{-11}$ m$)$	3.35	[40]
ϵ_{c-o} $(10^{-22}$ J$)$	7.75	[41]
σ_{c-o} $(10^{-11}$ m$)$	3.15	[41]
l_{c-o} $(10^{-11}$ m$)$	1.13	[36]
ϵ_{iso} $(10^{-22}$ J$)$	13.8	[42]
σ_{iso} $(10^{-11}$ m$)$	3.75	[42]

[a] Intermolecular potential parameters given here are related to
the potential parameters of Refs [27-30] through
$4\epsilon_{\alpha\beta}$ $(\sigma_{\alpha\beta})^6 = e_{\alpha\beta}$; $4\epsilon_{\alpha\beta}$ $(\sigma_{\alpha\beta})^{12} = d_{\alpha\beta}$
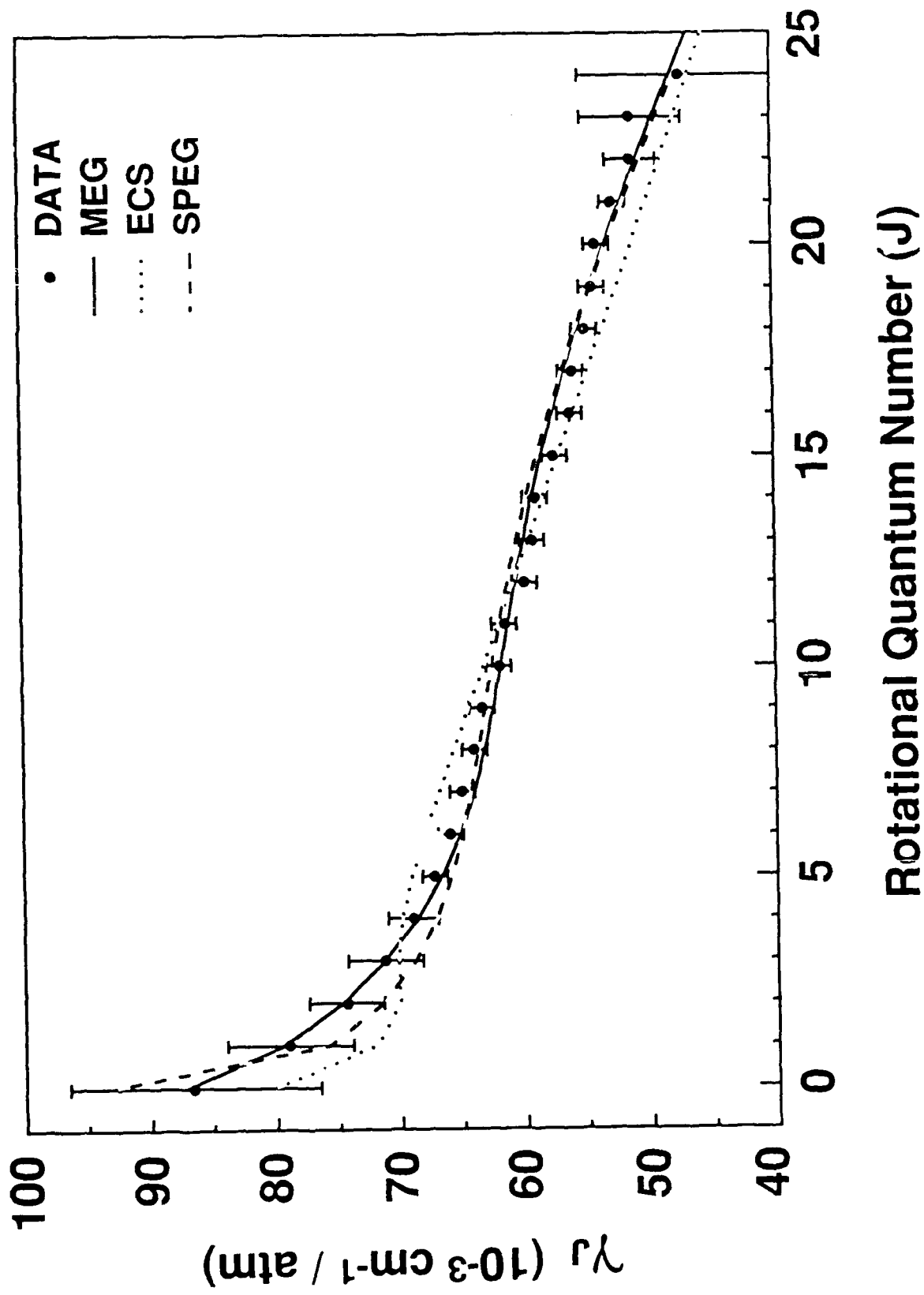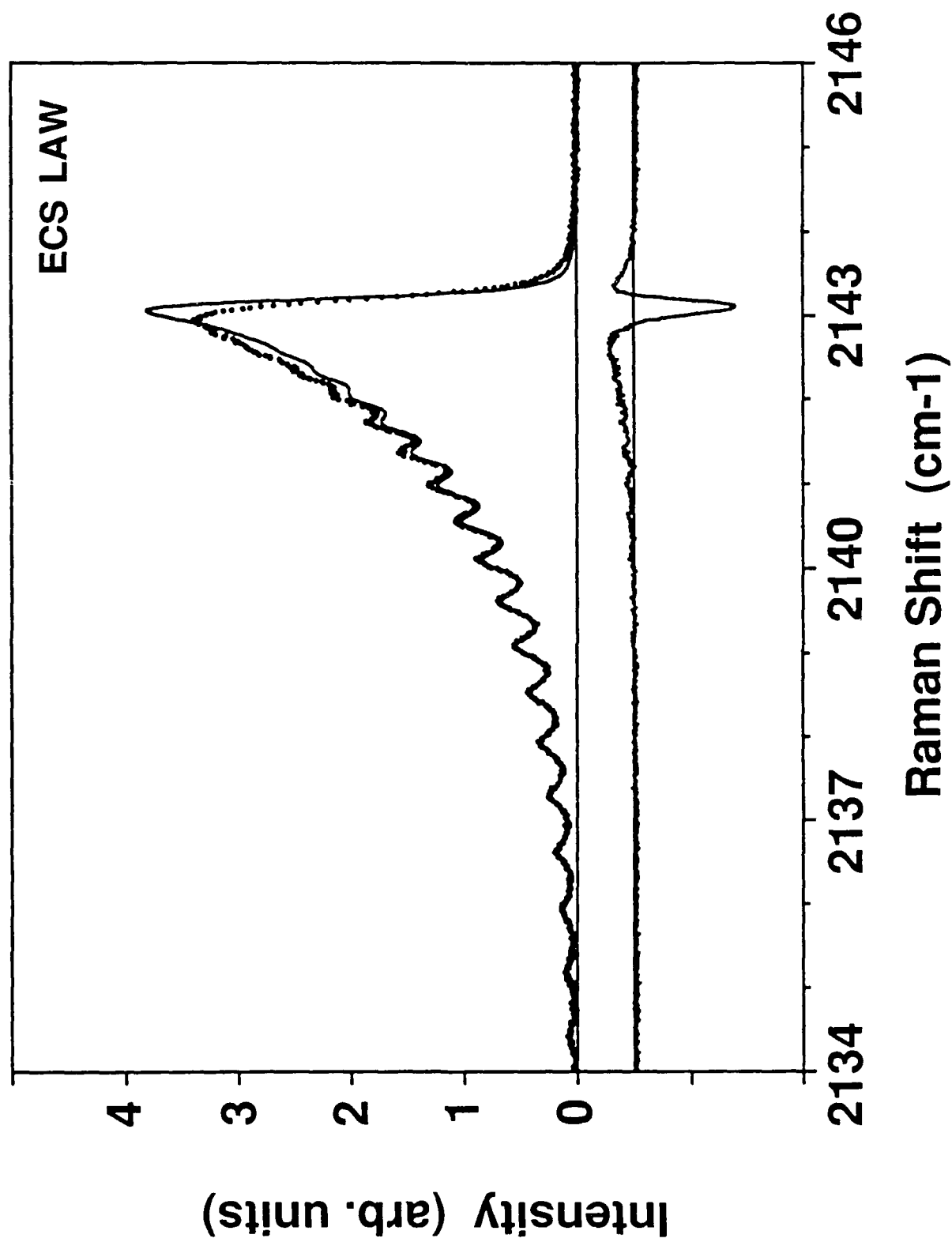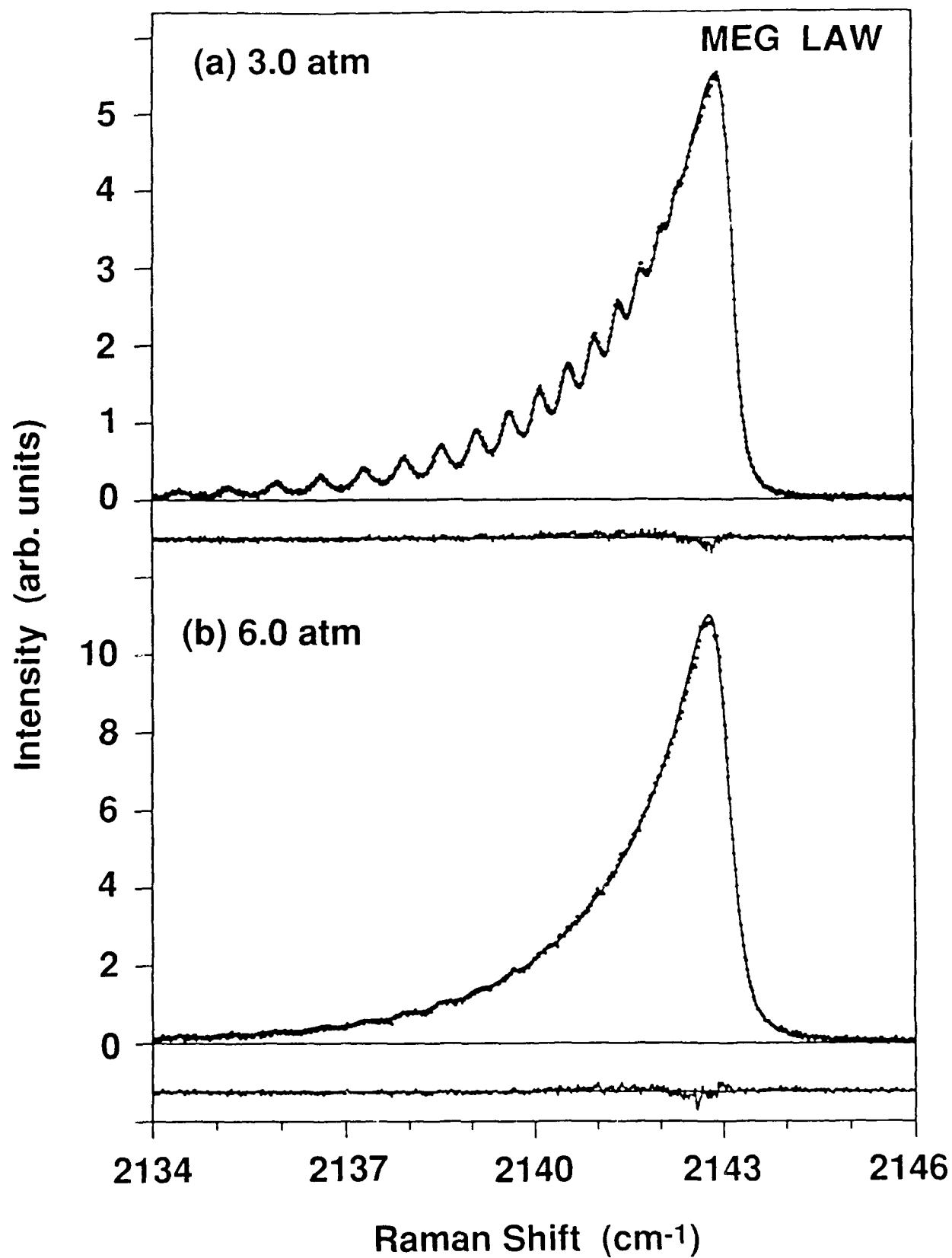and $|r_{1c}| + |r_{1o}| = l_{c-o}$.

FIG 1

ECS LAW

Intensity (arb. units)

Raman Shift (cm-1)

FIG 2

FIG 3

(a) 3.0 atm

SPEG LAW

(b) 6.0 atm

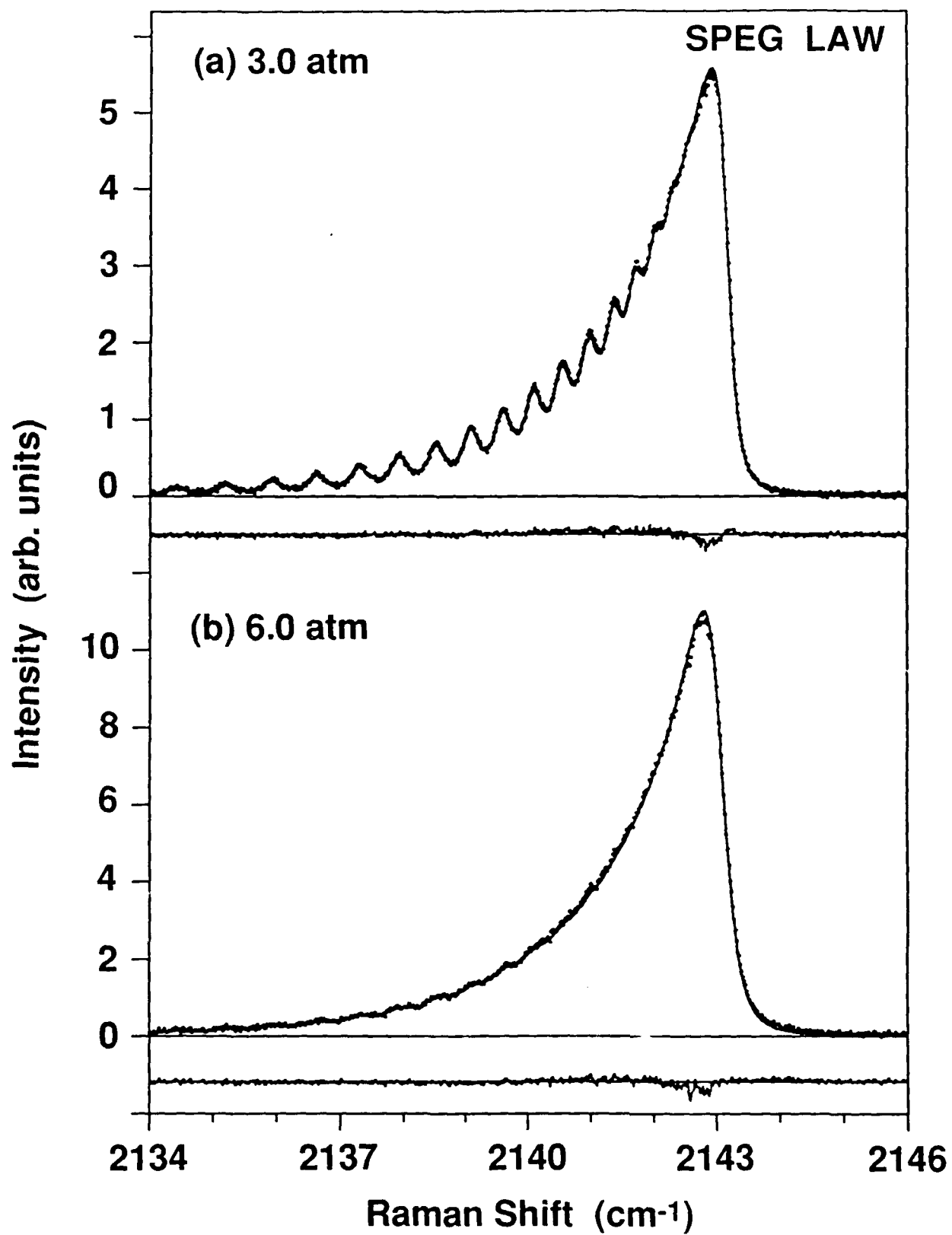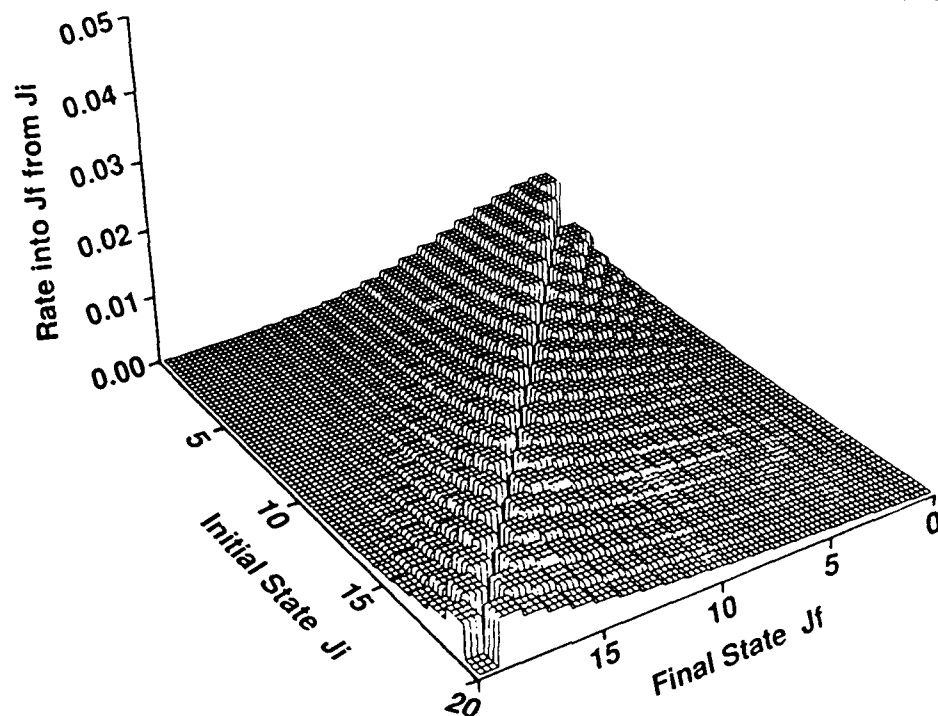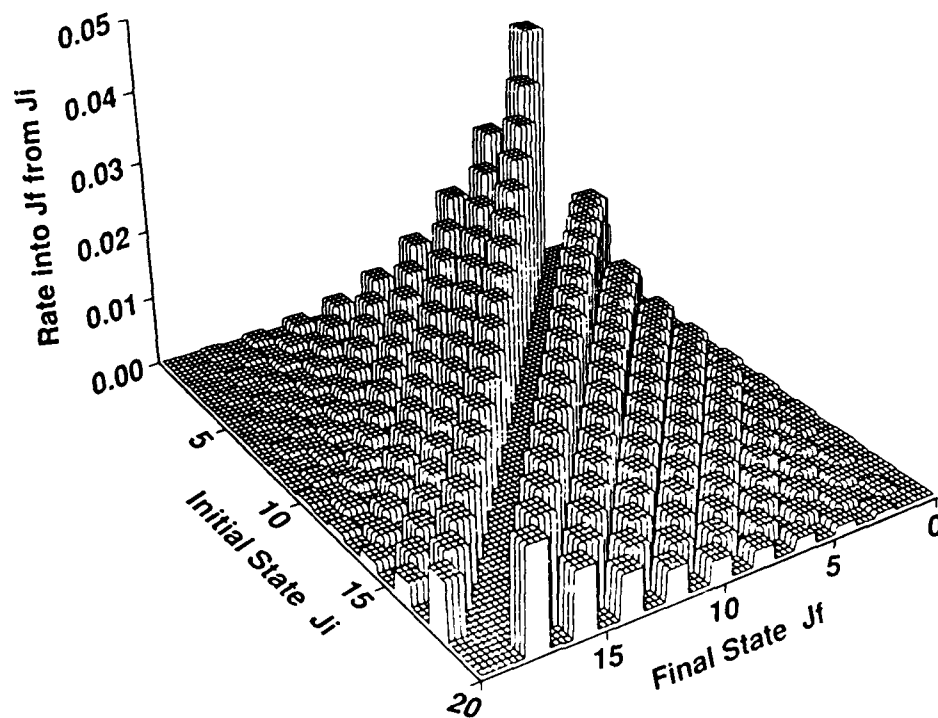Intensity (arb. units)

Raman Shift (cm⁻¹)

FIG 4

CO:CO MEG LAW (A)

CO:CO SPEG LAW (B)

FIG 5

Observation of a Speed-Dependent Collisional Inhomogeneity in H_2 Vibrational Line Profiles[*]

R. L. Farrow, L. A. Rahn, and G. O. Sitz[†]

Combustion Research Facility

Sandia National Laboratories

Livermore, California 94551-0969

and

G. J. Rosasco

Center for Chemical Technology

National Institute of Standards and Technology

Gaithersburg, MD 20899

Abstract

We report observations of inhomogeneous broadening in the vibrational line profiles of a gas in the "impact" density regime. In measurements up to 27 amagat (where the spectra are dominated by collision broadening), non-Lorentzian, asymmetric features are observed in Raman Q-branch transitions of H_2 dilute in a heavy perturber gas. We compare these measurements with an inhomogeneous line-profile model based on collisional shifts that strongly depend on the (thermal) speed of the H_2 radiator. Quantitative agreement is obtained only when speed-changing collisions are considered, which result in spectral line narrowing.

1

The collisional broadening of an isolated rotation-vibration transition of a gas is considered to be in the impact regime[1] when (a) the collision duration is small compared to the inverse of the collisional width, (b) the latter is large compared to the Doppler width, and (c) the collisional width and shift have no significant dependence on relative molecular speeds. Such conditions have been shown theoretically[2] to produce Lorentz profiles. Experimental studies[3] of collisional broadening in pure H_2 have successfully employed these assumptions for densities well above the Dicke minimum[4] for the Doppler effect (~2.5 amagat for pure H_2) and below densities where the finite duration of collisions becomes important (~100 amagat). However, measurements of the temperature dependence of H_2 collisional shift coefficients[3,5] indicate that such shifts depend significantly on relative speed, in apparent violation of (c). In considering spectra at densities in the Doppler regime, Berman,[6] Ward *et al.*,[7] and Nienhuis[8] demonstrated that such speed-dependent shifts (and/or speed-dependent collision widths) can lead to asymmetries and/or additional inhomo-geneities in the line profile. Berman, Pickett[9] and Luijendijk[10] showed theoretically that these effects generally persist to higher densities, i.e., to the collision-broadened regime. While examples of speed-dependent line profiles in the Doppler regime have been reported in atomic[11] Ca and rovibrational HF and HCl spectra,[12] to our knowledge none have been observed in a purely collision-broadened line.

In this Letter, we report observations of line profiles in Raman Q-branch transitions of H_2 perturbed by Ar that exhibit asymmetries and Gaussian-like cores at densities normally considered to be in the impact regime. For dens' ,s from 3.6 to 14 amagat at room temperature the non-Lorentzian features do not vary, , ,iough the width of the profile increases linearly. Spectra measured at constant density (~14 amagat) show a marked increase in the non-Lorentzian features with increasing temperature. The features occur at densities well above the Dicke minimum (~1 amagat for H_2-Ar) and yet below those for which finite collision-duration

2

effects[13] or collision-induced scattering[14] contribute to the Raman spectrum. We show that the anomalies can be explained by inhomogeneous broadening that arises from strong variations in the collisional shift with radiator speed. This interpretation is supported by a line-profile model based on speed-dependent shift cross-sections derived from measurements of the Q-branch line shifts of the H_2-H_2 and H_2-Ar systems at different temperatures. The model also incorporates the effects of speed-changing collisions, which coherently narrow the (speed-dependent) inhomogeneous part of the profiles. Such collisions are most likely when the masses of radiator and perturber molecules are similar, explaining why these inhomogeneities are less important in self-broadened gases.

The high-resolution inverse Raman (IRS) experiment[15] employs a pulse-amplified, tunable pump laser (~22 ns pulse duration) and a cw probe laser, providing a spectral resolution of 45 MHz (FWHM). Q-branch transition frequencies were obtained using a travelling corner-cube wavemeter. The highest peak intensity produced at the focus of the beams was kept below ~2 GW/cm^2 to eliminate Stark effects, which have been known to produce asymmetries.[16] The sample gases were contained in high-pressure, high-temperature furnace with temperature controlled to an accuracy of +50, -25 K. We measured gas pressure with transducers accurate to better than 1% of the indication and computed amagat density units using virial coefficients given in Ref. 17. The gases were mixed in the sample chambers while monitoring partial pressures and the compositions were verified to within ±2% by mass spectrometry.

The most compelling experimental evidence for a radiator-speed-dependent mechanism is summarized as follows: We observed non-Lorentzian line profiles only for perturbers with masses much greater than that of the H_2 radiator (for Ar, Kr, and N_2, but not for He or H_2). For such systems, a radiator's absolute speed largely determines its relative speed in collisions.[7] Strong variations in the collisional shift

3

with relative speed are evidenced by strong temperature dependences observed in the density-shift coefficients. Thus, radiators with different speeds will be characterized by different vibrational transition frequencies, giving rise to an inhomogeneity. The observed temperature dependence of the asymmetry further supports the speed-dependent mechanism. Finally, we observe rapid narrowing of the asymmetry with increasing H_2 partial pressure, which we believe indicates the important role of speed-changing collisions in determining the line profile. Only results that critically define the line-profile model will be presented here.

Experimental values of the H_2 $Q(1)$ line shifts for Ar and H_2 perturbers at temperatures from 295 K to 1000 K are listed in Table I. The Ar line-shift coefficients were determined by measuring $Q(1)$ spectra in 1:1 mixtures of H_2 and Ar at densities from 14 to 46 amagat. We fit the data to Lorentzian profiles (a good approximation for this mixture composition) to obtain observed shifts, then corrected these for self-shift contributions using the pure-H_2 coefficients measured by Rahn and Rosasco.[18]

We modeled the $Q(1)$ spectral profile, including the line shift, in H_2-Ar mixtures by assuming that the collisional shift depends on the relative speed between H_2 and the perturber. The speed-changing rate of H_2 resulting from H_2-Ar collisions was taken to be comparable to the rate of vibrational dephasing by Ar, but for H_2-H_2 collisions it was assumed to be much faster than the dephasing by H_2. Also, we assumed the following empirical form for the $Q(1)$ shift cross-section averaged over impact parameter:

$$\sigma(\upsilon_{rel}) = a\upsilon_{rel} + b + \frac{c}{\upsilon_{rel}}, \tag{1}$$

where υ_{rel} is the relative speed between radiator and perturber, and a, b, and c are adjustable parameters. Here, σ has units of cm^{-1}/amagat per cm/s. The radiator-speed-dependent shift coefficient was obtained from:

$$\delta(\upsilon_{rad}, T) = \int f_m(\mathbf{v}_{rad} + \mathbf{v}_{rel}, T)\upsilon_{rel}\,\sigma(\upsilon_{rel})\,d\mathbf{v}_{rel}, \tag{2}$$

4

in cm^{-1}/amagat, where v_{rel} is the relative velocity. Note that if $f_m(v, T)$ is the Boltzmann distribution of perturber velocities, $f_m(v_{rad}+v_{rel}, T)$ gives the distribution of relative velocities seen by a radiator of velocity v_{rad}. For comparison with the observed line shifts, we integrated $\delta(v_{rad}, T)$ over the Boltzmann distribution of radiator velocities: $\delta(T) = \int f_M(v_{rad}, T) \, \delta(v_{rad}, T) \, dv_{rad}$.

Two sets of parameters a, b, and c in Eq. (1) were adjusted[19] to obtain agreement between $\delta(T)$ and the line-shift measurements for each collider pair (H_2-Ar and H_2-H_2; see Table I). The resulting $\sigma(v_{rel})$ for H_2-H_2 is in excellent agreement (better than ± 1 Å^2 from 0.005 to 0.1 eV) with the collision-energy-dependent shift cross-section reported by Kelley and Bragg.[3]

We now show that the line profiles observed for the H_2-Ar system can be modeled using the speed-dependent shift cross-section (Eq. 1). Examples of the non-Lorentzian nature of these profiles are shown in Figs. 1a and 1c, where spectra of $Q(1)$ from mixtures of 2(mole)% H_2 in Ar at total densities of 13.9 and 13.7 amagat, and temperatures of 295 K and 1000 K, respectively, are plotted. The solid curves are best-fit Lorentzian profiles and associated fit residuals. Note that the residuals increase substantially at 1000 K, but maintain a similar shape. Similar effects were observed for $Q(0)$ and $Q(2\text{-}4)$.

An inhomogeneous line profile is computed using $\delta(v_{rad}, T)$ from Eq. (2) in the expression for a speed-dependent Lorentzian profile:[6,10]

$$I_{inhom}(\omega) = \frac{1}{2\pi} S(\omega, \gamma, T) + c.c. \equiv \frac{1}{2\pi} \int \frac{f_M(v_{rad}, T)}{\gamma(T)\rho - i[\omega + \delta(v_{rad}, T)\rho]} dv_{rad} + c.c. \quad (3)$$

Here, γ is the coefficient for the dephasing width (HWHM), ω is the detuning from the zero-density Raman frequency, and ρ is the density in amagat. This expression is similar to that for a speed-dependent Voigt profile,[6-8] except that we have assumed that $\gamma(v_{rad}, T) \sim \gamma(T)$ and that the Doppler-shift term ($k \cdot v_{rad}$) is much smaller than

$\gamma\rho$ due to motional narrowing.[20] The former assumption is based only on the fact that no speed-dependence of the broadening was required to describe our results.

The inhomogeneous profile given by Eq. (3), which neglects speed-changing collisions, is generally in poor agreement with experimental asymmetric spectra in that it overestimates linewidth and asymmetry. However, if speed-changing collisions are present and occur more frequently than dephasing collisions, scattering amplitudes associated with different speed-groups can coherently interfere, resulting in spectral narrowing. This narrowing and symmetrization are analogous to that produced in Doppler profiles by *velocity*-changing collisions, and can significantly alter the shape of the speed-dependent profile. We included speed-changing collisions using a hard-collision approximation analogous to that for Dicke narrowing,[21] resulting in a final expression for the line shape:

$$I(\omega) = \frac{1}{2\pi} \frac{S(\omega, \gamma + v, T)}{1 - v\rho S(\omega, \gamma + v, T)} + \text{c.c.}, \qquad (4)$$

where v is the frequency of speed-changing collisions. Note that as $v \rightarrow 0$, $I(\omega) \rightarrow I_{\text{inhom}}(\omega)$, but as v becomes larger than both γ and the width of I_{inhom}, $I(\omega)$ narrows to a Lorentzian profile of half-width γ. Note that, unlike motional narrowing of the Doppler effect, varying the total density alone does not affect the degree of narrowing, since the width of I_{inhom} and $v\rho$ both scale linearly with density.

To calculate the model spectra in Fig. 1b and 1d (2% H_2 in Ar), we used Eq. (4) and varied γ, v, and a frequency offset for best fit. (The latter is necessary because the model can vary from observed transition frequencies by up to 0.5×10^{-3} cm^{-1}/amagat) The resulting γ and v were respectively 2.4 and 8.3 at 1000 K, and 2.4 and 6.3 at 295 K, in units of 10^{-3} cm^{-1}/amagat. The temperature dependence of v (the speed-changing frequency) is found to be comparable to that of β, the frequency of velocity-changing collisions.[20] However, the magnitude of v is only ~8% of β, implying that the H_2 *speed* is conserved even after several *velocity*-changing

6

collisions with Ar. The inefficiency of Ar in changing the speed of H_2 is presumably due to the large mismatch in mass and average speed. The best-fit values for γ (the dephasing frequency) were essentially the same; thus, the increased width observed at 1000 K results mostly from inhomogeneous broadening. Remarkably, we find that homogeneous (dephasing) broadening produces only ~25% of the total width in this case.

The model is also found to successfully describe the observed narrowing and symmetrization of the profiles as H_2 concentration increases at constant temperature. We measured spectra from a series of gas mixtures at constant total density and temperature but with varying composition. The anamolies were strongest in mixtures of 0.5% H_2 in Ar (we did not investigate greater dilutions), but were nearly indiscernible in 20% mixtures at 295 K. For 50% H_2 at 295 K, the profile was Lorentzian to within our experimental uncertainty, ±1% of the peak intensity. More-over, the linewidths of the profiles, as determined from either best-fit Lorentzian or spline functions, exhibited remarkable deviations from a linear mixing rule (i.e., a dependence on the mole-fraction-weighted sum of perturber broadening coefficients). This effect appears as a curvature in linewidths plotted against H_2 mole fraction (symbols in Fig. 2b). We have observed similar nonlinear dependences in coherent anti-Stokes Raman spectroscopy (CARS) linewidths of H_2 in Kr, and in IRS linewidths of D_2 in Ar.

The line profiles corresponding to the IRS data in Fig. 2b were analyzed by varying the broadening and narrowing coefficients (γ and v in Eqs. 3 and 4) for best fit to each profile (described below), and by employing a mole-fraction-weighted sum of the previously determined H_2 and Ar shift functions [$\delta(v_{rad}, T)$] for each mixture. The results for 295 K are shown in Fig. 2a. Using the linearly varying coefficients shown by the solid lines in Fig. 2a, the model accurately describes the dependence of

7

linewidth on H_2 mole fraction (Fig. 2b) and is also in excellent agreement with the observed spectral profiles (not shown).

Some of the values for γ and v indicated by data points in Fig. 2a could not be obtained by unconstrained fitting. At H_2 concentrations of 50% and higher the Lorentzian nature of the experimental profiles provided poor sensitivity to the relative magnitudes of γ and v. Here, we used a linear extrapolation for v which had an intercept for pure H_2 equal to the known velocity-changing collision rate, β.[20] (This line, shown in Fig. 2a, was found to be consistent with the v-values for low H_2 concentrations.) The associated coefficients for γ were obtained by fitting with fixed v. Thus using $v = \beta$ for pure H_2, the model predicts that ~15% of the collision width is due to inhomogeneous broadening. For H_2-Ar collisions, about half of the width is found to be inhomogeneous, and v is predicted to be ~10 times lower than the pure-H_2 value, corresponding to only ~5% of β for H_2-Ar.[20]

Similarly consistent results were obtained at 1000 K, although only three mixtures were investigated (2%, 50%, and 100% H_2). For pure H_2, 80($\pm$15)% of the total linewidth was determined to be homogeneous, and v was equal to 60($\pm$20)% of β computed for 1000 K.[20]

We also investigated the dependence of the line profiles on total density, primarily in 2% H_2-Ar mixtures at ~295 K. Recall that the model [Eq. (4)] predicts an invariance of the line *shape* with respect to density. That is, if we normalize the detuning by density ($\omega = \omega'\rho$), then ρ enters the line profile only as a proportionality constant. Consistent with this property, we found that to within our uncertainties the best-fit values for γ and v were independent of density over the range 2.8-14 amagat.

References

1. A. Ben-Reuven, Adv. Chem. Phys. **33**, 235 (1975).

2. See, for example, G. Peach, Contemp. Phys. **16**, 17 (1975).

3. J. D. Kelley and S. L. Bragg, Phys. Rev. A **34**, 3003 (1986), and references therein.

4. R. H. Dicke, Phys. Rev. **89**, 472 (1953).

5. W. K. Bischel and M. J. Dyer, Phys. Rev. A **33**, 3113 (1986), and Ref. 3.

6. P. R. Berman, J. Quant. Spectrosc. Radiat. Transfer **12**, 1331 (1972).

7. J. Ward, J. Cooper, and E. W. Smith, J. Quant. Radiat. Transfer **14**, 555 (1974).

8. G. Nienhuis, J. Quant. Spectrosc. Radiat. Transfer **20**, 275 (1978).

9. H. M. Pickett, J. Chem. Phys. **73**, 6090 (1980).

10. S. C. M. Luijendijk, J. Phys. B **10**, 1735 (1977).

11. I. Shannon, M. Harris, D. R. McHugh, and E. L. Lewis, J. Phys. B: At. Mol. Phys. **19**, 1409 (1986).

12. J. P. Looney, "Comprehensive Theory for the Broadening, Shifting, and Narrowing of HF and HCl Fundamental Band Absorption Profiles," Doctoral Thesis, Pennsylvania State University, December, 1987.

13. Ph. Marteau, C. Boulet, and D. Robert, J. Chem. Phys. **80**, 3632 (1983), and references therein.

14. See for example, J. Borysow and L. Frommhold, "The Infrared and Raman Line Shapes of Pairs of Interacting Molecules," in *Phenomena Induced by Intermolecular Interactions*, ed. G. Birnbaum (Plenum Press, New York, 1985), pp. 67-93.

15. L. A. Rahn and R. E. Palmer, J. Opt. Soc. Am. B **3**, 1166 (1986).

16. R. L. Farrow and L. A. Rahn, "Optical Stark Effects in Nonlinear Raman Spectroscopy," in *Raman Spectroscopy: Linear and Nonlinear*, J. Lascombe and P. V. Huong, eds. (Wiley, New York, 1982), pp. 159-160.

17. J. O. Hirschfelder, C. F. Curtiss, and R. B. Bird, *Molecular Theory of Gases and Liquids* (Wiley, New York, 1964).

18. L. A. Rahn and G. A. Rosasco, to be published elsewhere.

19. The values we obtained for a, b, and c for Ar (H_2) perturbers were: $a = 6.0$ (3.8) $\times 10^{-14}$ s^2/cm^3 amagat, $b = 4.6$ (2.9) $\times 10^{-8}$ s/cm^2 amagat, $c = -2.205$ (-1.32) $\times 10^{-2}$ cm^{-1}/amagat.

20. We calculated β using $\beta = kT/mD$ as discussed in Ref. 21, where the diffusion coefficient, D, was computed per Ref. 17.

21. S. G. Rautian and I. I. Sobel'man, Sov. Phys. Usp. **9**, 701 (1967).

Table I

Collisional line-shift coefficients $\delta(T)$ for the $Q(1)$ transition of H_2 at different temperatures, measured with IRS, and compared to fitted model results. The coefficients are expressed in 10^{-3} cm^{-1}/amagat; figures in parentheses indicate experimental uncertainties in the last digit(s).

Temperature (K)	H$_2$-Ar		H$_2$-H$_2$	
	Exp. $\delta(T)$	Theo. $\delta(T)$	Exp. $\delta(T)$[a]	Theo. $\delta(T)$
295	-12.0(1)	-11.4	-3.20(3)	-3.2
450	-8.2(1)	-8.3	0.70(1)	-0.05
750	-2.7(2)	-3.0	5.85(8)	5.4
1000	0.86(40)	1.0	9.16(14)	9.5

[a]Ref. 18 except for the 295-K value, which is from Ref. 5. The value for 750 K is interpolated between measurements at 725 K and 1000 K. Due to its simplicity, the uncertainty in the model is ~0.5 × 10^{-3} cm^{-1}/amagat; thus the disagreement at 450 K is not considered significant.

Figure Captions

1. Experimental IRS spectra (data points) of the $Q(1)$ transition of H_2 broadened by Ar at 295 K and 1000 K. The H_2 mole fraction is 2% and the total densities are 13.9 and 13.7 amagat, respectively. The data are compared to best-fit Lorentzian profiles and to the model profile described in the text. The model includes inhomogeneous broadening arising from radiator-speed-dependent collisional shifts.

2. (a) Best-fit collision-broadening (γ) and -narrowing (ν) coefficients, indicated by symbols, obtained from IRS spectra of the $Q(1)$ transition of H_2/Ar mixtures at 295 K and 7.3 amagat total density. (These coefficients are used by the proposed line-profile model.) Also plotted are best-fit straight lines through the data.

    (b) Spectral linewidths determined from fitting Lorentzian profiles to the data (symbols) and to the theoretical profiles (curve) calculated using the corresponding parameters in (a). The CARS measurements will be described fully elsewhere.
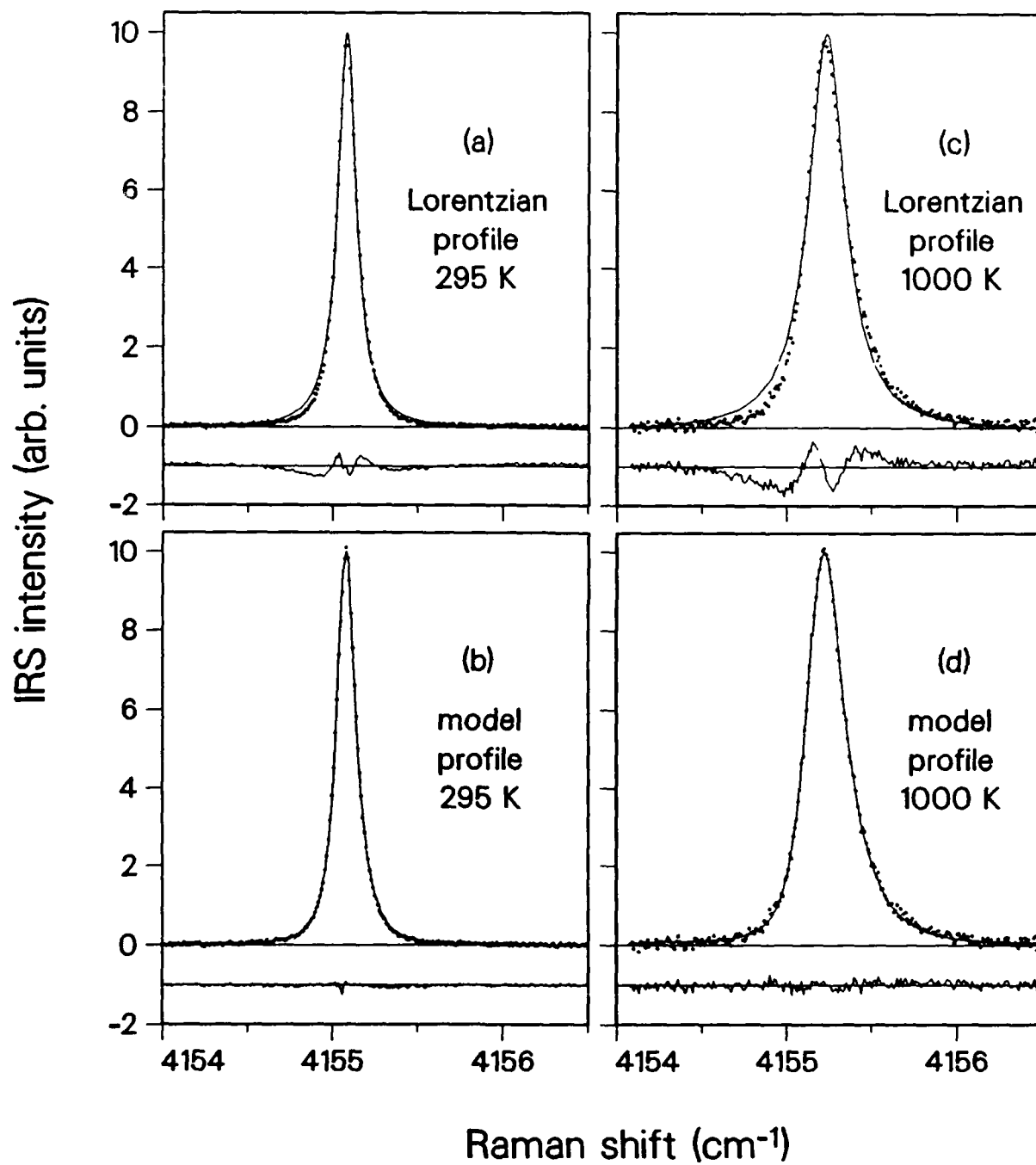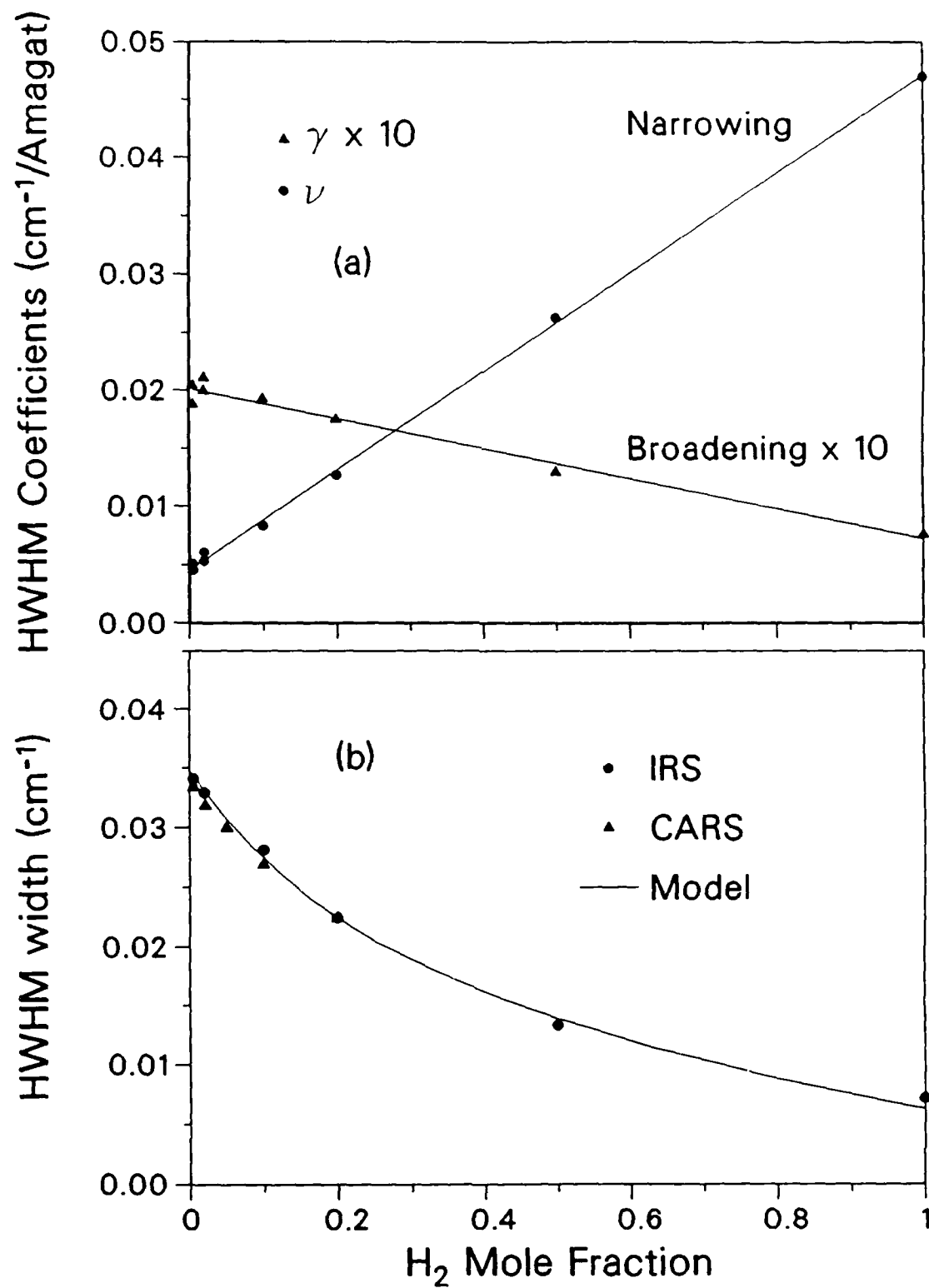
Fig 1

Fig 2